

DEVELOPMENT OF A HEAT-SEALED FLUID CHANNEL SYSTEM FOR
PHYSIOLOGICALLY TARGETED TEMPERATURE CONTROL

AN ABSTRACT

SUBMITTED ON THE 16TH DAY OF APRIL 2018

TO THE DEPARTMENT OF BIOMEDICAL ENGINEERING

IN PARTIAL FULLFILLMENT OF REQUIREMENTS

OF THE SCHOOL OF SCIENCE AND ENGINEERING

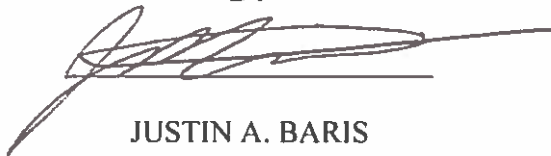
OF TULANE UNIVERSITY

FOR THE DEGREE

OF

MASTER OF SCIENCE IN BIOMEDICAL ENGINEERING

BY



JUSTIN A. BARIS

APPROVED BY:



MICHAEL J. DANCISAK, PH.D.
DIRECTOR



KATHERINE RAYMOND, PH.D.



LARS G. GILBERTSON, PH.D.

ABSTRACT

Current methods for temperature modulation of people who perform repetitive, fatiguing, or ergonomically unfavorable tasks, are costly and do not provide long-lasting comfort. These systems have extreme temperature fluctuations and during extended tasks, require periodic garment changes. Previous developments in our lab have shown the need for a better controlled, less invasive, and more targeted method of providing heat transfer for the reduction of muscle fatigue and physiological tremor and to improve task performance. A model of aluminum plating was fabricated to create heat-sealable Mylar® constructs, allowing for targeted fluid flow to the deltoid region, a high-density zone in the upper extremity. A proof of concept has been quantified in the ability of Mylar® to be sealed and for fluid flow to be incorporated. ASTM F88 peel testing was able to quantify the system's strength-to-material thickness and strength-to-sealing time relationships. A burst testing apparatus was also designed and used to further quantify the strength of the fluid channel system via ASTM D642. A valve connection system to incorporate flow between high-density zones was also designed. Further work is necessary to quantify thermal transfer properties and promote full integration of the design into existing garments, but proof of concept in sealing Mylar® fluid channel system for physiologically-based temperature modulation has been achieved.

DEVELOPMENT OF A HEAT-SEALED FLUID CHANNEL SYSTEM FOR
PHYSIOLOGICALLY TARGETED TEMPERATURE CONTROL

A THESIS

SUBMITTED ON THE 16TH DAY OF APRIL 2018

TO THE DEPARTMENT OF BIOMEDICAL ENGINEERING

IN PARTIAL FULLFILLMENT OF REQUIREMENTS

OF THE SCHOOL OF SCIENCE AND ENGINEERING

OF TULANE UNIVERSITY

FOR THE DEGREE

OF

MASTER OF SCIENCE IN BIOMEDICAL ENGINEERING

BY



A handwritten signature in black ink, appearing to read 'Justin A. Baris', is written over a horizontal line.

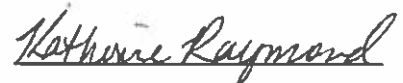
JUSTIN A. BARIS

APPROVED BY:



A handwritten signature in black ink, appearing to read 'Michael J. Dancisak', is written over a horizontal line.

MICHAEL J. DANCISAK, PH.D.
DIRECTOR



A handwritten signature in black ink, appearing to read 'Katherine Raymond', is written over a horizontal line.

KATHERINE RAYMOND, PH.D.



A handwritten signature in black ink, appearing to read 'Lars G. Gilbertson', is written over a horizontal line.

LARS G. GILBERTSON, PH.D.

**© Copyright by Justin A. Baris, 2018
All Rights Reserved**

ACKNOWLEDGEMENTS

Justin would like to thank Dr. Michael Dancisak for his constant support throughout this project and allowing the opportunity to work and learn from him for the past several semesters. Additional thanks go to Dr. Katherine Raymond and Dr. Lars Gilbertson in their design expertise and in serving as great resources for ideation, IP protection, and literature review. Dr. Ronald Anderson's help with ADMET testing was instrumental. Thank you to Dr. Lee Murfee with his help in presentation formatting and research support. Additionally he would like to note contributions from Antonius Prader in 3D CAD Design help and setup of experimentation. Dr. Cedric Walker and Chase Schober's help with CNC machining, CAM processes, and acrylic fabrication was also invaluable in the completion of this project. April Aguiard for her unwavering moral support, and last but most certainly not least, he would like to thank his parents, friends, and family for their constant support throughout this process.

TABLE OF CONTENTS

ACKNOWLEDGEMENTS	ii
TABLE OF CONTENTS	iii
LIST OF TABLES	vii
LIST OF FIGURES	viii
CHAPTER 1: INTRODUCTION	1
I.1. Clinical Condition	1
I.2. Current Technologies	1
I.3. Project Description	2
I.4. Proof of Concept	3
I.5. Assumptions and Limitations	4
I.6. Operational Definitions	5
CHAPTER 2: REVIEW OF LITERATURE	7
II.1. Impact of Temperature on Task Performance	7
II.2. Muscle Fatigue	9
II.2.1. Surgical Tasks	10
II.2.2. Industrial and Manufacturing Tasks	13
II.2.3. Athletics Applications	15
II.3. Physiological Tremor	17
II.4. Cooling Interventions	18
II.4.1. Ice-Pack Method	23
II.4.2. Liquid-Cooling-Warming Garments	27
II.4.3. Cooling Garment Prior Art	29

II.4.4. Tube-Suit	32
II.5. Personal Protective Equipment (PPE)	35
II.6. Valve Design Prior Art	37
CHAPTER 3: MATERIALS AND METHODS	40
III.1. Design Requirements	40
III.2. Materials	42
III.2.1. Mylar®	42
III.2.2. Aluminum	46
III.2.3. 3D Printer	47
III.2.3.1. PLA	47
III.2.3.2. PETG	48
III.2.4. Acrylic	49
III.3. Sealing Patterns.....	49
III.4. Fluid Pressure Calculations.....	51
III.5. Determination of Heating Element	53
III.6. Plate Fabrication	58
III.6.1. Plywood	58
III.6.2. Aluminum	62
III.7. Testing with Grill Construct	64
III.7.1. Temperature	65
III.7.2. Pressure	65
III.7.3. Sealing Protocol	67
III.8. ADMET Peel Testing (ASTM F88)	69
III.8.1. Sample Preparation Protocol	70
III.8.2. Test Protocol	73
III.8.3. Data Collection and Analysis	75
III.9. ADMET Burst Testing (ASTM D642).....	75

III.9.1. Fixed-Platen Testing Apparatus	75
III.9.2. Sample Preparation Protocol	77
III.9.3. Test Protocol	78
III.9.4. Data Collection and Analysis	79
III.10. Valve Design	79
III.11. Assembly of FCS	81
CHAPTER 4: RESULTS	85
IV.1. Temperature Testing of Sealing Press Device	85
IV.2. ASTM Peel Testing	87
IV.2.1. Data Aggregation	87
IV.2.2. Two-Way ANOVA	88
IV.2.3. Method of Sample Break	92
IV.3. ASTM Burst Testing	100
IV.3.1. Sample Preparation	100
IV.3.2. Data Aggregation and Analysis	100
CHAPTER 5: DISCUSSION	106
V.1. Overview	106
V.2. Temperature Testing	107
V.3. Fluid Pressure Calculations	107
V.4. Peel Testing	110
V.5. Burst Testing	111
V.6. Manufacturing Concerns	114
V.7. Further Design Considerations and Future Work	117
V.8. Conclusions	120
APPENDIX	
Appendix A - Bernoulli and Reynolds Number Equation Variables	121
Appendix B - Method of Sample Break (ASTM International, F88)	122

Appendix C – Temperature Test Data	123
Appendix D - Peel Test Data	126
Appendix E- Burst Test Data.....	130
List of References	131
Biography.....	140

List of Tables

Table 1 – Temperature subcategories and corresponding temperature ranges in WGBT (Adapted from Pilcher, et al. 682-698)	8
Table 2 – Design requirements for physiologically targeted LCWG	40
Table 3 – Design requirements for valve connection system	41
Table 4 – Notable thermal properties of 6061-T6 Aluminum (uncoated) (Adapted from Aerospace Specification Metals, Inc.)	47
Table 5 – Temperature and dwell time conditions for sample preparation protocol. (Adapted from ASTM International, E171)	71
Table 6 – Data aggregated based on seal area	88
Table 7 – Aggregated data from ASTM F88 testing	89
Table 8 – Aggregated data from ASTM F88 testing via method of break and delamination.....	94
Table 9 – Thickness vs. method of break in ASTM F88	98
Table 10 – Dwell time vs. method of break in ASTM F88	99
Table 11 – ASTM D642 burst strength (lbs) with two outliers eliminated	102
Table 12 – Aggregated deformation results from ASTM F88	106

List of Figures

Figure 1 – Percent reduction in task performance based on temperature subcategories. (Pilcher, et al. 682-698)	8
Figure 2 – Simulated Laparoscopic Surgical Tasks on a Lapsim Trainer a) with arms in “ideal” posture, and b) arms in “elevated” posture. (Galleano et al. 329-333).....	11
Figure 3 – Percentage change in mean frequency of Brachioradialis (Left) and Mid-Deltoid (Right) contraction. Linear regression with 95% confidence interval in control groups (top lines) and surgical groups (bottom lines) (Slack, et al. 651-657)	12
Figure 4 – Time to Fatigue for selected muscle groups at beginning of day (left) vs. end of day (right). (Halim et al. 31-42)	14
Figure 5 – Pre-fatigue and post-fatigue 3DVE differences (degrees) based on joint. (Tripp, et al. 90-98).....	16
Figure 6 – Time to Functional Fatigue after Exercise in Novice and Experienced Cohorts with and Without Cooling Intervention. (Jensen, et al. e126-e130)	21
Figure 7 – Suture Experiment Time after Exercise in Novice and Experienced Cohorts with and Without Cooling Intervention. (Jensen, et al. e126-e130)	21
Figure 8 – CoolOR Zipper Vest with Cool 58 Packs. (Polar Products, Inc.)	24
Figure 9 – Surface (Left) and 2cm subadipose (Right) temperature vs.time. (Merrick, et al. 28-33)	26
Figure 10 –“System and Method for Providing Even Heat Distribution and Cooling Return Pads” (Dunning, et al.)	30
Figure 11 – Targeted Cooling Apparatus for Lower-Extremity Cooling. (Zacoi)	32

Figure 12 – Tube-suit embodiment. (Koscheyev, et al.).....	33
Figure 13 – Proximal arm vasculature and muscle groups. (Cultua).....	34
Figure 14 – Stackhouse Surgical Gown with included helmet component. (Stackhouse, et al.)	36
Figure 15 – Shrinkage vs. Temperature of 1mil (Left) and 7.5mil (Right) Mylar® sheets. (Dupont Teijin Films). Lines correspond with polymer orientation: MD = machine direction, TD = transverse direction	44
Figure 16 – Tensile Strength vs. Time at 150 °C. (Dupont Teijin Films). Specimens are tested with ASTM D882 (ASTM International, D882)	44
Figure 17 – “Teardrop” Sealing Scaffold based on the Anatomy of the Deltoid Group	50
Figure 18 – Reynolds Number Calculation Based on velocity and diameter of FCS (Adapted from Benson; Engineer’s Edge) (See Appendix A)	53
Figure 19 – Seal strength of several polyethylene polymers based on temperature. (Farley, et al.)	54
Figure 20 – T-Thermocouple in place on Bottom Grill Plate	55
Figure 21 – Material melts due to Soldering Iron, leading to ineffective seal.....	56
Figure 22 – Temperature testing setup in “closed” grill position	57
Figure 23 – Fabrication of ½” thick plywood plate constructs	59
Figure 24 – 1 st iteration plywood plating snapped in to grill construct	60
Figure 25 – 2 nd Iteration Plywood Plates	61
Figure 26 – 3 rd Iteration Plywood Plates.....	61
Figure 27 – 4 th Iteration Plywood Plates.....	62
Figure 28 – 5 th Iteration Plywood Plates.....	62

Figure 29 – Final Iteration Manufactured in 6061 Aluminum on Grill Construct	63
Figure 30 – Isometric View of Current Aluminum Plating with spaces for valve connection	64
Figure 31 – 20lb weight stack added to top of grill construct for sealing. Applied for each dwell time in sample preparation	66
Figure 32 – Sheet placed in tension on scrap piece of 6061 Aluminum for sealing process	68
Figure 33 – Sample preparation template with distinct areas for ASTM F88 Peel Testing	70
Figure 34 – Seal preparation dimensions for ASTM F88 (ASTM International, F88)	72
Figure 35 – “Unsupported” specimen technique (ASTM International, F88)	74
Figure 36 – Sample tested in ASTM F88, unsupported technique with reference string behind	74
Figure 37 – Fixed-platen testing apparatus outfitted on the ADMET testing machine	76
Figure 38 – Sample preparation template made from Plywood with distinct areas for ASTM D642 Burst Testing	78
Figure 39 – Specimen placed in test apparatus for ASTM D642 Burst test	79
Figure 40 – 1 st Valve Iteration (Modification of Ferber)	80
Figure 41 – 2 nd Valve Iteration	80
Figure 42 – Two valve iterations with tapered ends	81
Figure 43 – Deformation of PLA valves with application of direct heat. Front, Top, and Bottom Views of deformation (clockwise from top left)	83
Figure 44 – Tissue clamping forceps holding valve and Mylar® in tension for application of heat to area	83
Figure 45 – Snap configuration in deltoid FCS to allow for 3D deformation compensation	84

Figure 46 – Temperature profile of unmodified sealing press (n=5 trials)	86
Figure 47 – Temperature profile of modified sealing press (n=5 trials)	86
Figure 48 – Average time to reach sample preparation temperature (to nearest 30 seconds) (p<0.001; n=5 trials)	87
Figure 49 – Relative Standard Deviation of ASTM F88. Taken as standard deviation divided by mean, multiplied by 100 (Keeny, Texas A&M)	90
Figure 50 – Mean Peel Strength by Material Thickness in Pounds (Error Bars: +/- 1 SD)	91
Figure 51 – Mean Peel Strength by Dwell Time in Pounds (Error Bars: +/- 1 SD)	91
Figure 52 – Thickness and Dwell Time Interaction via Means of Strength	92
Figure 53 – Graph of position vs. load in sample undergoing a material break with delamination.....	93
Figure 54 – Graph of position vs. load in sample undergoing an adhesive peel without delamination.....	94
Figure 55 – Method of Sample Break vs. Strength (lbs) (Error Bars: +/- 1 SD). Material Break and Both (Material Break and Adhesive Peel) showed significant differences (p<0.001) compared to Adhesive Peel alone	95
Figure 56 – Presence of Delamination vs. Strength (lbs) (Error Bars: +/- 1 SD). Delamination showed significantly higher peel strength than No Delamination (p<0.001)	96
Figure 57 – Aggregated Results of Delamination and Method of Sample Break Interaction	97
Figure 58 – Thickness vs. Method of Break in ASTM F88 (shown as percentage of samples)	98
Figure 59 – Dwell Time vs. Method of Break in ASTM F88 (shown as percentage of samples)	99

Figure 60 – Plot of Load vs. Position in ASTM D642 Burst Test	101
Figure 61 – Boxplot to detect presence of outliers in Burst Strength. Two outliers were found in the 10-second dwell time condition. Outlier is defined as ≥ 1.5 -times the inter-quartile range	102
Figure 62 – Burst Strength (lbs) results of ASTM D642 Burst Test (Error bars: +/- 1 Standard Deviation) (p=0.047)	103
Figure 63 – Deformation (in) results of ASTM D642 Burst Test (Error bars: +/- 1 Standard Deviation) (p=0.068)	105
Figure 64 – Laminar vs. Turbulent Flow Characteristics (Klabunde)	108
Figure 65 – Calculations of Peak Pressures in FCS with smallest cross-sectional area (See Appendix A)	109
Figure 66 – Fluid pressure calculations with internal diameter of $\frac{1}{4}$ " (.02083ft). (See Appendix A)	109
Figure 67 – Fluid pockets at >90-degree corners	113
Figure 68 – Material shrinkage during specimen preparation	116
Figure 69 – Isometric (Left) and Front (Right) views of additional FCS designs	118

Chapter 1: INTRODUCTION

1.1. Clinical Condition

This design project developed and tested the essential qualities of a key component for a Liquid-Cooling-Warming-Garment (LCWG) to help increase comfort and safety for workers in healthcare and industry, and athletes in extreme or repetitive work environments. Although outcomes may be different for each individual user, development of a system to control comfort levels in critical task environments may improve efficiency and safety for the individual users. This system can be further incorporated into existing technologies to provide a targeted, physiological temperature modulation.

1.2. Current Technologies

Developments in full-body cooling systems have shown a significant decrease in muscle fatigue in long-duration exercise. As many tasks can be extremely labor-intensive, an adoption of this type of cooling system into pre-existing technologies is a natural step in improving overall task performance. Current LCWG systems require large fluid volumes and pressures, so the development of a compartmentalized system to cool targeted heat exchange areas of the body is vital.

For example, technologies currently exist for the cooling of surgeons and surgical staff in an operating room, but they are bulky, constrictive, and place temperature

reducing “ice-packs” in an ineffective and wasteful fashion (Polar Products). Other vests have a fluid flow component, but do not exchange thermal energy in strategic locations, which can cause large temperature fluctuations in core body temperature, creating further discomfort for the user (Cincinnati Sub-Zero Products, Inc.; Hamilton Sustrand Corporation). Additionally, these systems are extremely costly and must be re-sterilized between uses, so the need for a cost-effective and disposable system is clearly demonstrated.

1.3. Project Description

The objective of this project is to create a component of a LCWG that incorporates customizable cooling reservoirs into a “Multi-Zone Cooling/Warming Garment” as similarly described in its US Patent (Koscheyev, et al.). This technology was revised to expand and adapt to other tasks in a different application from its intended, aeronautical use. The novel portion of this project is the newly developed fluid channel system (FCS) that can be attached to existing protective garments to cool or warm targeted parts of the body in a compartmentalized fashion. The FCS can be adjusted for anthropometric variations and user preference. The idea to use a Mylar®-constructed suit attachment was based upon: its light material weight, extreme thermal and chemical resistance, ease of sealing and great adhesion properties. The material in the FCS is both puncture and tear resistant (Andritz Group). The FCS is a channeled garment of fused Mylar® that has 3D printed materials as the structural basis for valves that connect to fluid inlet and outlet ports. The new low-profile valve design allows for fluid-flow throughout each high-density zone.

This cooling flow in specialized patterns allows for cooling distribution among high-density tissues that allow for exudation of heat from the body (Koscheyev, et al.). High density tissues are defined by Koscheyev, et al. as areas of the body that are in close proximity to large bony structures, have low fat deposits, and/or have large amounts of vasculature.

When discussing a connection system to integrate the fluid-flow between different high-density tissue areas in these Mylar® constructs, valves from wine and beverage dispensers are of particular note (Nielsen). Several of these designs have a sleek, low profile valve (referred to as a “Butterfly Valve”), which prevents puncture of thin-film bags (De Muinck and Sondaar). When combined with the Mylar® in the FCS, there is minimal impact on task performance, a key design parameter.

1.4. Proof of Concept:

In order to establish a proof of concept, the Deltoid muscle group of the acromial and deltoid regions has been chosen for design iterations and materials testing. This determination was made because it is typically a high use muscle group for upper extremity tasks. Additionally, scaling design iterations for other regions of the body can be easily achieved.

Several channel design iterations have been created to examine the most effective fluid-flow between the two sheets of Mylar®. In order to prevent fluid buildup, high pressures leading to rupture of the garment, or impairment of upper-extremity tasks, several important design parameters were taken into consideration. Particular care was taken to avoid sharp, 90-degree corners in the sealed fluid flow patterns, because these

can cause pressure buildup with stagnant fluid pockets (K. H. Beij). Furthermore, reproducibility and manufacturing considerations are especially important for consistent reservoir sealing and fluid flow.

Another area of interest for this particular project was the development of a sealing system that allows for a reproducible fluid channel system (FCS) that can be attached to different portions of the user's personal protective equipment (PPE). To allow for a consistent flow channel dimension and a consistent cooling effect, a "sealing press" was developed for this application. The method for sealing a biaxially-oriented polyester film has also been well studied and patented (Bassett et al.).

An appropriate design was established for the deltoid area, a valve system to allow for low-profile fluid flow was developed. This is a critical step in allowing the incorporation of this system into existing technologies and not disrupting the user's range of motion and/or ability to complete tasks.

1.5. Assumptions and Limitations:

Throughout this experimentation it is noted that the acromial and deltoid region is a high-density tissue area that can be temperature-controlled to prevent upper-extremity fatigue. The heat transfer properties of this region are extremely complex, particularly with the large movements of this muscle group that some workers and athletes may experience, particularly those performed in orthopedic or laparoscopic surgeries, assembly line work, repetitive motions in office settings, and exercise conditions. This is a particularly necessary region of the upper extremity that could benefit from this localized cooling effect. It has been demonstrated through preliminary work that the

design of this individually- sealed channeling system can be modified to any particular high density zone throughout the body such as (but not limited to): lumbar, sural, antebrachial, and scapular regions. The particular channeling design can also be modified to accommodate larger (or possibly smaller) fluid volumes to attenuate more targeted heat transfer to a desired region.

1.6. Operational Definitions

Average seal strength – average force per unit width of seal required to progressively separate a flexible material from a rigid material or another flexible material

Burst strength – a measure of the internal pressure necessary to rupture a package or seal.

Comfort – self-reported measure of a worker’s ability to perform their tasks without a marked increase in difficulty. This is individual-dependent and based on a number of factors such as: ambient temperature, body position, and duration of task.

Dwell Time - time materials are held in the press to seal or fuse materials. Dwell time ranges from 10 to 30 seconds for materials used in this project at press temperatures of 150° C.

Fatigue – physiological fatigue, which can result from extended periods of muscle exertion, large temperature increases, and can impair judgment and physical abilities. This is different from pathological fatigue, which can be observed in many neurodegenerative conditions (ALS, Parkinson’s, Multiple Sclerosis) as a symptom of a medical condition.

Heat seal – the result of bonding surfaces by controlled application of heat, pressure, and dwell time.

High-Density Tissues – Areas of the body that are in close proximity to large bony structures, have low fat deposits, and/or have large amounts of vasculature.

Liquid-Cooling-Warming-Garment (LCWG) – A device that allows for fluid-flow to heat and cool a user’s body in order to improve their performance at a specific task and maintain their self-reported level of comfort.

Maximum seal strength – maximum force per unit width of seal required to separate progressively a flexible material from a rigid material or another flexible material, under the conditions of the test.

Mylar®™ - Biaxially-Oriented Polyethylene Terephthalate (BOPET); A polyester film used in numerous food packaging, electrical, and insulating applications.

Seal integrity – (1) characteristics of the seal that ensures that it maintains label claim(s), acceptable quality, and adequately contains the product; (2) characteristics of the seal, which ensures that it prevents the ingress of microorganisms under specified conditions.

CHAPTER 2: REVIEW OF LITERATURE

II.1. Impact of Temperature on Task Performance

A major contributing factor that needs to be considered when performing repetitive motor tasks is the effect of temperature. There is strong evidence to show that temperature has a significant impact on task performance both physically and cognitively, particularly in environmental conditions above 90 degrees Fahrenheit and below 50 degrees Fahrenheit (Pilcher, et al. 682-698). This application can be applied to a wide range of performers in these extreme temperature environments, for example in manufacturing, healthcare and athletics.

Pilcher, et al. performed a meta-analytic review of 23 studies on the effects of temperature on performance in adverse task conditions. They were able to determine that there was a significant decrease in task performance in both hot-and-cold temperature conditions (Pilcher, et al. 682-698) with other factors considered such as: task duration, “pre-conditioning” to temperature conditions, and type of task being performed. An aggregate of these results can be seen (Figure 1), with average percent difference compared to neutral temperature ranges. The temperature ranges can be found aggregated (Table 2) based on Wet Globe Bulb Temperature (WGBT), a quantitative measure of heat stress that takes environmental temperatures and other factors into consideration. This was first invented by the United States Military as a means of prevention of heat illness and takes radiant heat exposure, air temperature, and wind speed into account (Budd 20-

32). If the temperature in the respective study was not reported in WGBT, it was converted using the following equation, with Effective Temperature (ET) measured as the environmental temperature (Pilcher, et al. 682-698): $WGBT = (ET - 13.1) / 0.823$

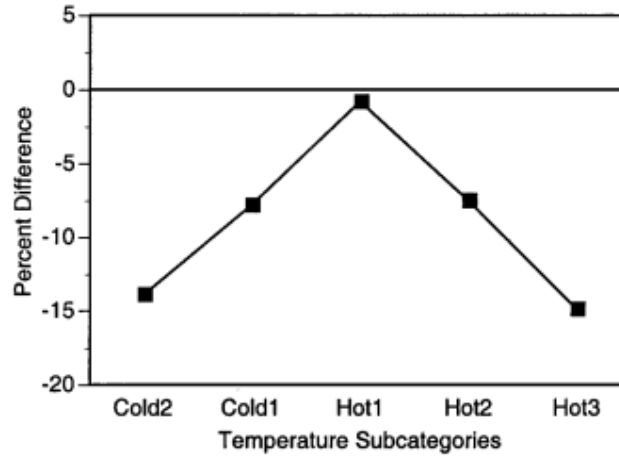


Figure 1: Percent reduction in task performance based on temperature subcategories. (Pilcher, et al. 682-698)

Temperature Subcategory	Temperature Classification Range, WGBT
Cold2	< 50°F (10°C)
Cold1	50-64.9°F (10-18.28°C)
Hot1	70-79.9°F (21.11-26.62°C)
Hot2	80-89.9°F (26.67-32.17°C)
Hot3	≥90°F (32.22°C)

Table 1: Temperature subcategories and corresponding temperature ranges in WGBT. (Adapted from Pilcher, et al. 682-698)

From the data collected by Pilcher, et al., it was confirmed that the largest detriments in performance occurred under the coldest conditions (13.91% average) and hottest conditions (14.88% average). Extrapolated over the course of entire shifts, these can lead to dramatic decreases in productivity. Particularly for workers in these extreme conditions, a method of temperature modulation is absolutely critical.

II.2. Muscle Fatigue

It has long been speculated that there is a relationship between muscle fatigue and task impairment, particularly with repetitive movement tasks. There is further evidence to suggest that muscle fatigue could be a contributing factor to task impairment in high temperature conditions (Pilcher, et al. 682-698).

Repetitive movement disorder (RMD) is a chronic overuse condition affecting muscles, nerves, and/or joints leading to inflammation and pain (Fuller, et al. 1043-1052). This is seen particularly in movements that cause prolonged or high resistance loads in upper-extremity muscle contraction. Fuller et al. noted that repetitive muscle use generally leads to reduced functional capacity of that muscle, commonly referred to as fatigue. Additionally, postural muscle fatigue increases postural sway, suggesting that motor control centers are affected by the fatigue of these muscle groups in long-duration quiet standing (Corbeil, et al. 92-100). Both repetitive tasks and static positioning can affect muscle fatigue, thus demonstrating the need for fatigue-reducing intervention methods as specific as physiologically based, targeted cooling.

II.2.1. Surgical Tasks

The term Surgical Fatigue Syndrome (SFS), which is marked specifically by mental exhaustion, reduced dexterity, increased irritability and impaired judgment, tends to occur after four uninterrupted hours in the operating room (Cuschieri 9-19). Although this is one particular time frame for SFS to occur, environmental factors such as ambient temperature, evaporative cooling effects, and airflow in the operating room can affect this time scale. Particularly in laparoscopic surgeries, the ergonomically unfavorable stances and arm positioning can be a major factor leading to this condition (Cuschieri 9-19; Berguer, et al. 466-468; Galleano, et al. 329-333). Cuschieri went on to suggest in his review of the Whither Minimal Access Technique that a “teamwork approach” or the use of prolonged rest periods might be able to mitigate the effects of SFS (Cuschieri 9-19). However, this may lead to increased surgical time and cost, additional time under anesthesia for the patient, and more hospital resources being consumed for each surgery. The use of other interventions to prevent SFS is of great necessity.

Berguer et al. found that EMG activity in the thumb and forearms of the surgeons had significant increases in both peak and total muscle effort (Berguer, et al. 466-468). This work suggests that laparoscopic surgeries were much more taxing on the surgeon’s key, engaged muscle groups compared to typical open surgeries that may be more biomechanically and ergonomically favorable. Galleano et al. suggested that the use of armrests in this type of surgery may be beneficial to increase physician comfort and task efficiency but showed no significant decrease in surgical task time (Galleano, et al. 329-333) (Figure 2). The abduction of the shoulders in particular is a “stressed” position that can cause prolonged contraction of the deltoid, scapular, and acromial muscle groups.

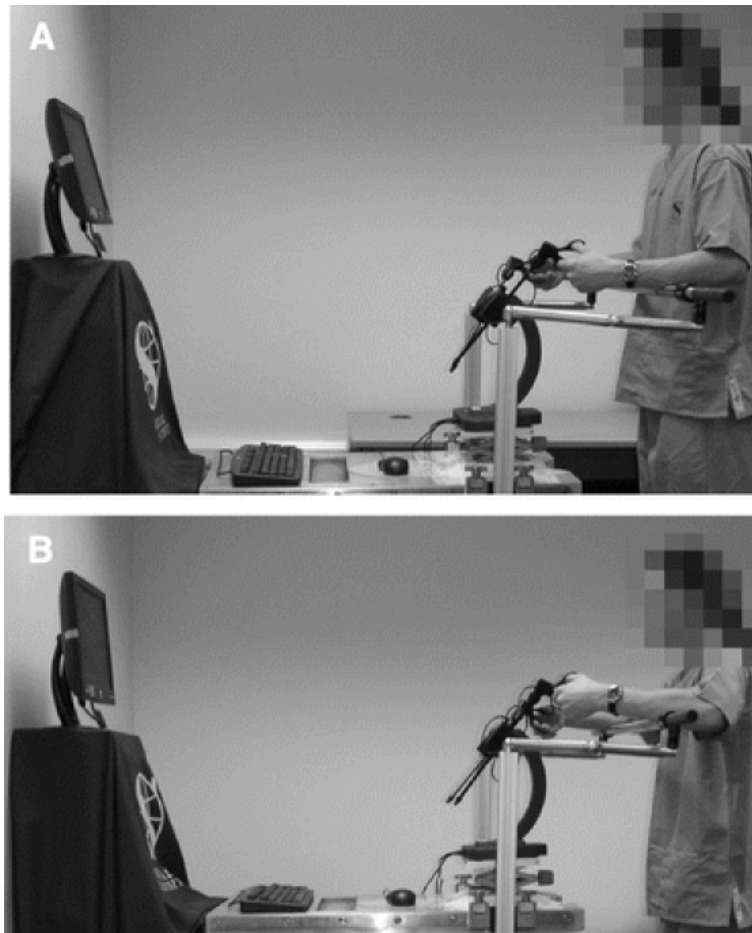


Figure 2: Simulated Laparoscopic Surgical Tasks on a Lapsim Trainer a) with arms in “ideal” posture, and b) arms in “elevated” posture. (Galleano et al. 329-333)

Maffiuletti and Lepers took a survey of 38 orthopedic surgeons to demonstrate the impact of muscular fatigue on a surgeon’s typical day. 84% of surgeons classified some form of muscular fatigue consecutive to an operative day with the back and lower extremity muscles being particularly affected (Maffiuletti and Lepers). Slack, et al. studied the effects of operating time on muscular fatigue compared to 20 control subjects performing deskwork and showed a significant increase in muscular fatigue in an 8-person ENT surgical group (Slack, et. al 651-657).

Fatigue has been correlated with a mean shift in the frequency of muscle contraction to lower frequencies (Roman-Liu, et al. 671-682; Dimitrova and Dimitrov 13-36). The mean decrease in EMG frequency was shown to be significantly greater (1.6x) in the brachioradialis than the mid-deltoid, but the noted decrease in frequency in both groups suggests an increase in the fatigue of surgeons vs. control (Figure 3).

Interventions suggested by the group to mitigate the effects of this fatigue include: performing complex or fatiguing tasks towards the beginning of procedures, taking breaks during long-duration operations, and offering a change of surgeons when fatigue begins to affect surgical performance (Slack, et al. 651-657). More practical measures are necessary to mitigate this fatigue to prevent disruption of operating time or cost.

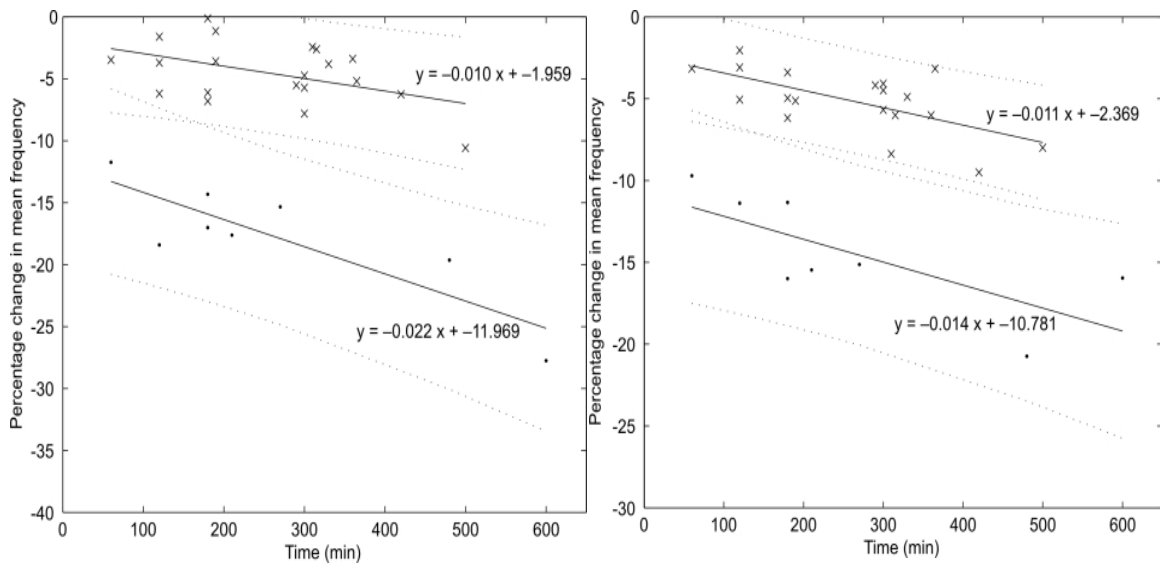


Figure 3: Percentage change in mean frequency of Brachioradialis (Left) and Mid-Deltoid (Right) contraction. Linear regression with 95% confidence interval in control groups (top lines) and surgical groups (bottom lines) (Slack, et al. 651-657).

II.2.2. Industrial and Manufacturing Tasks

Particularly seen in the manufacturing and food services industry, repetitive motion tasks can lead to increased fatigue and pathological conditions for workers. Work-related overuse injuries cause significant cost for manufacturing and industrial companies in both healthcare-related and lost-production capacities. However, lack of movement in lower-extremities can also lead to a significant increase in muscle fatigue, with corresponding psychological fatigue (Halim, et al. 31-42). A study of occupational hazards found that static postures, repetitive arm movements, working with hands above shoulder height, and direct load bearing to be particular causes of Cumulative Trauma Disorders (CTDs) in the soft tissues of the shoulder region (Sommerich, et al. 697-717). Shoulder abduction was a particularly telling risk factor for the presence of Occupational Cervicobrachial Disorder (OCD) in repetitive movement tasks (Kilbom and Persson, 273-279). A preliminary study performed by Kilbom and Persson identified key risk factors and consequences for ergonomically unfavorable work conditions in the manufacturing industry. They found that long-duration flexing of neck and upward extension of arms led to a significant increase in shoulder injury at both one and two years follow up (Kilbom and Persson, 273-279).

Halim et al. analyzed both psychological fatigue via an occupational survey and quantitative muscular fatigue via surface electromyograph (sEMG) in assembly-line production workers. Although not to significance ($p < 0.05$) for all muscle groups, there was a positive correlation between perceived psychological fatigue and sEMG muscle fatigue. Additionally, functional time to fatigue in these groups was dramatically

decreased as the day went on, leading to decreased performance later in work shifts for both metal stamping and handwork operators (Figure 4) (Halim et al. 31-42).

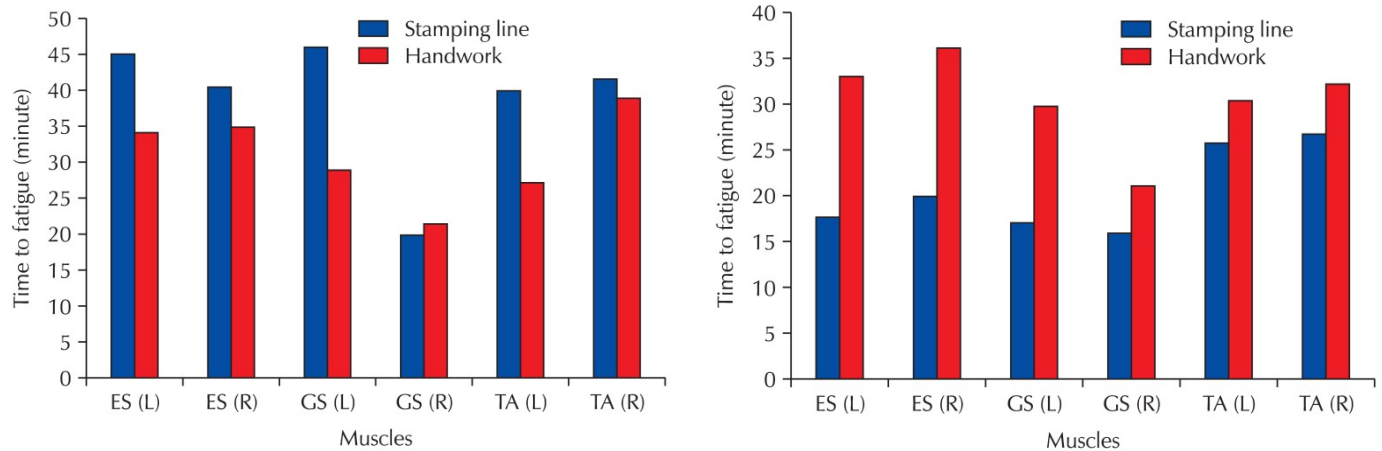


Figure 4: Time to Fatigue for selected muscle groups at beginning of day (left) vs. end of day (right). (Halim et al. 31-42)

Nur et al. analyzed the correlation between production standard time and muscle fatigue rate for industrial assembly-line workers. At each respective speed, average time to fatigue was measured with surface EMG measurements quantifying a 15% Maximum Voluntary Contraction (MVC) decrease as “functionally fatigued”. This corresponded with a shorter time to fatigue as the time to produce products became more difficult (Nur et al. 2323-2326).

II.2.3 Athletics Applications

A vast area of consideration that must be addressed for performance detriments due to muscle fatigue is athletics. Many studies have shown a quantitative decrease in performance with muscle fatigue conditions in baseball (Tripp, et al. 90-98; Erickson, et al. 762-771), basketball (Montgomery, et al. 1135-1145) and soccer (Rampinini, et al. 227-233). Furthermore, research has shown that overall proprioception shows quantitative decreases due to muscle fatigue (Carpenter, et al. 262-265), which could affect athletes as well as other individuals.

Tripp, et al. investigated the affects of functional fatigue on the arm positioning in baseball throwing experimentation. They used 3-dimensional variable error (3DVE) scores, to quantify the differences in 3-dimensional position in both pre-and-post fatigue conditions. Fatigue significantly increased the 3DVE error scores and correlates with a significant change in arm positioning that could lead to injury, poor biomechanics, and decreased performance. (Tripp, et al. 90-98) (Figure 5). Erickson, et al. in their study of adolescent pitchers, further demonstrated this biomechanical breakdown. They showed significant increases in fatigue, pain, and decrease in velocity with increases in pitch count (Erickson, et al. 762-771). These measure are indicative of fatiguing muscles and compensation to keep performance consistent with increasing pitch count.

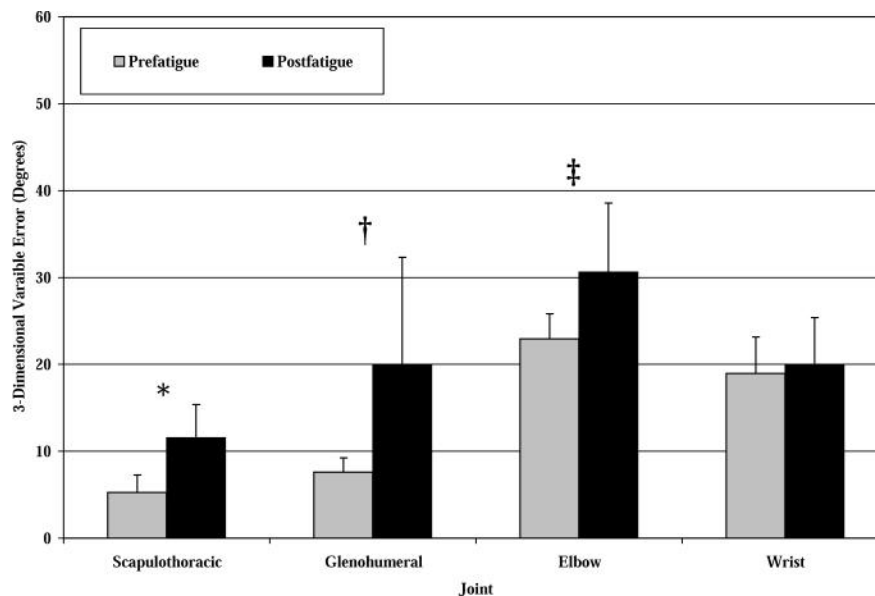


Figure 5: Pre-fatigue and post-fatigue 3DVE differences (degrees) based on joint. (Tripp, et al. 90-98)

Basketball athletes were also shown to have a quantitative performance deficit in muscle fatigue conditions. Montgomery, et al. looked at muscular fatigue not only over the course of individual games, but the cumulative affects that fatigue can accrue during several games in short succession. Players who used cold-water immersion and compression showed an average improvement of 1.5% in line-drill tests over just three days of fatigue (Montgomery, et al. 1135-1145). Interesting results were found by Rampinini, et al. in terms of athletes from teams of varying levels of success in professional soccer. This group found that players from less successful teams completed significantly more physical work than the players from more successful teams. Less successful team's players displayed more total distance covered (+4%), "high intensity running" (speed > 14 km/h) (+11%), and "very high intensity running" (speed >19km/h) (+14%). This correlated with higher involvements with the ball, short passes, successful

short passes, tackles, dribbling, shots and shots on target in the more successful group (Rampinini, et al. 227-223). Carpenter, et al. demonstrated the affects of muscle fatigue on proprioception relationships in the shoulder joint. A 73% increase in rotational motion was seen before perception of motion in a post-exercise condition (Carpenter, et al. 262-265), which is indicative of a lower degree of proprioception. This significant increase in motion can lead to injury, lack of positional awareness, and lack of ability for task completion in fatiguing exercise conditions.

II.3. Physiological Tremor

A physiological tremor can be defined as involuntary neuromuscular movements with no clinical significance and can be correlated with numerous conditions including: anxiety, withdrawal, and physical exhaustion (Jankovic and Stanley, 460-465). There is a body of evidence to suggest that involuntary movement of skeletal muscle groups can be exacerbated by individualized muscle fatigue and can cause significant hindrance to task performance (Slack et al. 137-141; Hsu and Cooley, 323-327). Particularly with fine motor activities necessitated in healthcare, industrial, and manufacturing capacities, a physiological tremor can lead to significant health and safety issues for workers.

Morrison, et al. directly demonstrated the correlation between muscle fatigue and physiological tremor. There was an observed increase in both limbs' finger tremor although only one limb was exercised, suggesting that there is a bilateral effect on unilateral exercise (Morrison, et al. 609-621). The task-specific nature of physiological hand tremor was investigated for surgical applications by several studies (Hsu and

Cooley, 323-327; Slack, et al. 137-141). Slack, et al. was able to show that there was a 8.4-fold increase in surgeon's hand tremor vs. control groups over an entire workday (Slack, et al. 137-141). This shows that the detail and precision that is required of surgery-specific tasks can lead to a particularly high level of physiological tremor as the day goes along. Although there was only a slight increase from 1.305 +/- 0.581 mm to 1.818 +/- 1.078mm in average hand tremor amplitude preoperatively to postoperatively, the tip of the surgical instrument will show proportionally greater amplitude of tremor (depending on the length of the instrument) (Slack, et al. 137-141). Hsu and Cooley further quantified the affects of exercise on hand tremor in microsurgical applications. There were significant increases in time spent outside of the target ($p < 0.02$ for both upper-body and aerobic exercise) and total number of excursions from the target ($p < 0.02$ for upper-body exercise; $p < 0.01$ for aerobic exercise). There was a noted, but not significant increase in both conditions after 2 hours post exercise.

A literature review found a lack of quantitative studies on the affects of physiological tremor in other applications beyond surgery. However, the fine motor movements and sustained muscle activity seen in other tasks (athletics, manufacturing, food services, etc.) could exacerbate the affects of physiologic tremor on performance.

II.4. Cooling Interventions

As seen in the prior art, the impacts of muscle fatigue and resulting conditions (psychological fatigue, postural imbalances, RMDs, and physiological tremor) necessitates interventions beyond those ordinarily seen in healthcare and industrial

applications. Several sources suggest the use of a “shift work approach” to mitigate the effects of muscle fatigue and finger tremor (Berguer, et al. 466-468; Cuschieri 9-19; Galleano, et al. 329-333; Halim, et al. 31-42; Nur et al. 2323-2326) but these are impractical due to cost and time constraints. Others suggest periodic breaks and doing particularly detailed tasks early in workdays (Cuschieri 9-19; Nur et al. 2323-2326; Slack, et al. 651-657) but these would also increase costs and scheduling issues in many industries. Therefore, other methods of intervention to reduce subject fatigue and mitigate performance losses must be investigated. Based on the significant findings that temperature can also play a role in performance decreases (Pilcher, et al. 682-698) and the effects that temperature modulation can have in improvement of exercise performance (Bongers, et al. 377-384), the use of temperature modulation is a particularly novel approach to prevent task performance decreases.

Healthcare and manufacturing techniques can be extrapolated into a form of low-intensity, long-duration exercise; therefore the positive benefits of cooling interventions can be used to prevent muscle fatigue and performance decreases in these applications that are generally reserved for just athletic areas. Several studies have shown the positive impacts of cooling interventions to increase performance (Jensen, et al. e126-e130; Lakie, et al. 35-42; Stevens, et al. 829-841).

Lakie, et al. was able to show the positive impact of a cooling intervention to decrease the amplitude of physiologic tremor in their study measured via sEMG. They immersed one arm in cool water for 5 minutes and saw a striking reduction in tremor amplitude as well an increase in amplitude under similar warm water conditions. The authors note that the size of muscle twitch has a direct relationship to temperature: the

higher the temperature, the stronger the muscle twitch force (Lakie, et al. 35-42). This is indicative of the physiological response of the human muscle fiber to temperature and that cooling interventions are necessary to mediate this response.

Jensen, et al, demonstrated the impacts of cooling interventions in surgeons to prevent fatigue and decrease physiological hand tremor. This group looked at the efficacy of cooling interventions in increasing the functional time to fatigue and decreasing the physiologic hand tremor observed in a post-exercise condition. Both novice (surgeons with less than 5 years experience; maximum age of 35 years old) and experienced (surgeons with greater than or equal to 10 years experience; minimum age 50 years old) groups were tested in this experimentation. The participants were asked to flex and extend their dominant wrist with a 5lb weight until they reached the point of functional fatigue: where they could no longer maintain range of motion within 10 degrees of their baseline measure. They were then asked to complete a suture experiment with corresponding tremor measured at completion of five continuous running sutures. When observed with a cooling intervention, there was no significant decrease in hand tremor for the novice cohort, but a significant decrease in physiologic tremor for the experienced surgeon ($p < 0.05$). Furthermore, a positive correlation was seen in both an increased functional time to fatigue (Figure 6) and decreased suture time (Figure 7) for both experimental groups with initiation of a cooling intervention (Jensen, et al. e126-e130). This suggests that for all groups (for the experienced group especially), there is a benefit to targeted cooling interventions to prevent the effects of fatigue and increase functional capacity in specific tasks.

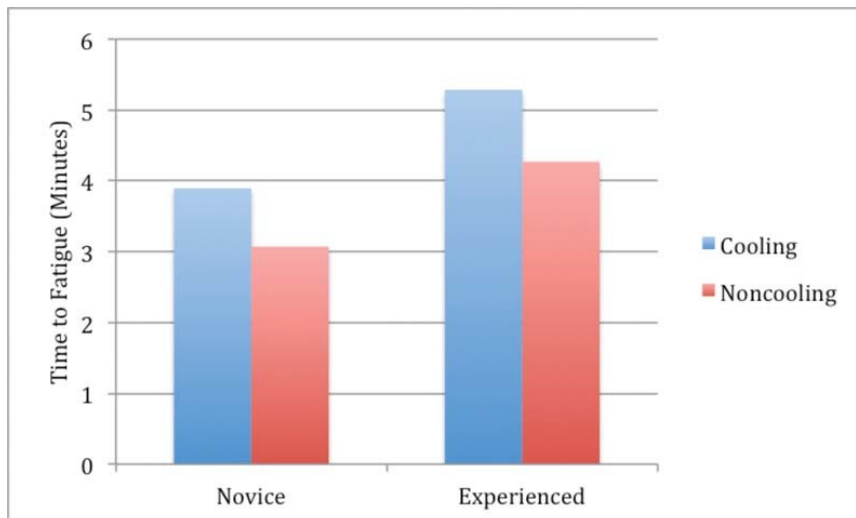


Figure 6: Time to Functional Fatigue after Exercise in Novice and Experienced Cohorts with and Without Cooling Intervention. (Jensen, et al. e126-e130)

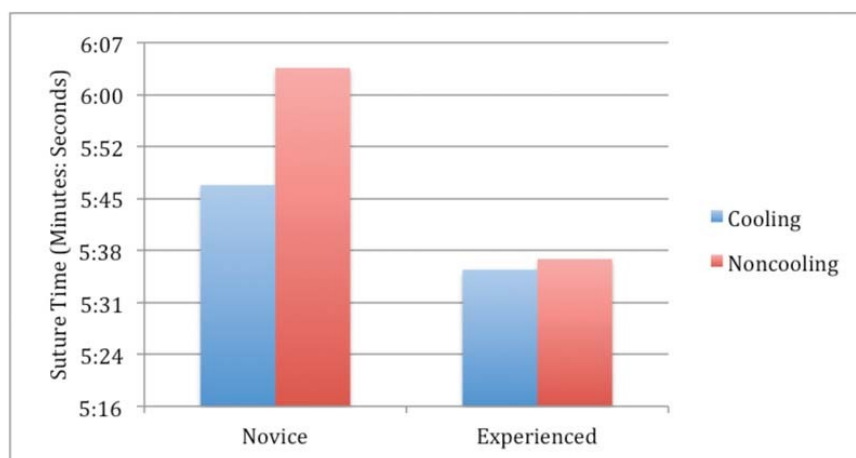


Figure 7: Suture Experiment Time after Exercise in Novice and Experienced Cohorts with and Without Cooling Intervention. (Jensen, et al. e126-e130)

There is further evidence to suggest that cooling interventions applied during a task (mid-cooling) as opposed to before the initiation of the task (pre-cooling) may be more effective in allowing for sustained performance. Stevens, et al. attempted to elucidate a correlation between performance improvements and cooling modalities (ice

packs, ice slurry ingestion, menthol sprays, and torso cooling garments) applied at different intervals both pre-and-mid-exertion. They suggest that there are several ways by which heat affects performance. The central nervous system's biochemical pathways and psychophysiological components (perceived effort and comfort) are of particular interest in the application of mid-exercise interventions. Furthermore, they discuss limitations of particular mid-cooling interventions such as regulations against interventions in sports performance, the limited studies on "elite" athletes, and the cost-benefit relationship of added weight during competition (Stevens, et al. 829-841).

Eijsvogels, et al. in their study of master's runners (42 +/- 10 years), also saw a mid-cooling intervention's effectiveness. Subjects were asked to run a 5-km time trial on a treadmill at 25 degrees C with and without a cooling intervention. They were able to demonstrate quantitatively that the use of a cooling vest significantly decreased participant heart rate, decreased skin temperature and improved thermal comfort over all control trials (Eijsvogels, et al. 840-846). Limitations in the use of a torso-cooling apparatus are discussed in II.4.2.

Several sources note that there are rules preventing the use of some systems in individual sports such as cycling, but other sports (such as certain running governing bodies) do not have specific prohibitions for these types of systems (Eijsvogels, et al. 840-846; Stevens, et al. 829-841) and they are in widespread use in sports such as auto racing. There are also no limitations on the use of these interventions in training and could help lessen the affects of muscle fatigue and high heat on performance during long-duration exercise. Further evidence also suggests they can prevent overuse injuries in a similar fashion (Eijsvogels, et al. 840-846).

Although there may be noted limitations in athletics applications, these would have no bearing on the efficacy of a similar system for industrial or healthcare workers. The sub-maximal “exercise” conditions of repetitive movement tasks could still see benefits from this per-cooling intervention.

II.4.1. Ice-Pack Method

Current technologies for the cooling of healthcare, industry, and athletics professionals do exist on the market. One preferred cooling method is the use of ice-pack vests or garments that use frozen liquid to cool large regions of the user’s abdomen and torso. Many limitations with this method are evident.

As seen with the CoolOR Zipper Vest with Cool58 Packs (Polar Products, Inc.) ice packs are distributed in a vest system to be worn under personal protective equipment (PPE) for healthcare professionals (Figure 8). These vests carry with them several key limitations. First, they are extremely expensive at \$200 per vest, with \$100-\$200 for additional ice packs. Next, they impart a large amount of added weight to the user (between 4-7.5 pounds for icepacks alone). Ice packs need be changed periodically (after approximately 3 hours) in surgical and sterile work environments, which can cost time and cause inconvenience to users. Finally, it is difficult to control large temperature fluctuations as the manufacturer suggests modifying number of layers worn beneath the garment as a way to control temperature (Polar Products, Inc.).



Figure 8: CoolOR Zipper Vest with Cool 58 Packs. (Polar Products, Inc.)

Cleary, et al. studied the efficacy of this specific product in their study of American Football athletes. This group was subjected to 60 minutes of intense duration exercise (outdoors; in the sun) and 30 minutes of recovery (outdoors; in the shade) both with and without the use of cooling interventions. This experiment was able to show several critical things about the use of cooling interventions for task improvement and recovery. There was a significant decrease in perceived exertion scale rating, perceived thirst scale rating, and other qualitative comfort measures (Cleary, et al. 792-806), however there was no significant difference in cooling vs. non-cooling in cardiovascular responses, core temperature, and other performance metrics. These findings show that sensation of heat was improved, but quantitative athletic performance was not improved in this application. The authors also stated that several of the participants noted that the vest “lost some cooling capacity” as the duration of the experiment wore on. They further note that prior literature noted the decrease in nerve conduction velocity with the application of cold-water immersion and ice packs (Cleary, et al. 792-806). The

application of icepacks showed a significant decrease in sensory and motor neuron conduction velocity by 31.9% and 4.2%, respectively (Herrera, et al. 581-591). This sensation and motor loss could be particularly dangerous in the targeted applications of LCWGs for task-based work in industry and healthcare. Injury can occur to the worker or others if they do not have sensation or lose motor function abilities in the highly specified industrial and healthcare settings. In addition, there are numerous studies that demonstrate the lack of consistency and effectiveness of icepack cooling methods. The thermodynamic properties of heat exchange are particularly complex, with combinations of conduction, convection, and evaporation all playing key roles (Merrick, et al. 28-33) and are not fully understood for individual cooling modalities.

Merrick, et al. attempted to elucidate correlations between different cooling modalities and temperature exchange areas in human tissues. This group tested wet ice, icepacks, and a cool gel (commercially available as “Flex-i-Cold”) all against a control group. They found that there was significantly better heat exchange in cooling modalities that underwent a phase transition during the course of their treatment application (i.e. melting). This however was only seen at a relatively shallow 1cm-subadipose tissue, with the 2cm-subadipose tests showing no significant difference between modalities (Merrick, et al. 28-33) (Figure 9). One particular flaw with this study was that the group was operating under the assumption that the coldest modality (one that produced the most temperature change) is the best for cryotherapy. Although this may be true post acute injury (Merrick, et al. 241-245), this is not necessarily true post-exercise or post muscle fatigue. The inflammatory responses seen after acute injury have shown to be mitigated by the implementation of cryotherapy (Merrick, et al. 241-245), but the level of

inflammation in a post-exercise condition is difficult to quantify. Thus, the beneficial results of these cryotherapy methodologies are difficult to extrapolate to post-exercise conditions.

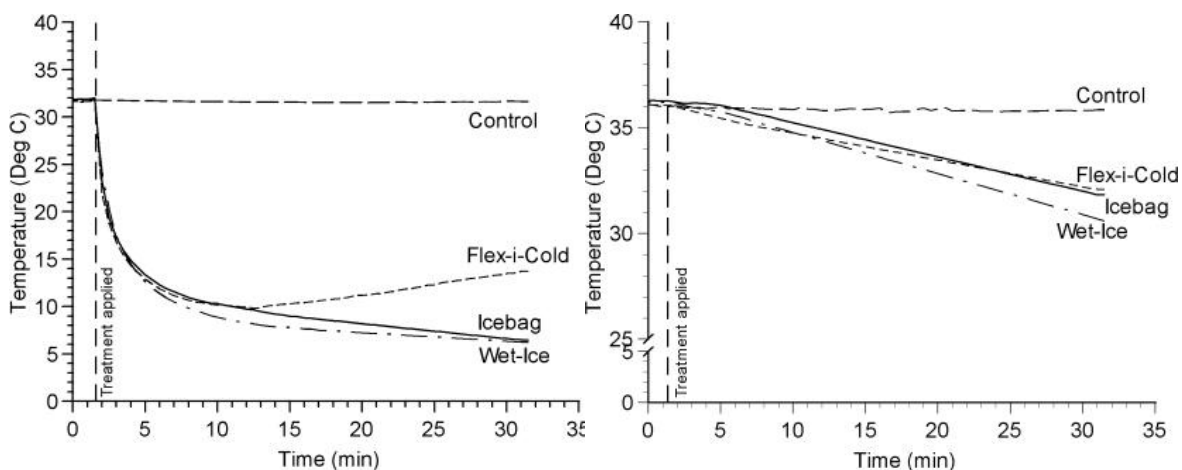


Figure 9: Surface (Left) and 2cm subadipose (Right) temperature vs.time. (Merrick, et al. 28-33)

Another particularly important factor noted by Walton, et al. was the large variability of measurements taken on different muscle groups on different subjects. Although they used sheep in their study of the penetration depth of icepack treatments, they noted that even in the same individual animal, “readings from different limbs were rarely identical”, even with the same treatment parameters (Walton, et al. 294-300). This shows the wide anatomical and treatment variations that can occur with the application of icepacks, rendering them an ineffective and inefficient method of providing a targeted cooling affect. Human studies have shown similar results, with wide anatomical and

physiological differences in temperature decreases with application of cold treatment (Hartviksen, 79-84; Reader and Whyte, 396-402).

II.4.2. Liquid-Cooling-Warming Garments

An additional method of providing cooling relief to task-oriented individuals is the use of Liquid-Cooling-Warming Garments (LCWGs) that use temperature controlled fluid (i.e. water, saline, or air) to cool the user. These systems have been shown to provide a qualitative comfort improvement, however the literature is mixed in the efficacy of some of these systems.

Eijsvogels, et al. suggest that although a torso-cooling apparatus like the one used in their study is effective in decreasing localized skin temperature, there are several key factors that limit the efficacy of this type of system. They note that there was no significant performance improvement or decrease in core body temperature seen in athletes with a cooling intervention applied (Eijsvogels, et al. 840-846), although a decrease in core body temperature would provide more performance benefit in long-duration aerobic exercise than in industrial and healthcare applications. Homeostatic control mechanisms are absent in the individual limbs that are present in the central “core” of the body (Lakie, et al. 35-42). This is evidence that the physiological response to a decrease in core body temperature (shivering, less motor control, etc.) may cause the inverse effect and increase tremor size: rendering torso and full body cooling systems insufficient in the reduction of tremor amplitude.

Eijsvogels, et al. is merely a preliminary investigation of the efficacy of these systems for “per-cooling” (use during tasks) and another important factor noted in this

study was the temperature gradient between skin temperature and the cooling vest, which decreased significantly as the trial went on. This temperature gradient subsequently limited the cooling capacity of the vest and its use showed no increase in performance compared to the non-cooling intervention. Performance decreases in higher temperature conditions be mediated by such a cooling intervention, although there was no quantitative performance improvements in ambient conditions using full-torso cooling (Eijsvogels, et al. 840-846; Pilcher, et al. 682-698).

Filingeri, et al. directly studied the affects of “mild evaporative cooling” applied directly to the torso in heat-affected long duration aerobic exercise (Filingeri, et al. 200-210). This cooling modality is a type of LCWG that uses pre-wetted materials to cool a user through evaporation, greatly reducing the weight and increasing the wear-ability of garments. One drawback to this type of system is that it required this “pre-wetting” and would not be practical outside of aerobic exercise (running, cycling, etc.) due to the preparation methods necessary in healthcare and industrial settings.

Quantitative comfort measurements (perceived wetness, perceived exertion level) were combined with qualitative performance measurements (core temperature, skin temperature, heart rate) to show the affects of this cooling intervention applied both pre-and-during-exercise. There were similar effects of lowered local and mean skin temperature in both pre-and-during-exercise cooling, Interestingly, there were greater qualitative levels of comfort in perceived exertion as well as quantitative decreases in heart rate shown with the mid-cooling intervention (Filingeri, et al. 200-210).

Although many of the benefits of this mid-cooling intervention may be difficult to quantify, the comfort improvements for the athletes shows the benefit of these mid-exercise cooling interventions. They decrease perceived exertion and stave off many of the psychological affects of high temperature conditions. Furthermore, although core body temperature may not be sufficiently reduced with cooling interventions, the symptoms and effects of a rise in core body temperature can be mitigated with the use of such cooling systems.

II.4.3. Cooling Garment Prior Art

Vast prior art exists in the arena of cooling systems intended to increase performance, particularly for industrial and healthcare applications. Several of these methods and technologies are discussed herein and their different modalities are evaluated. This is by no means an exhaustive list, but gives an indication of some technologies previously developed.

The “Medical Cooling Vest and System Employing the Same” created and patented by W. Clark Dean is a medically specific system to cool healthcare workers under their Personal Protective Equipment (PPE). This vest attempts to provide several safeguards against puncture and leakage with its use of ambient pressure technologies (Dean). This is however a torso cooling system that has shown limited efficacy in performance increases, with large temperature fluctuations, and uncertain outcomes (Eijsvogels, et al. 840-846; Pilcher, et al. 682-698). This system also adds an additional layer of material and is worn over other garments, which could counteract the intended cooling affect (Duke). Placing a barrier of a shirt (scrubs in this case) will further slow

evaporation and mitigate decreases in localized skin temperature. One important consideration with this methodology is their mention of the need for sterility of fluid (Dean), particularly important in healthcare and other sterile manufacturing arenas.

Another methodology uses conductive layers for electrical heating of specified heat-exchange areas. Dunning, et al. describe a “System and Method for Providing Even Heat Distribution and Cooling Return Pads” (Figure 10). This system uses electricity, which is great for generating heat and could be beneficial for their intended warming applications, but would be less efficacious in cooling techniques. They do mention a “cooling layer” but its intention is to cool the other layers, and not the contact area with the user (Dunning, et al.).

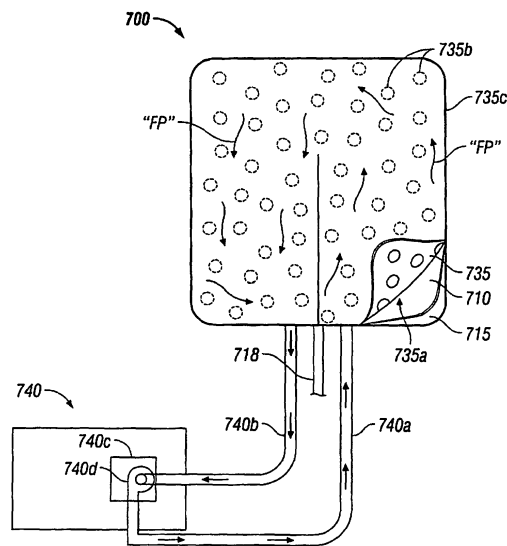


Figure 10: “System and Method for Providing Even Heat Distribution and Cooling Return Pads” (Dunning, et al.)

Another patent by Ellis, et al. discloses a personal warming system meant specifically for hospital settings. Several key factors are noted in this patent for the x-ray-procedure warming garment. This is another electrical heating element that is noted for its cost effectiveness, sterility, and controllability – things that are lacking in other systems in the hospital setting (Ellis, et al.).

An apparatus with broad-reaching implications is disclosed in “Body Heating/Cooling Apparatus” by Jenkins. This particular system is another torso vest that has a “flexible, continuous channel with a serpentine pattern throughout and also includes the mention of a pump to control fluid-flow. One limitation that is discussed specifically in the patent is that it is only rated “for as long as two hours depending on the selection of the materials and ambient temperatures” (Jenkins). This is an impractical and short length of time that is a limiting factor in its efficacy for industrial and healthcare applications specifically. A targeted cooling approach would also be more effective in providing longer-lasting cooling relief.

Other garments include a “Patient Temperature Control System with Variable Gradient Warming/Cooling” (Koewler), “Configured Pad for Therapeutic Cooling Effect” (Molloy), and “Apparatus for Controlling the Temperature of an Area of the Body” (Zacoi). Koewler incorporates that use of automatic sensing of temperature (and subsequent modulation without physician adjustment), Molloy specifies film thicknesses that are effective for effective heat transfer, and Zacoi uses a targeted cooling approach (Figure 11), all of which are factors that must be evaluated. These systems do have specific drawbacks that include bulky tubing systems, fluid-circulation issues, and heat

exchange ineffectiveness but portions of these are important prior art for design consideration.

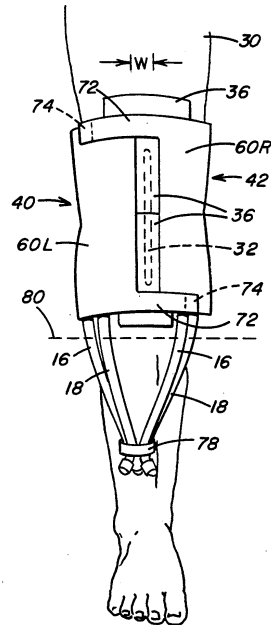


Figure 11: Targeted Cooling Apparatus for Lower-Extremity Cooling. (Zacoi)

II.4.4. Tube-Suit

Koscheyev, et al. from the University of Minnesota describes in their US Patent a “Multi-Zone Cooling/Warming Garment” that is much of the basis for this project (Figure 12). Its current use in aeronautics by NASA is easily adaptable (with slight modifications) to numerous manufacturing, healthcare, and athletics applications.

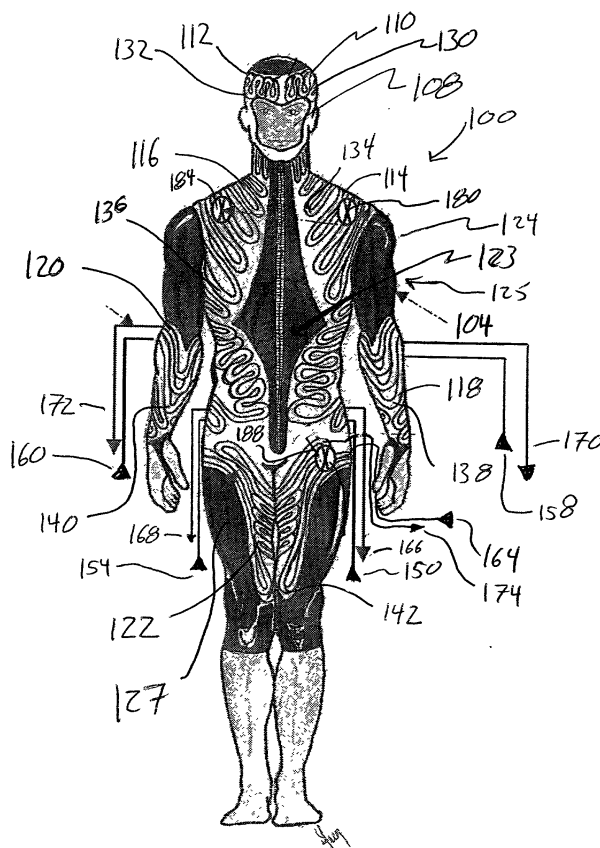


Figure 12: Tube-suit embodiment. (Koscheyev, et al.)

Several key design specifications and features of this product are detailed in this patent filing with particular emphasis on “High Density Tissues” that are the physiological targets of this temperature modification intervention. These tissues are found to have “superior blood vessel distribution, heat conductivity, and heat transport capability to and from the blood” (Koscheyev, et al.) which allows for this garment to be efficient in providing heat transfer. Another important factor they note is the ability to reduce weight and size of garments with this approach. The high vascularization of areas is also of particular importance in designing a physiologically relevant garment (Koscheyev, et.al) and helps to justify the choices of the deltoid and acromial regions of the shoulder seen later in our design. Of particular note are the subclavian, axillary,

brachial, and cephalic veins that run directly inferior and medial to the deltoid muscle group. The middle, posterior, and anterior deltoid are further of particular interest due to their large muscle bodies and proximity to the superficial skin surface which allows for the most efficient heat transfer (Figure 13). Coupled with the functional fatigue, physiological tremor, and injuries associated with these areas in repetitive upper motion tasks, the physiological basis for the design of our system is clearly demonstrated. The ability of the system to incorporate feedback mechanisms (temperature sensing, other biological parameters, etc.) and compensate accordingly is another important design aspect that could be incorporated into more effective garments.

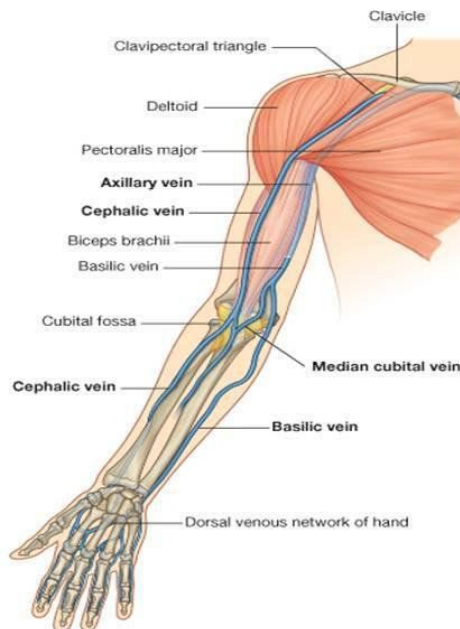


Figure 13: Proximal arm vasculature and muscle groups. (Cultua)

One obvious drawback of this system that is not addressed is the difficulty for manufacture of tubed garments and difficulty of incorporation into existing technologies. The PPE discussed in section II.4 necessitates full integration into prior art, as the tube-suit described by Koscheyev, et al. is an additional garment layer. Furthermore, the bulky tubing and connection systems could be seen as a hindrance to movement and performance in particular for repetitive motion, upper extremity movements.

II.5. Personal-Protective Equipment (PPE)

A key element in the development of a LCWG is a lack of disruption to current personal protective equipment (PPE) systems that are commercially available. Once the LCWG component can be incorporated into one particular application, its broader applications in many industries can be demonstrated. PPE exists in several industries for purposes discussed herein (Anderson, et al; Stackhouse, et al.; VanDerWoude; VanDerWoude and Campbell).

The Stackhouse Surgical Gown by Stackhouse, et al. is the gold standard used in orthopedic surgeries (Figure 14). It is made of barrier materials that prevent biological fluid contact with the wearer and is easily positioned on the shoulders, has a permanent face-screen for protection in the hood, and a rip seam in order to be quickly removed and disposed of (Stackhouse, et al.). An obvious drawback to this system is its bulk and covering of key heat-transfer structures in the human body. Over 40% of the body's heat is emitted through the head (Koscheyev, et al.) and is trapped in this system. Although there is mesh to allow for ventilation in the back portion of the gown, there is insufficient heat evacuation from this type of equipment.

component in the development of our system. This system is designed with patients in mind for both pre-operative and post-operative cooling/warming conditions (Anderson, et al.) but this concept can be extrapolated for other healthcare, manufacturing, and athletic applications.

II.6. Valve Design Prior Art

An additional design objective to be included in the Fluid Channel System (FCS) is valves that allow for fully integrated fluid flow between different high-density regions. Controlling fluid flow into and out of tubing and fluid channel systems can be problematic for a number of reasons. First, there can be impedance of fluid flow that can cause leakage and sterility issues, particularly in the medical realm. Next, the 3-dimensional profile of inlet and outlet valves can cause user discomfort. Finally, incorporation of inlets/outlets into thin-film materials (without significant use of adhesives) has proved particularly difficult in our experimentation.

Significant prior art for inlet/outlet valves exist in numerous applications including medical (Anderson, et al.; Brister), beverage dispensing (Bond and Ulm; De Muinck and Sondaar; Nielsen and Dige), and others (Hagihara; Smolko and Kevorkian). Although these are by no means a comprehensive list of prior art, important design considerations can be abstracted from aspects of these systems.

An “Interface for Use Between Medical Instruments and a Patient” discusses important aspects of sterility and safe interfaces between patients (Anderson, et al). This is an important consideration in healthcare (surgical and otherwise) and other manufacturing applications – the ability to prevent leakage and contamination resulting

thereafter. Although this deals with barrier materials between an ultrasound transducer and a patient, they also discuss the ability of the material to transfer HIFU heat energy for patient treatment (Anderson, et al.), which is something to take into consideration for targeted temperature control applications. In the realm of medical device connection systems, Brister describes the use of a “cylinder within a cylinder” connection system to incorporate connective fluid flow between regions (Brister). This is not a particularly simple application, but it does allow for a “push-fit” connection system between two different valves to allow for air to flow between tube and intragastric device (Brister). The “push-fit” would allow for easy access and setup of the system and is a particularly novel way to prevent fluid leakage from inlet/outlet connections. This is a design consideration that was most certainly taken into account.

Solutions for fluid packaging have evolved significantly over the decades, however advancements in fluid packaging for thin film materials offer key design criteria that were considered in our system. The beverage dispensing “Bag-In-A-Box” (BIB) system valves described by both Bond and Ulm and Nielsen and Dige are particularly intriguing for our design intent. They are integrated with thin-film materials to allow uninterrupted flow between bladders of material and outside. They also feature a “puncture” system to allow for dispensing to start (Bond and Ulm; Nielsen and Dige). With modification, a valve that is extremely sleek with a low profile could have substantial benefits when incorporated into the FCS. The “low profile” valve system is also seen in the “Butterfly Valve” patented by De Muinck and Sondaar and guides a key design requirement: simple integration into the thin-film barrier material without puncture, leakage, or blockage. The system uses a lever to cut off flow (De Muinck and Sondaar)

which would possibly be included in further iterations of our valve design to divert flow to particular HD regions and not others, all with a turn of a switch.

A self-sealing system with a vacuum, allows for unidirectional flow and for the system to self-contain in the absence of fluid pressure (Hagihara). This could be an additional way to prevent fluid leakage if connections were to be disconnected. Furthermore, the equalization of pressure on both sides of the valve is an important consideration (Smolko and Kevorkian) and the use of vacuum systems can help equalize the internal and external pressure differences in fluid flow systems.

The final design iteration that is of particular note is the prior art of fluid drip bags. Many applicable systems have fluid valves integrated into IV and other medical drip bags. Those described by Niedospial and Quirico, Pardis have the added benefit of being currently in use in the medical field so there is at least some familiarity with their connection systems by medical professionals.

CHAPTER 3: MATERIALS AND METHODS

III.1. Design Requirements

The purpose of this project is to create a component for a physiologically based Liquid-Cooling-Warming-Garment (LCWG) to allow for targeted heat transfer from system to wearer. Several key design criteria of the system are incorporated into Tables 2 and 3 below. This project has two distinct parts: 1) the sealed, channeled garment system to allow for physiologically targeted fluid flow, and 2) development of a “valve connection system” to allow for flow between reservoirs positioned over targeted high-density regions and fluid cooling systems. Proof of concept was being tested in the ability of these distinct parts to be designed, fabricated, and tested for optimal conditions. These design criteria were taken from prior art, the biomechanical aspects of physiologically targeted cooling, and significant manufacturing concerns.

Design Requirements
1. Lightweight material
2. Sufficient fluid flow
3. No significant fluid pressure buildups
4. Physiologically targeted
5. No movement impedance for user
6. Easily and reproducibly manufactured
7. Durable enough to withstand internal and external pressures
8. Easily scalable/adjustable design
9. Incorporated into existing garments

Table 2: Design requirements for physiologically targeted LCWG.

<u>Design Requirements</u>
1. Easily manufactured
2. Slim, with low profile
3. No exposed sharp edges
4. Proper fill density to allow uninterrupted flow
5. Incorporated into FCS with heat

Table 3: Design requirements for valve connection system.

Particularly notable in designing the functional requirements of this system was Rose and Dobb's patent for "Tubed Lamination Heat Transfer Articles and Method of Manufacture". This prior art incorporated lamination surrounding fluid carrying tubes, but reinforced several of the key functional design requirements (Rose and Dobbs). Thin-film lamination materials fulfill many of these LCWG design requirements. They are extremely lightweight, can be molded to the physiological shape of particular regions, and are easy to work with in laboratory and manufacturing conditions. Furthermore, depending on thickness and overall material weight, it can be easily incorporated into existing protective equipment. Finally, thin-film sheets can be "heat-sealed" to themselves without the use of adhesives, further allowing for manufacturing advantages.

In terms of the valve connection system, any number of plastic-type valves could be incorporated into the design of the overall fluid channel system (FCS). However, integrating the valves without large amounts of adhesives would prove to be particularly challenging in the development of this system. Literature has shown that the use of certain spray adhesives (and other glues) may help in the sealing of these systems (Arcade Museum), and needs to be studied in further work for its efficacy. Furthermore,

low-profile valves have been incorporated with many thin-film materials in food, medical, and beverage applications (De Muinck and Sondaar; Nielsen and Dige, etc.). The fact that these valves already are used in liquid-barrier applications further justifies their use as prior art for the formation of the valve's functional requirements.

III.2. Materials

III.2.1. Mylar®

Biaxially-oriented polyethylene terephthalate (BoPET) made by Dupont Tejjin Films (known by the trade name Mylar® and used interchangeably throughout) is a common synthetic, polyethylene material used for a number of different applications. These applications include imaging, decoration (metallic birthday balloons), food packaging, thermal applications, and protection for thin films (Andritz Group; Kellene; Pfister, Schaar). BoPET has high chemical resistance, thermal stability, seal-ability, and acts as an efficient barrier to oxygen and water (Andritz Group). It is most notable for its use in several food applications including MRE (Meal-Ready-to-Eat) bags in use by the military and “do-it-yourself survivalists” and in several bagged beverage applications commercially available. For the purposes of this project, the ease of heat-sealing and the thermal stability were vital in the choice of BoPET. Its material properties make it a prime candidate for this heat-sealing application. It is particularly easy to work with in its food grade form and is easily heat-sealed to itself when pressed together for short durations (Farley, et al.). Its construction (in the form purchased) is that of an envelope with three sides sealed and one held open. It is also of multiple layer construction as is consistent with its application in NASA weather balloons (Staugaitis and Kobren). This

was an important consideration when looking at the presence of layered delamination in peel testing.

Dupont Teijin Films lays out many of the key material properties for this application in their specification sheet titled “Mylar® Polyester Film”. One compounding factor to the material properties is the sheet thickness because a thicker material transfers less heat from system to user and is more rigid in terms of flexibility. This is an important consideration particularly for manufacturing and thermal conductivity purposes. For this reason, three thicknesses of BoPET were chosen for testing in this study to determine their feasibility as a part of the FCS. The tested thicknesses were 2mil (.002in), 5mil (.005in), and 7.5mil (.0075in) to allow for a variety of pliability, heat transfer properties and sealing characteristics.

The first important factor in this material data is the “Shrinkage vs. Temperature Properties”. Particularly when heat-sealing a particular material, the high temperatures applied could cause significant material shrinkage and distort the finished product. Mylar® however, shows very little shrinkage even when faced with temperatures required to seal two sheets together. Both the 1-mil and 7.5-mil thickness show approximately a 1.75% and 1.6% material shrinkage respectively (at 150 °C ambient temperature) (Dupont Teijin Films) (Figure 15), which was initially thought to be an insignificant amount. This would later prove to make the manufacturing of our FCS inefficient and challenging. Combined with the tensile strength characteristics of the material after heating for extended periods at 150 °C (Figure 16), the shrinkage and tensile strength losses are not a particular concern for this application. This was

experimentally tested in this study using both peel and burst testing to confirm the specifications in the data sheet.

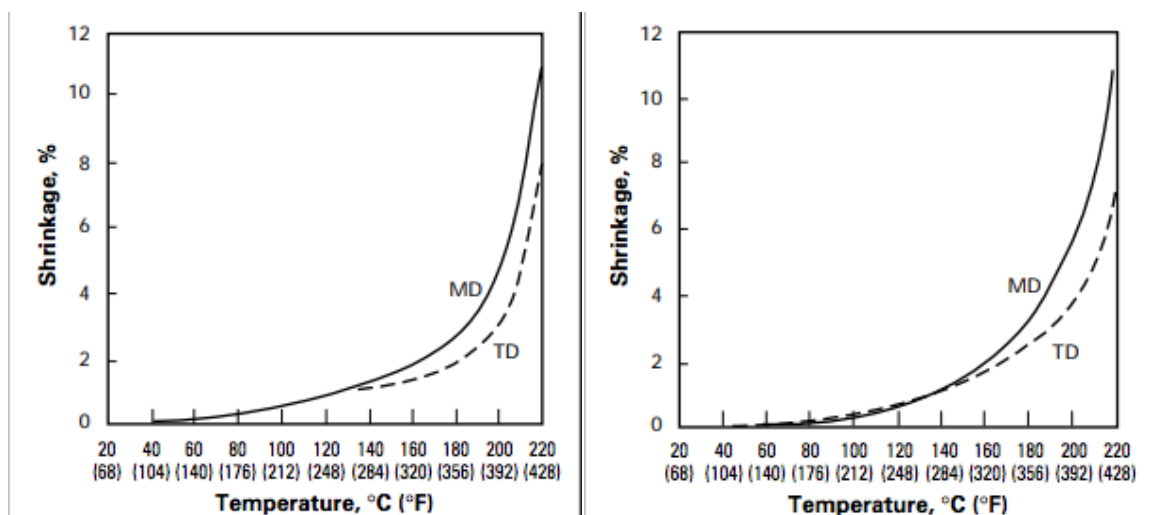


Figure 15: Shrinkage vs. Temperature of 1mil (Left) and 7.5mil (Right) Mylar® sheets. (Dupont Teijin Films). Lines correspond with polymer orientation: MD = machine direction, TD = transverse direction.

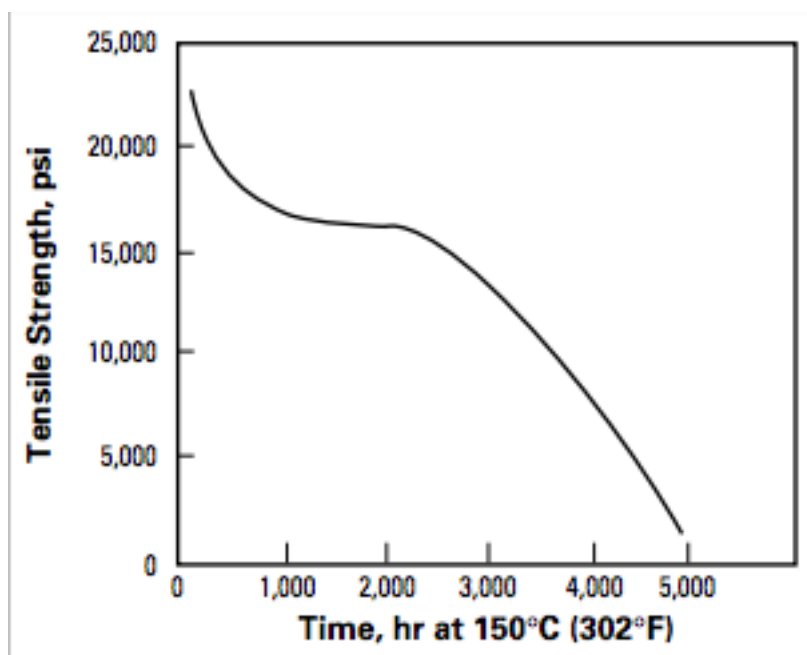


Figure 16: Tensile Strength vs. Time at 150 °C. (Dupont Teijin Films). Specimens are tested with ASTM D882 (ASTM International, D882).

Another important consideration noted in the product specifications is the operating temperatures for which this thin-film is rated. As seen in Figure 16, even after exposure to 150 degree Celsius heat for 2,000 hours, the material is still rated for upwards of 15,000 psi of tensile strength (Dupont Teijin Films). This is well beyond the anticipated operating pressures of the FCS. Furthermore, Dupont rates Mylar® to be particularly effective from -70 °C to 150 °C under “normal stress conditions”, as well as from -250 °C to 200 °C when “the physical requirements are not as demanding”. For the LCWG application the physical requirements of the material are not demanding since the stresses and temperatures stay in a more physiologically relevant range. As a result, material creep is not of particular concern.

Material creep (deformation under long-term stress below the yield strength of a given material) can be a significant factor in applications where adverse temperatures and/or pressures are applied to a material. The affects of creep could change the strength profile of a material and possibly compromise the ability of the FCS to perform optimally. Dupont Teijin Films notes that Mylar® is unusually resistant to creep even in high pressure and temperature conditions. At room temperature (25°C to 30°C) after 260 hours at 2.98 kpsi there was a measured creep of 0.1% and after 1000 hours at 3.00 kpsi, another experiment showed a miniscule 0.2% deformation. Furthermore, at 100 °C and 0.5 kpsi for 4000 hours, there was only 0.9% material deformation (Dupont Teijin Films). This is well beyond the service life and operating conditions anticipated the FCS, so creep is not a concern for this application. As a result, creep was not measured in this study, but needs to be quantified in further experimentation

III.2.2. Aluminum

In the design process, a review of probably press plate materials showed the need for a soft, workable metal that could be used to fabricate a system for heat-sealing thin-film materials in a consistent, repetitive fashion. 6061-T6 Aluminum was used to fabricate the heat seal press plates.

6061-T6 aluminum was chosen due to its high strength, workability, and resistance to corrosion. It combines a high tensile strength (45,000 psi), high shear strength (30,000 psi), and particularly effective thermal properties for a heat transfer application (Aerospace Specification Metals, Inc.). This allows the material to maintain its strength while still able to be machined on a CNC.

Thermal properties of particular note are the small coefficient of thermal expansion, high thermal conductivity, and high melting temperature (Table 4). An additional concern with the specificity of the sealing pattern that was later chosen was the possible warping of 6061 aluminum plating. This would be caused by the temperature fluctuation of the plating from room temperature (approximately 20 °C) to upwards of 150°C. Due to the fact that the melting point range of this particular aluminum alloy is well above the operating temperatures of the sealing system, there is no concern that the aluminum plating would warp, particularly in the intricate sealing pattern design discussed later.

Thermal Properties	
Coefficient of Thermal Expansion (CTE), 250 C	25.2 $\mu\text{m}/\text{m}\cdot^{\circ}\text{C}$
Thermal Conductivity	167 W/m-K
Melting Point	582-652 $^{\circ}\text{C}$

Table 4: Notable thermal properties of 6061-T6 Aluminum (uncoated). (Adapted from Aerospace Specification Metals, Inc.)

III.2.3. 3D Printer

An important and effective tool for use in this project was the use of novel 3D printing technologies. These tools were effective for rapid prototyping of both the initial sealing scaffold and later, the valves integrated into the FCS. Simple file format changes allowed for files to be converted from SolidWorks parts, directly into STL files, and then sliced and printed on 3D printers. Furthermore, any design flaws could be easily visualized and assessed in a particularly cost-and-time effective fashion. Several materials were used in the 3D-printing process.

III.2.3.1. PLA

Poly-Lactic Acid (PLA) is a ubiquitous polymer that is used in many 3D printing and biomaterial applications. It is noted for its ease of manufacture, moldability, and relative strength to weight ratio. It has a melting point of 165 $^{\circ}\text{C}$ and glass-transition temperature of 55 $^{\circ}\text{C}$ (Farah, et al.) which make this material particularly adept for the FCS valve connections. This material was used for initial sealing scaffolds and later valve iterations. Furthermore, its low material weight and the ability of the 3D-printers to adjust material infill density and extrusion temperature make PLA the ideal material for use in the reservoir valve developed here.

III.2.3.2. PETG

Because the manufacturing process employed for the valve system involved applying direct heat to the BoPET material in order to form a seal, there was initial concern that PLA's low melting temperature would cause deformation of the 3D-printed parts. This was found to be true when direct heat was applied. Until further prototyping confirmed that its use was not necessary, Polyethylene-terephthalate-glycol modulated (PETG) was used in place of PLA for valve designs. In manufacturing where higher heat and faster production times are of concern, PETG (or other polypropylene materials) may be a better option.

PETG is another type of polymer that is used in rapid-prototyping and 3-D printing applications. It has a notable higher extrusion temperature than other commonly used plastics for printing and was chosen as such for its resistance to heat-seal temperatures applied directly to valves in order to incorporate them in the BoPET FCS construction. PETG needs a high extrusion temperature (250 °C), high bed temperature (100°C), and tends to string at high temperatures with the use of a cooling fan in printing (Matter Hackers; All3DP). As a result, the PLA material was determined to work better for the current construction of the FCS. Although not used currently, the idea to use plastics with higher-temperature ratings may be beneficial, particularly in ambient temperature conditions where there may be direct contact of valve connectors to temperatures that exceed those required to melt PLA and other similar polymers.

III.2.4. Acrylic

In order to construct the burst test device for applying uniform pressure for compressing the reservoirs as described in the burst test protocol (ASTM International, D642), a scrap piece of 1-inch acrylic was used. The specification lays out that the two sides of the compression device need to be “flat to within 0.01in for each 12in in length” and the acrylic fits the criteria (ASTM International, D642).

III.3. Sealing Patterns

Once Mylar® was chosen as the construction material of the FCS, one of the particular “High Density Tissues” given in the prior art (Koscheyev, et al.) was chosen as a basis for proof of concept (Deltoid muscle group). This specific zone was chosen because it is scalable, covers a large amount of heat-transfer surface area, and fatigues easily in several types upper-extremity tasks. Designs considerations for this region could easily be scaled and incorporated into other high-density tissue regions in the arms, legs, and on the torso.

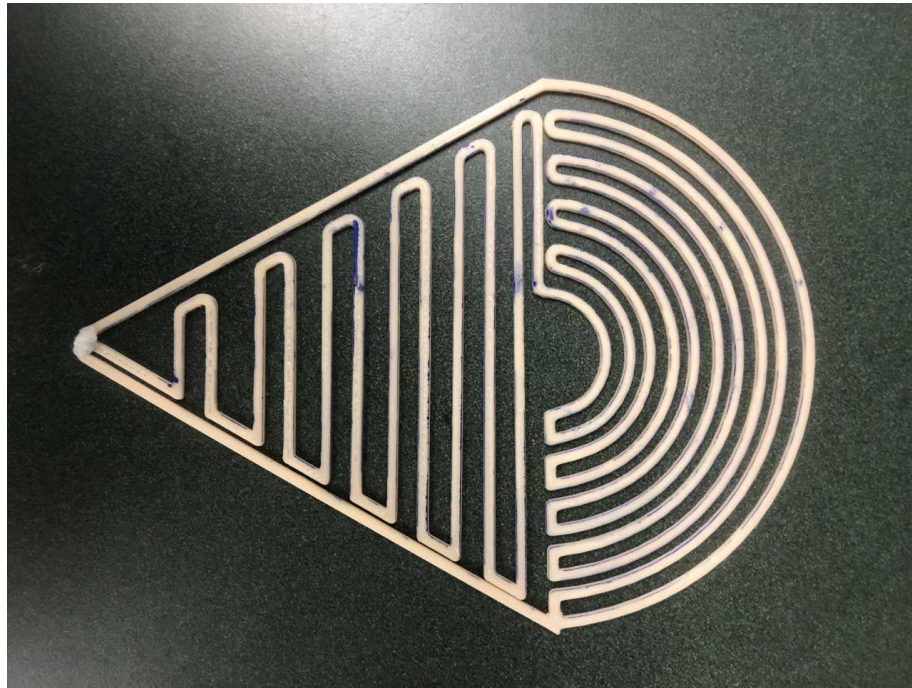


Figure 17: “Teardrop” Sealing Scaffold based on the Anatomy of the Deltoid Group.

Several versions of sealing patterns were chosen and modeled in SolidWorks, with the tentative design being a complex “teardrop” shape (Figure 17). It measures 8 inches long by 5 inches wide, with a semicircle portion at the proximal end, converging to an outlet at the distal end (hence the “teardrop” shape). In order to allow for a sufficient fluid flow, the scaffold was designed with 0.125-inch-wide channels and 0.125-inch space for the heating element. The first SolidWorks iteration was 3-D printed to allow for a sealing “scaffold” used to guide sealing with a heating element and the Mylar® sheets. Due to the nature of the initial designs and the PLA scaffold used, the inner sections were flexible which did not facilitate using handheld heating elements for sealing. Additionally, this scaffold construct left room for significant sources of human error. Dwell time and seal path were extremely difficult to control, so a better sealing

system was clearly needed. Later sealing methods attempted to mitigate the affects of human error as a key design criteria.

III.4. Fluid Pressure Calculations

Fluid pressures were based on the product specifications of the Fisherbrand™ Isotemp™ Refrigerated/Heated Bath Circulators (Thermofisher Scientific). This system pushes fluid at a pressure of 4.4 psi and at a rate of 3.96 gallons/minute (Thermofisher Scientific). This system is well beyond the range necessary for this application, but 4.4 psi was used as the baseline for effective strength of the FCS in Bernoulli equation calculations. Other systems such as the Thermocube 200 (Solid State Cooling Systems) with a much lower flow rate (2 liters/min) would be sufficient in such small diameter fluid-channels as seen in our FCS. This system does have a static pressure of 10psi in its lowest state however, which could be too high for our FCS: further research has to quantify the pressures our system can fully handle (with a built-in factor of safety to be determined). The pressures placed on the system can be calculated using Bernoulli equations with simplifying assumptions. The assumptions are: the fluid is a constant density (assume water in this application), there is laminar flow, and the fluid is incompressible. Furthermore, it is assumed that there is a perfect fluid channel cylinder created with the diameter equal to the 0.125-in channels.

Key advantages are seen in our system when using Bernoulli's equation. First, the higher the fluid flow velocity, the lower the pressure seen in the fluid-channel system. This would be one way to mitigate the effects of pressure if they were found to be a factor in material strength. Additionally, there is a constant total pressure in a moving

fluid across the entire length of the FCS. The only area where this can cause issues is 90-degree pipe bends, where a small radius of curvature causes fluid pockets and pressure buildups (Beij). This design consideration was mitigated in later iterations of the sealing pattern design. Based on the calculation above, the absolute highest pressure our system would see with the above assumptions would be 5.23 psi (in the small bottleneck between upper and lower flow). An important thing to note is that these are simplifying assumptions made in order to get a baseline pressure measurement. In order to see the effects that other flow dimensions may have on the system, Bernoulli calculations were completed based on cross-sectional flow area that may be seen in the smallest area of the fluid channel system (there was a slight design flaw in the aluminum plating that allowed for a smaller cross-sectional area than the intended .125in). As Bernoulli's equation suggests, the smaller the cross sectional area, the higher the corresponding pressure (assuming same flow velocity). This is used as a simple comparison to determine the effects of changing the flow dimensions in further heat press plate iterations.

If the Reynolds number is high enough to create turbulent flow characteristics (high velocity, low viscosity, and/or large pipe diameter), there is an indication that it may be better for heat transfer characteristics. This is due to the presence of "layers" of fluid in laminar flow that insulate the temperature from the heat-exchange surface (Advantage Engineering, Inc.). For this FCS, Reynolds Number can be used to determine whether laminar or turbulent flow is expected (Figure 18).

$$Velocity = \frac{.53 \text{ ft}^3 / \text{min}}{\pi(.0104 \text{ ft})^2} = 1559.77 \text{ ft/min} = 7.92 \text{ m/s}$$

$$Reynolds \text{ Number} = \frac{\left(\frac{1000 \text{ kg}}{\text{m}^3}\right) \left(\frac{7.92 \text{ m}}{\text{s}}\right) (.0032 \text{ m})}{8.9 * 10^{-4} \text{ kg/m} * \text{s}}$$

$$Reynolds \text{ Number} = 28,476$$

Turbulent Flow (Re > 4500)

Figure 18: Reynolds Number Calculation Based on velocity and diameter of FCS (Adapted from Benson; Engineer's Edge) (See Appendix A).

This extremely high Reynolds number indicates that flow is inviscid and that essentially no viscous forces exist in this situation (Benson). This is effective for thermal transfer and shows that our system should be sufficient to facilitate this.

III.5. Determination of Heating Element

Farley, et al. confirms in their patent for “Heat Sealable Films and Articles Made Therefrom” that many polyethylene polymers show their highest strength when sealed between 110 and 160 degrees Celsius. Prior testing in our lab confirmed that these temperatures were sufficient to create a strong, permanent seal. Combined with the data collected from Dupont Teijin Film’s material specification and based on the representations of the data presented, 150 degrees Celsius was chosen as the baseline temperature for sealing and thus all sealing experimentation occurred at 150 degrees Celsius (+/- 5 degrees) (Dupont Teijin Films; Farley, et al.) (Figure 19). Additionally, several commercially available storage bag sealers for food grade BoPET are rated at 175

°C, further showing a temperature on the upper end of this range is more beneficial (USA Lab Equipment).

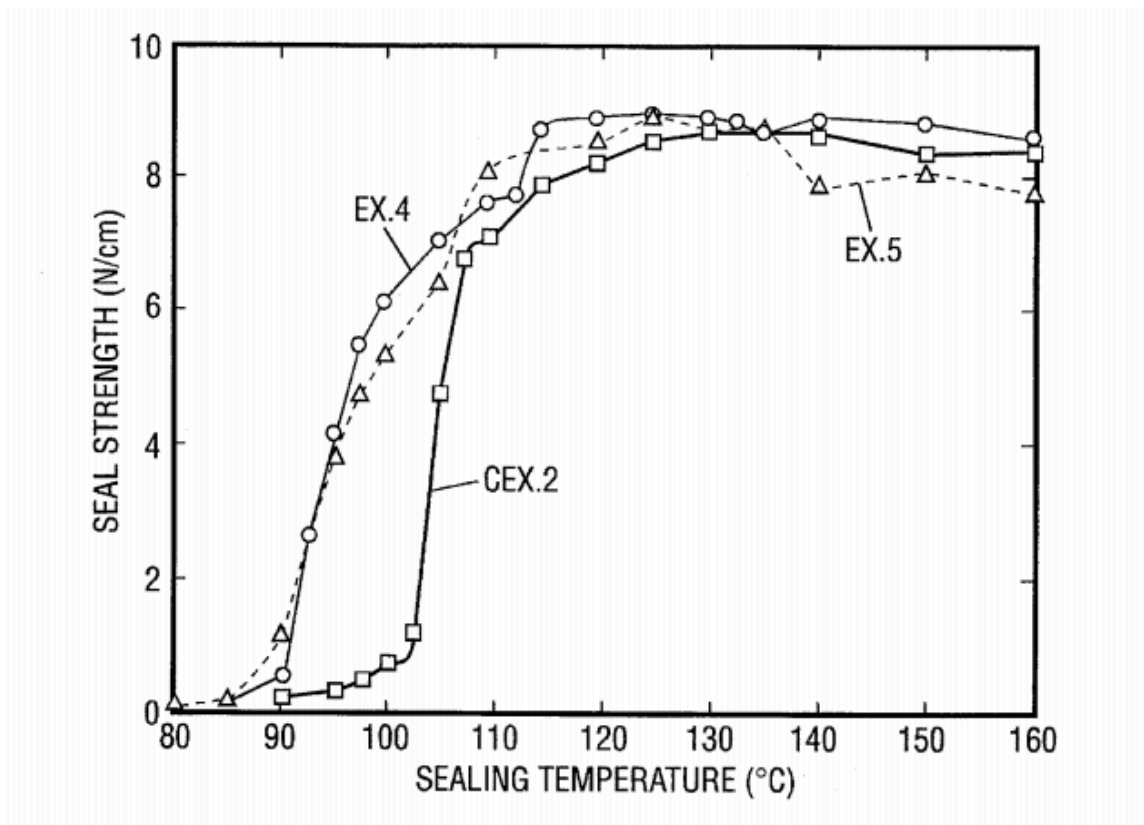


Figure 19: Seal strength of several polyethylene polymers based on temperature. (Farley, et al.)

Several temperature tests were performed to determine the appropriate heating element for use in this project. The element needed to be easily handled, allow for consistency in manufacturing, and eliminate human error in development of the targeted cooling systems. A T thermocouple made of Cobalt vs. Cobalt-Nickel was used for this experimentation in combination with a multimeter to measure its output (Omega Engineering Corporation). It is temperature rated for applications from -200 to 350 C° with a standard error of less than 1 C° at 0.1 C° intervals (Omega Engineering) and the apparatus itself was the appropriate dimension to work with all heating elements measured. This was particularly effective in measuring the temperature of the modified thin film press (Spectrum Brands), as the diagonal distance of the press plates was within fractions of an inch of the length of the thermocouple, allowing it to be fully integrated into the sealing system to measure temperatures (Figure 20).

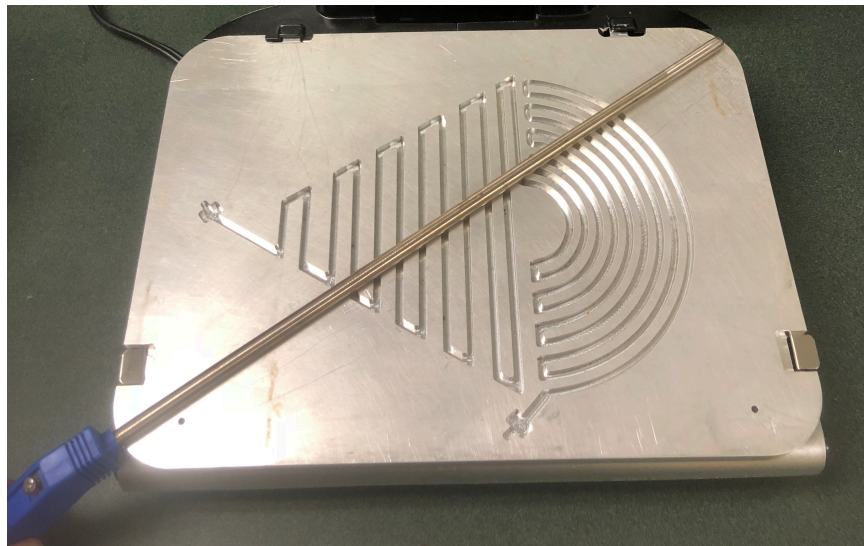


Figure 20: T-Thermocouple in place on Bottom Press Plate.

The first element used in temperature tests was a 30-Watt soldering iron (Chicago Electric Welding) that was adapted with a custom fitted aluminum tip (prior work at Center for Anatomical and Movement Sciences lab fabricated this system to seal Mylar®). The soldering iron is temperature-rated to reach approximately 390.5 C° (735 F°) (Harbor Freight Tools), which was shown to be excessively hot for an appropriate seal between two sheets of BoPET to be accomplished. The material melted after even a few seconds (Figure 21) in contact with the soldering iron and required a high degree of precision to accurately seal (especially the intricate “teardrop” pattern design). Even with the modified Aluminum tip and subsequent dissipation of heat, the temperature was far too high to create an effective seal.

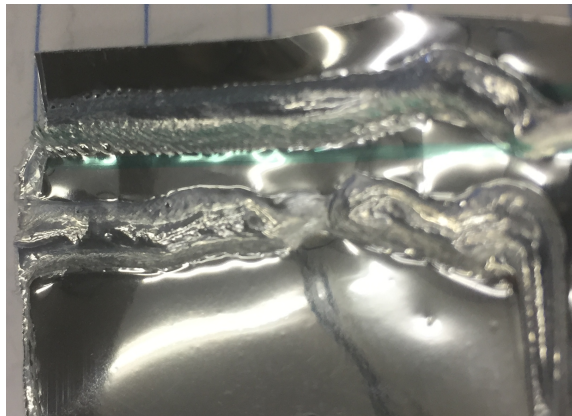


Figure 21: Material melts due to Soldering Iron, leading to ineffective seal.

Another attempt was made in sealing the BoPET film with a commercially available flat iron (Plug in GED™, Model #680609). The initial drawback to this model was its obvious lack of maneuverability and could not be used to seal patterns into the film, but was tested for its temperature rating (and how well it sealed the material at

different time intervals). The flat iron reached a stable temperature of 130-150C°. It was used in sample preparation for both peel and burst testing although not used in the actual design of the sealing pattern.

The final appliance that was measured for temperature and its heat-sealing properties was a modified sandwich grill press (Spectrum Brands, George Foreman™ Model GRP1060B). The press utilizes a multi-functional heating element that can be used for numerous applications. Although it is commercially available as a food cooktop, it incorporates a top and bottom plate that was projected to be ideal for sealing two sheets of material together. Temperature testing of this press found that if left in a closed position (two plates touching each other) sufficient sealing temperatures could be achieved (Figure 22). Due to the consistency of temperature and lack of human error in manufacturing, this press construct was used in further sealing of channeled constructs for use in the creation of BoPET reservoirs in most of the specimens and prototypes.

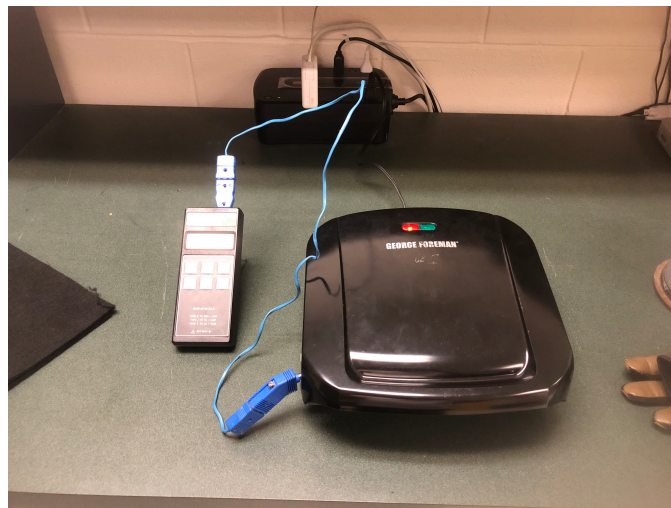


Figure 22: Temperature testing setup in “closed” press position.

III.6. Plate Fabrication

Since the George Foreman™ press is not fabricated specifically for sheets of BoPET to be heat-sealed between the two plates, design modifications were implemented to allow for thicker heat-sealing plates to be outfitted on the press. In order to accommodate thicker metal plating, the “snaps” on the upper and lower press faces were bent slightly larger than the manufacturer specifications. This would allow the heat-sealing plates to eventually snap in and snap out of the system. Additionally, small portions of the recesses for the “tabs” on the upper portion of the plating were removed to allow for a tight fit of the new plating system. This ensured that there would be no slippage of the plates during heat sealing.

III.6.1. Plywood

The 3-D printed scaffold pattern was laser-cut on two identical pieces of .25-inch-thick plywood. The design was taken from a SolidWorks part file and exported to a DXF file to interface with CorelDraw and the Epilog Laser Cutter in Tulane’s Makerspace. This was determined to be an appropriate step due to the ease of manufacturing and rapid prototyping capabilities with the use of plywood, while the ability to make minute design changes was exceedingly difficult with 6061-T6 aluminum.

The iterative design process for the plywood plates was time consuming due to the need for accuracy in final sealing design before manufacture of the plates in aluminum. Additionally, in order to fit in the press construct and make contact with one another, two sheets of ¼” plywood were glued together (Figure 23). The only difference between the top and bottom plates in all configurations is the fact that the top “tabs” are

approximately .2 inches closer together in the top plate than the bottom plate. The Epilog Laser Cutter was set to 11% speed, 100% power to raster the channel design into the front face and 10% speed, 100% power to vector the outside cuts through the piece of plywood. One important note is that these plates were designed under the assumption they would be pressed together to create the sealed construct as was later found to be ineffective in sealing.



Figure 23: Fabrication of 1/2" thick plywood plate constructs.

The first iteration of the plywood plating (Figure 24) attempted to directly take the 3D file of the “scaffold” that was created previously and raster it’s design into two plates that are mirror images of one another. Several issues were apparent with this design. First, the dimensions of the “tabs” on the ends of each plate that allowed them to set in directly to the heating element were the wrong dimension. Next, there was not enough space between the upper and lower portions of the design, and they were rastered together into one continuous channel. This would cause issues with fluid flow if a seal

were attempted with such a design. Finally, the curves on the bottom edges of the plates had too small of a radius of curvature, causing the plates to overhang from the end of the press – which could lead to issues later in the sealing process.



Figure 24: 1st iteration plywood plating snapped in to press construct.

The next iteration (Figure 25) saw changes in the overall outer plate shape and addition of a space for a small at the inlet. The dimensions of this valve area would later be changed to accommodate a larger, unsealed area for valve placement. Iterations 3 and 4 (Figure 26, 27) saw the additions of a valve area at the outlet and pilot holes for registration pins in order to line up the top and bottom plates for sealing. The final

iteration (Figure 28) decreased the size of the pilot holes and spatially shifted the position of the sealing pattern slightly towards the center of the plates. This iteration was determined to be the most feasible design for manufacture and was laid out for fabrication in Aluminum plating.

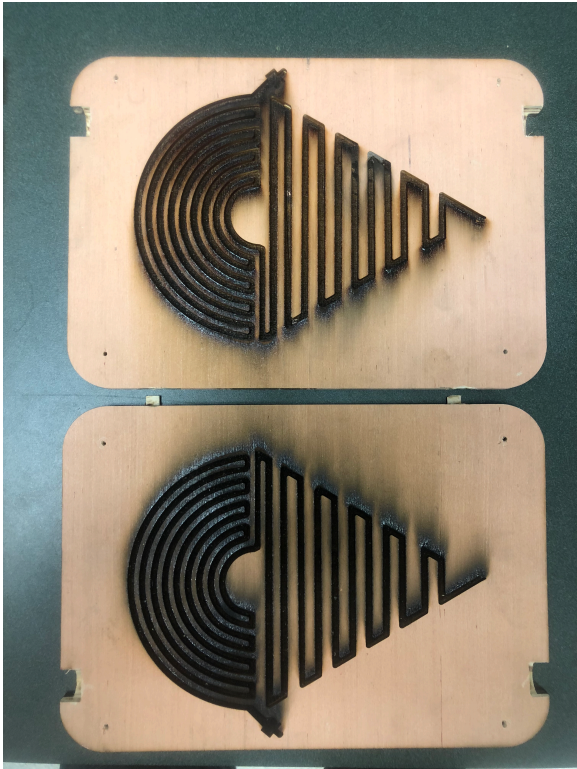


Figure 25: 2nd Iteration Plywood Plates

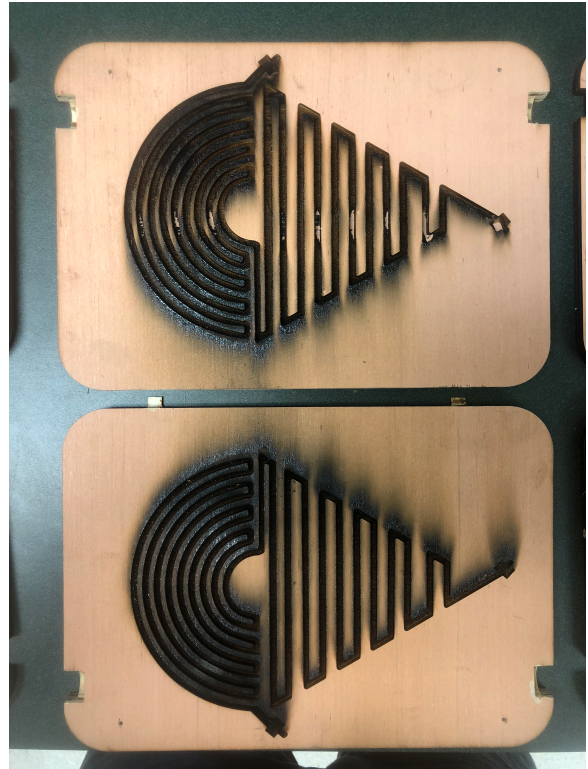


Figure 26: 3rd Iteration Plywood Plates



Figure 27: 4th Iteration Plywood Plates



Figure 28: 5th Iteration Plywood Plates

III.6.2. Aluminum

Manufacturing was attempted on the 4-Axis CNC Mill (Tormach, Inc.) in Tulane's Makerspace. The intricate channel design and corresponding complicated CAM design with extremely tight corners was outside of the scope of what could be manufactured on site, so production was outsourced to Laitram Machine Shop in New Orleans, LA. The final design was implemented in Aluminum and tested for fit on the press construct (Figure 29). The top and bottom portions fit together nicely with the aid of small registration pins placed in the pilot holes on the ends of the plates.

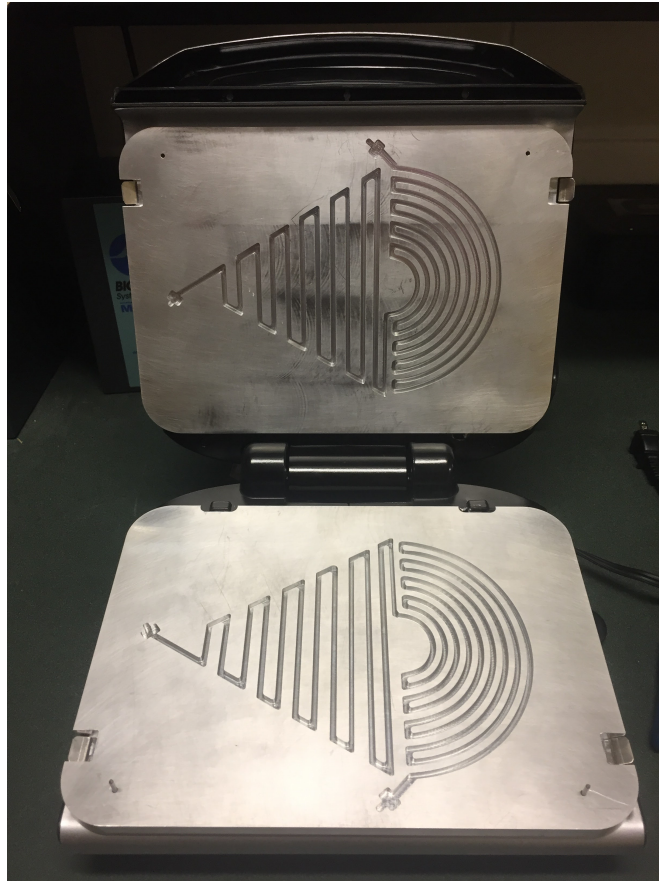


Figure 29: Final Iteration Manufactured in 6061 Aluminum on Press Construct.

Slight modification to the initial plate design was necessary in order to allow sufficient space for valve placement in the sealed construct. It was thought that all areas that were channeled out allowed for enough of a temperature differential to prevent a heat seal from forming, so space was only needed at the inlet and outlet portion. The current design with space for inlet and outlet valve connections can be seen in Figure 30.

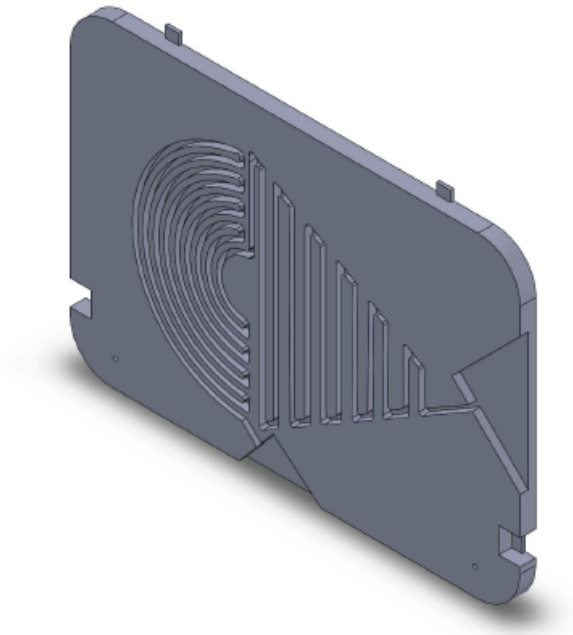


Figure 30: Isometric View of Current Aluminum Plating with spaces for valve connection.

III.7. Testing with Press Construct

Following the fabrication of the aluminum plating, the heat-transfer and pressure distribution properties of the modified press construct were quantified. This was necessary due to the new thickness, different material properties, and new dimensions of the heat seal plates. In order to confirm that the new construct would supply sufficient heat and pressure for sealing of BoPET, the press was temperature tested to determine that the range of temperatures was sufficient for sealing.

III.7.1. Temperature

It was shown that the thermal energy transferred on the press without modification was sufficient to allow for the sealing of the Mylar®, but the newly fabricated plates had unknown heat dissipation. Particularly of concern was their increased thickness, as it could not allow for sufficient distribution of heat to the inner press surface for heat sealing.

The temperature profile of both the off-the-shelf press construct and the newly fabricated aluminum plating were measured using the T-thermocouple and Omega Engineering voltage reader. The thermocouple was placed in between the press plates and temperatures were measured at 30-second intervals for 20 minutes and 30 minutes for the non-modified and modified press construct respectively. This experimentation was able to quantify the temperatures reached in the modified press construct and demonstrate that they were sufficient to provide the sealing temperatures required for the thin-film Mylar® to form a heat-seal. Maximum temperatures of 191°C and 177°C were measured in the unmodified and modified press respectively – well within the range needed to seal BoPET.

III.7.2. Pressure

Another important factor in the manufacturing of heat-sealed thin-film materials is the pressure placed on the system to force the material to come in direct contact with the heated surfaces. Although there is no definitive research into the ideal pressures for our combination of material thickness, temperature, and dwell time, there appeared to be a qualitative improvement in the performance of the sealing system when applying a

downward pressure on top of the press construct. This was done manually in initial testing, however needed to be consistent across all formats in order to allow for consistent sealing pressures.

A 20-lb weight was added on top of the system when sealing for the respective dwell-times used in experimentation (Figure 31). This was a standardized unit of measurement that could apply as a part of the FCS preparation protocol to allow for consistency in sealing pressure. Using a handheld pressure gauge (Chatillon Force Gauge, Model DFE II), the combination of the upper sealing plate and the additional 20lb weight applied a downward force of 14.2lbs (.18psi; based on sealing area). This same pressure was used consistently throughout all sample preparation, but further work would need to determine if this is the ideal seal pressure for the temperatures applied in this application.



Figure 31: 20lb weight stack added to top of press construct for sealing. Applied for each dwell time in sample preparation.

III.7.3 Sealing Protocol

A prior art search was unable to find literature to inform methodology of the most effective way to accomplish a seal between two sheets of BoPET in such a specific and detailed pattern. Much trial and error was necessary in order to determine the most appropriate FCS preparation protocol.

The first method that was used in attempting a BoPET heat seal was lining up the plates with the two registration pins and placing a sheet of Mylar® in between. The plates were then heated up to the appropriate temperature range (130-150 C) with the Mylar® already in place. This method was extremely inaccurate and caused much fluctuation with the temperatures imparted to the BoPET to form a heat seal. The sheets would undergo shrinkage at an uncontrollable rate, dwell times could not be controlled, and seal pressure was ineffective with just the weight of the aluminum plating.

The next method attempted was heating the plates to their appropriate temperature and then placing the sheets of Mylar® for sealing between top and bottom plates. There were several issues with this method. First, slight variability in the axial positioning of the top and bottom plates led to errors in lining up the sealing channels of the top and bottom plates. This caused the plates to create an ineffective seal in the intricate patterns required for fluid-flow in the FCS. The addition of registration pins to hold the top and bottom pieces flush and lined-up with one another attempted to remedy this issue. Unfortunately, the angle at which the plates line up with one another did not make this particularly user-friendly and caused additional issues in consistency and spatially lining up the top and bottom plates. One important factor that was not taken into consideration

when heating the top and bottom plates was the shrinkage the material would see when heated at these temperatures. Although it was chosen for its low shrinkage, the complexity of the design caused the effects of even a small amount of material shrinkage to be exacerbated. Furthermore, applying heat from both the top and bottom press plates did not facilitate a “channel” to develop – making this an ineffective method for creating the FCS constructs.

The final and most effective method involved placing the sheets of Mylar® on a room temperature, flat piece of scrap 6061-T6 aluminum in tension. This was then placed in the center of the press construct with the top, heated portion of the press pressed down onto the BoPET. This allowed for the channel design to be pressed on to the material. This proved to be the most consistent and effective way to apply heat, as the recesses in the top plate allowed for enough of a temperature differential to allow the Mylar® to a contact seal where the hot plate touched, leaving space for the fluid-channel voids to form. By placing the sheets in tension (Figure 32), the effects of shrinkage in the overall material were negated, and void spaces for fluid flow were able to form.



Figure 32: Sheet placed in tension on scrap piece of 6061 Aluminum for sealing process.

The use of only one plate with the channel design was an unexpected and key component to this project. This method was used in the remainder of the FCS sample preparation protocols with the additional .18-psi pressure at temperature ranges discussed below.

III.8. ADMET Peel Testing (ASTM F88)

In order to quantify the strength of the seals accomplished in the laboratory procedure, American Society for Testing and Materials (ASTM) standard F88, “Standard Test Method for Seal Strength of Flexible Barrier Materials”, was used to determine the load at break, elongation at material break, and method of sample break of the sealed FCS constructs (ASTM International, F88). As defined in the test standard, our developed FCS can be considered a flexible barrier material package that has been heat sealed in accordance with definitions laid out by ASTM International (ASTM International, F17).

Three sample thicknesses of BoPET were tested under the protocol laid out by ASTM International. Each of the thicknesses (2 mils, 5 mils, 7.5 mils) was tested under two dwell times of 10 seconds and 30 seconds. Each sample was tested at four distinct areas of seal pattern design. These areas were cut from the same area on each prepared sample with the use of a cutting guide constructed of ¼” plywood (Figure 33). This allowed for two “internal” and two “external” sealing areas to be tested to test the differences in strength at different areas. Although the bursting of the internal seals would not compromise the efficacy of the system, it is an important consideration to understand the possible differences in seal strength of different areas of the construct.

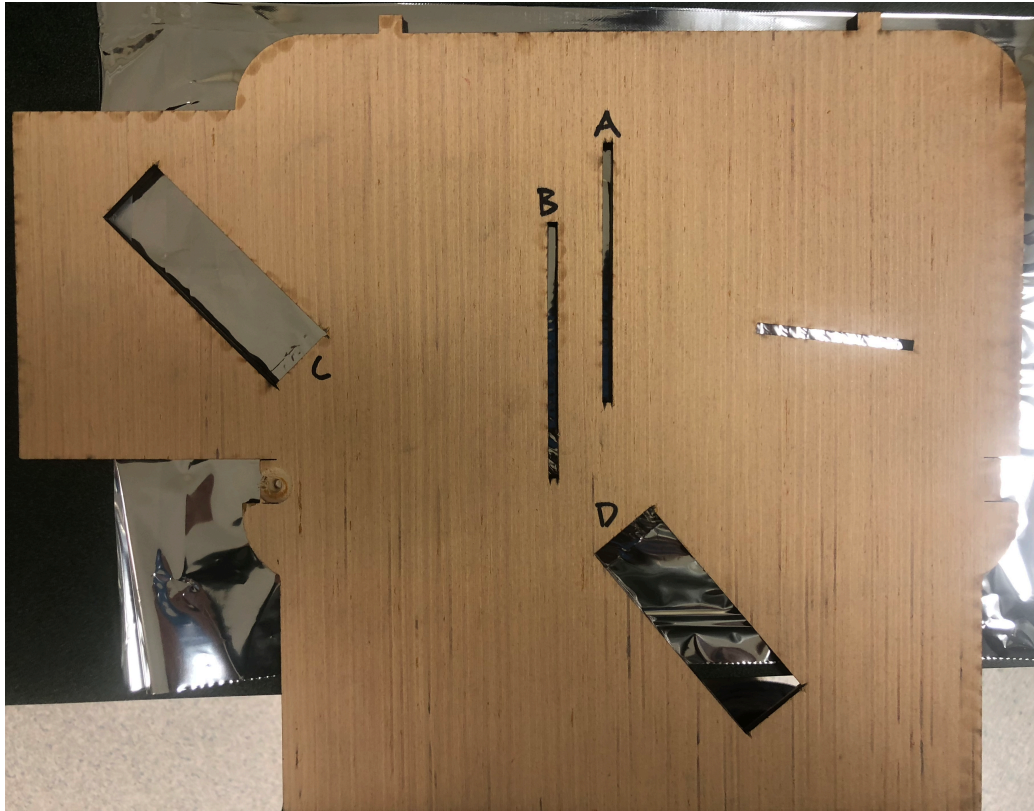


Figure 33: Sample preparation template with distinct areas for ASTM F88 Peel Testing.

III.8.1 Sample preparation protocol

In accordance with ASTM Standard E171, samples were prepared under the following conditions (Table 5). Many packaging materials do not exhibit a meaningful change in physical properties across the temperature and humidity ranges found in a general laboratory setting, and conditioning of samples is often not required in order to achieve useful test results and is often bypassed during routine testing (ASTM International, E171). For this reason, the humidity condition was not a factor in the sample preparation as there is no noted impact in prior literature to suggest that small deviations in humidity would affect the sample continuity. In order to maintain a small

effective range of humidity in sample preparation, all samples were prepared on the same day in the same laboratory setting.

Temperature (Seal): $150^{\circ} \pm 5^{\circ} \text{ C}$ [$302^{\circ} \pm 9^{\circ} \text{ F}$]
Temperature (Ambient): $20^{\circ} \pm 2^{\circ} \text{ C}$ [$68^{\circ} \pm 3.6^{\circ} \text{ F}$]
Humidity: N/A
Dwell Time: 10, 30 Seconds

Table 5: Temperature and dwell time conditions for sample preparation protocol. (Adapted from ASTM International, E171).

Samples were prepared with the methodology as follows: Seal press plates were heated to the seal temperature required to adequately seal constructs. The BoPET material (with respective thicknesses) was then placed in tension flat on a piece of 6061-T6-aluminum plating (with ends taped to create tension). Aluminum plating was placed in the path of seal design with for respective dwell time condition with a scrap piece of welding cloth (temperature resistant up to 2,000 degrees F) placed to protect the bottom plate. The bottom plate was protected to allow the heat to only be applied from the upper press portion and as not to affect the sealed pattern (with some portion of the Mylar® wrapping around to the bottom side of the aluminum plating).

Twenty pounds of additional weight was added to seal the constructs (beyond the force of the plate and press) for the individual dwell time to create a downward pressure of .18psi, which allowed for the plates to come in full contact with one another across their entire surface area. After removing the sealed FCS from the sealing press construct it was allowed to cool to ambient room temperature. The guide shown in Figure 35 was

then used to cut samples from each of the seal constructs according to dimensions required in ASTM F88.

One particular note in this sample preparation is that the test standard calls for samples to be prepared to 1" x 3" x seal width ("x") (Figure 34). The seal width was held consistent to .125in in order to test the smallest applicable seal width in the construct. Only .125in in width could be cut from sample areas A and B, but this was corrected in data analysis by normalizing to the 1in. seal width, to make sure the comparisons between groups were sufficient. Specimens that did not form a seal in sample preparation were eliminated from testing.

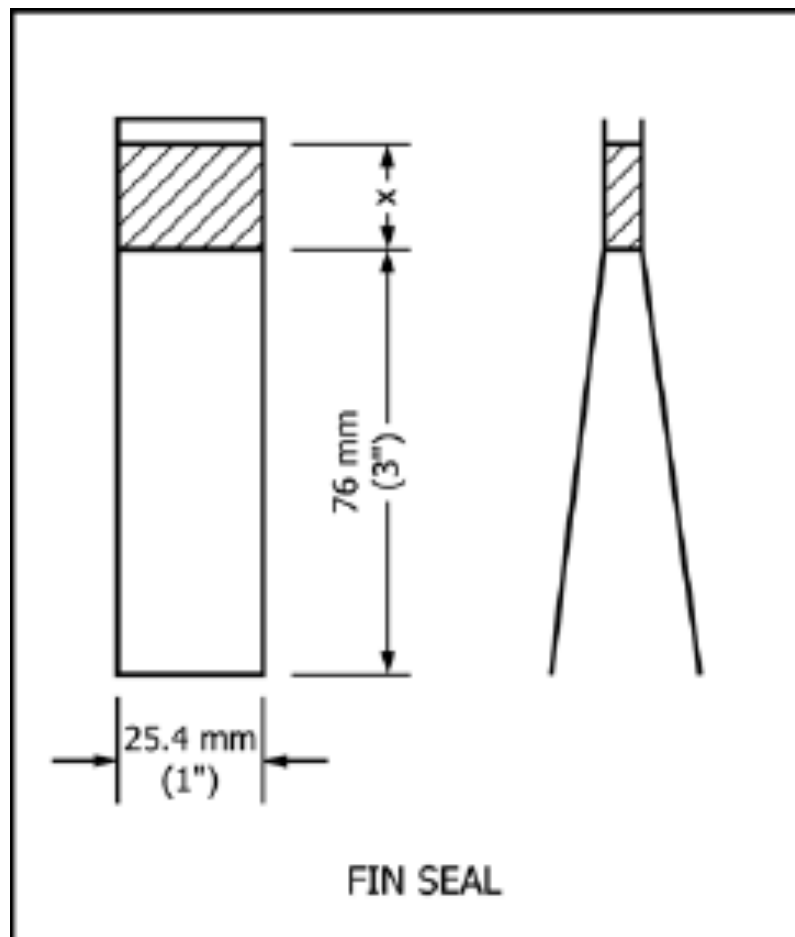


Figure 34: Seal preparation dimensions for ASTM F88. (ASTM International, F88).

III.8.2. Test Protocol

The ADMET MtestQuattro (ADMET, Inc.) testing apparatus was calibrated according to the manufacturer's recommendations. Each leg of the test specimen was clamped in the tensile testing machine with the sealed area of the specimen equidistant between the grips. In order to allow for better consistency, a string that was halfway between the two grips was used for reference (Figure 36). Since BoPET is a "less extensible material", the initial unconstrained specimen length (initial distance between grips) was set to 1 in (ASTM International, F88). The specimen was aligned laterally in the grips so the seal line was perpendicular to the direction of pull, allowing for a snug but unstressed position prior to the initial of the test. An "unsupported" technique was used (Figure 35) with each tail of the specimen secured in opposing grips with seal remaining unsupported while test was being conducted. The standard called for 8-12in[200-300 mm]/min grip displacement rate (ASTM International, F88). The seal was tested at a rate of grip separation of 10 in [250 mm]/min. For each cycle, the maximum force encountered as the specimen is stressed to failure was identified along with the mode of specimen failure (Appendix A). Peel strength of the system was measured in pounds/inch.

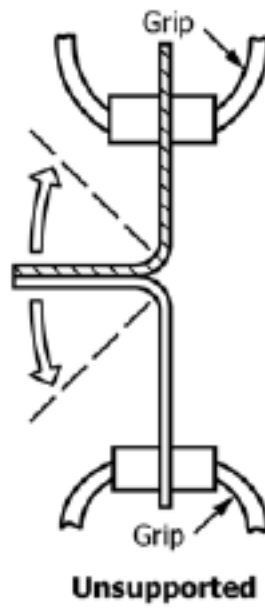


Figure 35: "Unsupported" specimen technique. (ASTM International, F88).

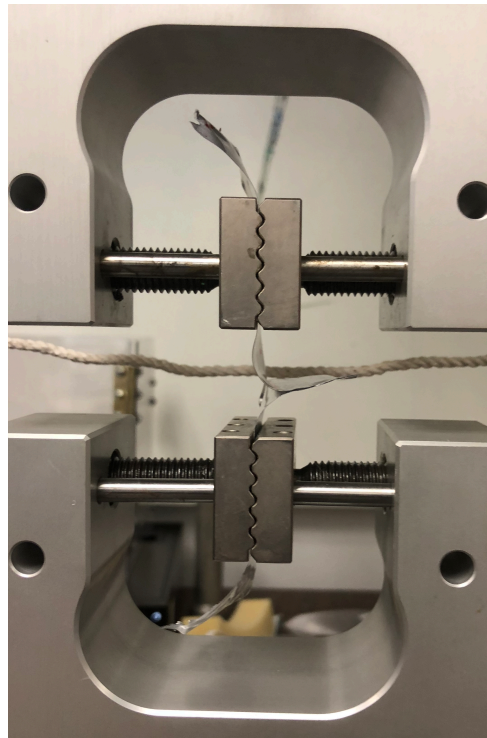


Figure 36: Sample tested in ASTM F88, unsupported technique with reference string behind.

III.8.3. Data Collection and Analysis

Data was collected for load at break, elongation at material break, and method of sample break for each specimen. Significance between dwell time and thickness groups was set to $p=0.05$ a priori. ANOVAs were performed in Microsoft Excel (Microsoft Corporation) and SPSS (IBM Corporation) in order to determine statistical significance of results.

III.9. ADMET Burst Testing (ASTM D642)

In order to further quantify the failure modes and FCS strength of the product developed, a modification of the “Standard Test Method for Determining Compressive Resistance of Shipping Container, Components and Unit Loads” was implemented (ASTM International, D642). This modification is applicable as a method to assess the seal strength of flexible barrier material to burst strength. A “fixed platen compression tester” was developed and used to place a compressive force on the pouch until a burst occurs (Figure 38) and the resulting force is recorded (Bernal).

III.9.1. Fixed-Platen Testing Apparatus

ASTM D642 specifies the “Fixed-Platen Testing Machine” as: “Two platens, flat to within 0.01 in. (0.25 mm) for each 12 in. (304.8 mm) in length, and one of which is movable in the vertical direction so as to compress the container between the platens” (ASTM International, D642). This was constructed out of $\frac{3}{4}$ ” acrylic scrap from Tulane University’s Makerspace. A lower box and upper were constructed to attach directly to the ADMET compression testing apparatus (Figure 37). The lower box was constructed in order to prevent fluid burst from damaging test equipment, thus $2\frac{1}{4}$ ” sides were added.

Furthermore, the upper platen is slightly smaller than the interior dimension of the lower box walls in order to allow for 3/16" clearance to compress the samples. The lower box was sealed with silicone to make it watertight. The inner face of the lower box and inner face of the upper platen are flat with one another to 0.1in for each 12in as per the test standard (ASTM International, D642). This was accomplished with Epoxy used to fill cracks in the upper portion and sanded flush with the rest of the surface.

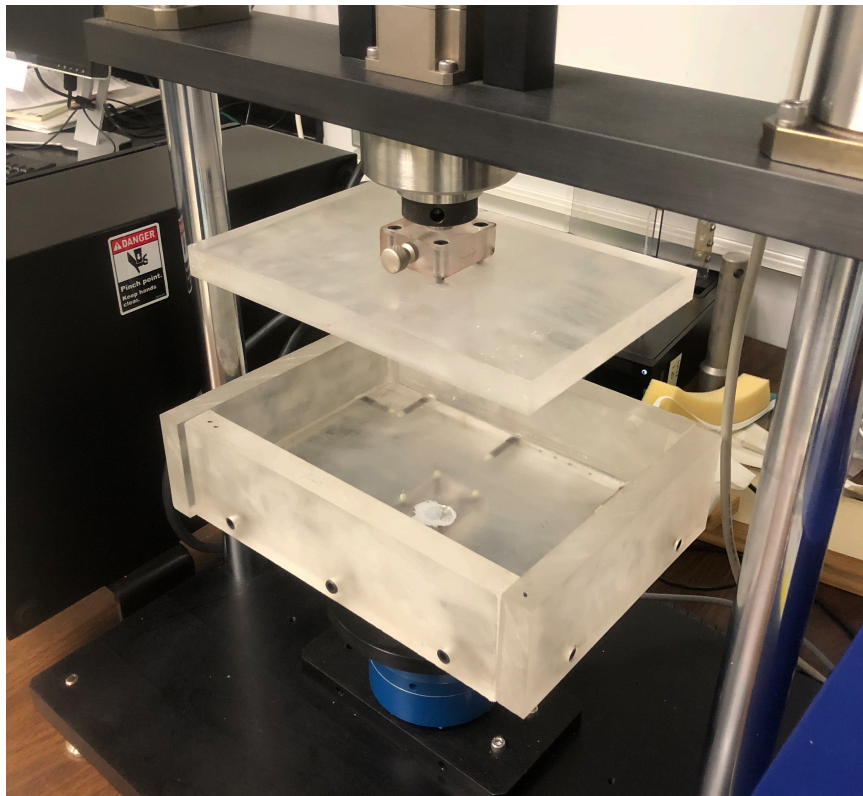


Figure 37: Fixed-platen testing apparatus outfitted on the ADMET testing machine.

III.9.2 Sample preparation protocol

Samples were prepared with the same methodology as described in section III.8.1 for the prior ADMET testing. However, the guide shown in Figure 38 was laser cut from ¼” plywood and was used to cut samples from each of the seal constructs according to dimensions required in to fit in the compression testing apparatus. Once these were cut to the appropriate dimension, the bottom portion of the FCS was sealed using the “Plug in GED™” flat iron and the interior channels were opened with a forced stream of fluid. This is necessary because this type of sealing can and did result in “three dimensional dots” to form on these internal channels that would impede fluid flow (Bletsos, et al.). These are defined as areas within the unsealed fluid channels that formed an incomplete “island” of sealed material due to the press method. This is an important manufacturing consideration that needs to be further studied in this particular application, because of residual micro-sealing within the fluid channels. To facilitate testing, samples were cut into top and bottom portions. The bottom segment was filled with water up to its capacity and sealed with the flat iron to close the open ends of the sample.



Figure 38: Sample preparation template made from Plywood with distinct areas for ASTM D642 Burst Testing.

Another important note is that based on the results and qualitative observations from the ASTM F88 peel testing, only 2 mil thicknesses were tested for 10-second and 30-second dwell times (2 groups).

III.9.3. Test Protocol

Specimen failure was defined as the point at which the burst of the FCS occurs. The specimen was centered on the lower platen of the testing machine in the same orientation (Figure 39). The top platen was brought into contact with the specimen to without the application of a pre-load. The machine was zeroed with the specimen on it and a continuous load was applied at a rate of 0.5in(12.7mm)/min until specimen failure (ASTM International, D642).

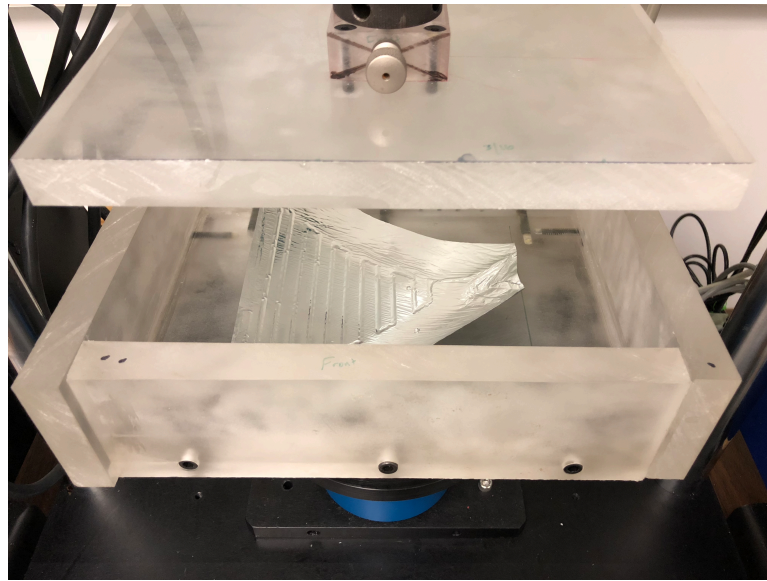


Figure 39: Specimen placed in test apparatus for ASTM D642 Burst test.

III.9.4. Data Collection and Analysis

Data was collected for load at burst and platen displacement for each specimen. Significance between preparation groups was set to $p=0.05$ a priori. A 2-tailed t-test between the dwell time groups was performed in SPSS (IBM Corporation) in order to determine differences.

III.10. Valve Design

Another issue that affects many of the current technologies available as Liquid-Cooling-Warming-Garments is a valve system that is bulky, expensive, and requires extensive tubing (Cincinnati Sub-Zero Products). Thus, a second aspect of this project is a SolidWorks design of a better valve-system that is less invasive and smaller than current technologies. This was done with 3-D printing techniques and incorporated into the sealed BoPET construction accomplished in previous steps.

The first design iteration was modeled off of the valve used in fluid drip bags manufactured by Pactech, Inc. (Ferber). These have a low profile and are easily accommodated into the outer seal area of the bag (Figure 40). Particularly of note are the indentations on the sides of the valve that allow for the shrinkage of the bag material into these areas. Furthermore, in the heat-sealing process, small portions of the valve material appear to have melted into the seal width, allowing for further strength in the seal around the valve connection.

The next design iteration of the valve connection system (Figure 41) was the addition of two more indentations to allow for extra gripping area for the Mylar®. This came with its own significant issue that was resolved in later iterations: the bottom of the valve created a sharp “lip” that could conceivably puncture the bag and allow for fluid leakage. This is a key issue, particularly if working in sterile environments as the leakage of non-sterile fluid could cause infection and/or contamination. Furthermore, this could lead to loss of effective cooling fluid and discomfort from the sensation of being wet.

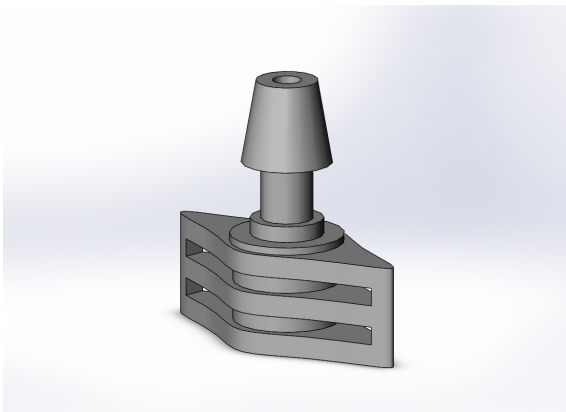


Figure 40: 1st Valve Iteration
(Modification of Ferber)

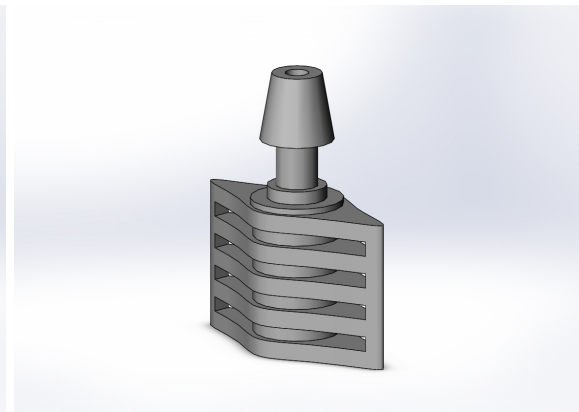


Figure 41: 2nd Valve Iteration

The current design iterations (Figure 42) taper the ends of the valve to eliminate this sharp lip and allows for increased fluid-flow area to prevent valve blowout and/or stress concentrations.

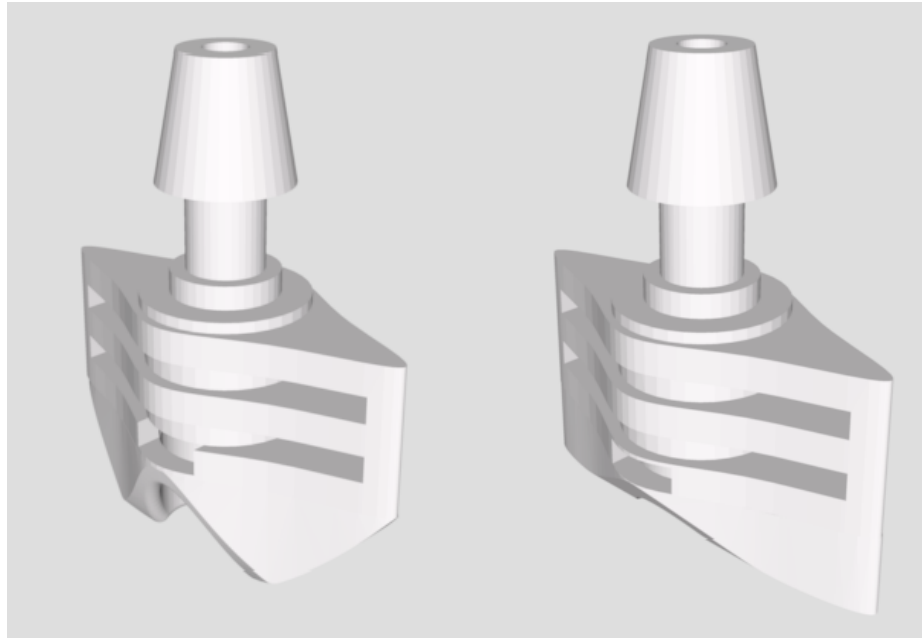


Figure 42: Two valve iterations with tapered ends.

III.11. Assembly of FCS

The initial idea was to eliminate the use of adhesive and purely use heat-sealing techniques to seal the 3D printed valves in between the layers of the Mylar® material. This caused several issues. First, the controlled application of heat was difficult to regulate and maintain. The Mylar® material was unable to heat seal directly into the recessed areas on the valve due to inconsistency in technique. Too much slack in material was allowed and the subsequent shrinkage of the Mylar® was not sufficient to grab the PET valves. Furthermore, when direct heat was applied with the flat iron in an attempt to

fuse the two materials together, the Mylar® was able to shrink and grab hold of the valve, but this subsequently caused the 3D printed material to reach its glass transition temperature and deform from its printed shape (Figure 43). This would cause continuity issues with the construction and could impede fluid flow.

A final heating apparatus was used to apply indirect heat to the layers of unsealed BoPET and the 3D printed valves: a heat gun used for heat shrink tubing (NEX, Inc.). This allowed heat upwards of 170 degrees Celsius to be applied indirectly to the area needing to be sealed. In combination with a small amount of Super Glue and the area being held in tension with two tissue clamping forceps (Figure 44), the valves were able to hold in the inlet and outlet portions of the construct and hold their place. Tests to quantify this strength are considerations for further work, but the addition of fluid flow to this construct will serve as proof-of-concept that the system can withstand fluid pressures without blowout.



Figure 43: Deformation of PLA valves with application of direct heat. Front, Top, and Bottom Views of deformation (clockwise from top left).



Figure 44: Tissue clamping forceps holding valve and Mylar® in tension for application of heat to area.

The final iteration of this FCS prototype includes the use of “snaps” to allow the system to be held in place with current garment systems and incorporated into existing technologies. These are placed strategically throughout the FCS construct to allow the system to be fixed adjacent to the wearer’s targeted high density tissue while still allowing for free range of motion (Figure 45).

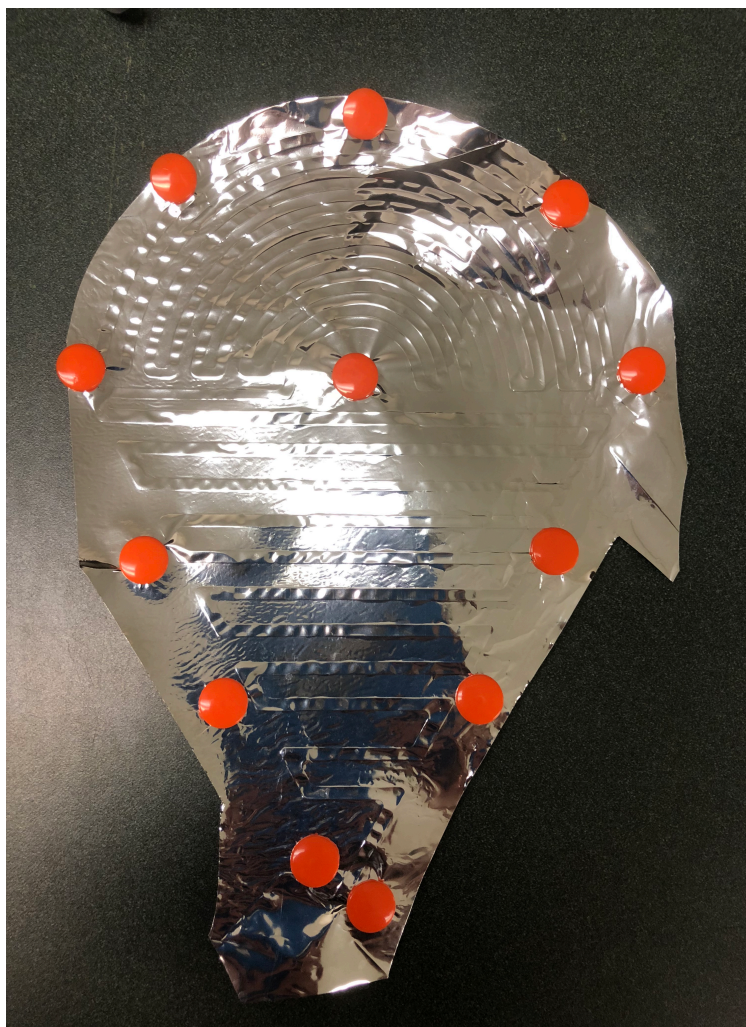


Figure 45: Snap configuration in deltoid FCS to allow for 3D deformation compensation.

CHAPTER 4: RESULTS

IV.1. Temperature Testing of Sealing Press Device

In order to quantify the temperature characteristics of the sealing press device, the temperature profile was completed across specific areas of the press plates. Temperature was measured at discrete time points (every 30 seconds) in a controlled laboratory environment with an average ambient room temperature of 18.9 °C. Temperatures were measured for 20 minutes and 30 minutes for the unmodified and modified press respectively (see Appendix B). The longer measurement time was a function of the heat dissipation in the thicker aluminum plates – they required much longer to reach their temperature plateau as shown in the data (Figures 46, 47, 48). After 30 minutes in the modified press construct experiment it was shown the temperatures necessary to seal the BoPET were attained, so tests were completed at this time point. It is possible that the system could have reached higher temperatures, but was of no consequence for the purposes of this project.

There was a significantly longer time ($t(4) = 38.463$, $p < 0.001$) to reach the required 150-degree sealing temperature used throughout the sample preparation (significance was set at $\alpha = 0.05$ for all statistical analysis). It took the modified press device 19.8 +/- 1.15 minutes vs. 8.4 +/- 0.22 minutes in the unmodified press to reach the necessary sealing temperature. Although pre-heat time was significantly longer than the

unmodified press, the fact that the modified plates did not affect the eventual temperatures reached in the press device was the key takeaway from this testing.

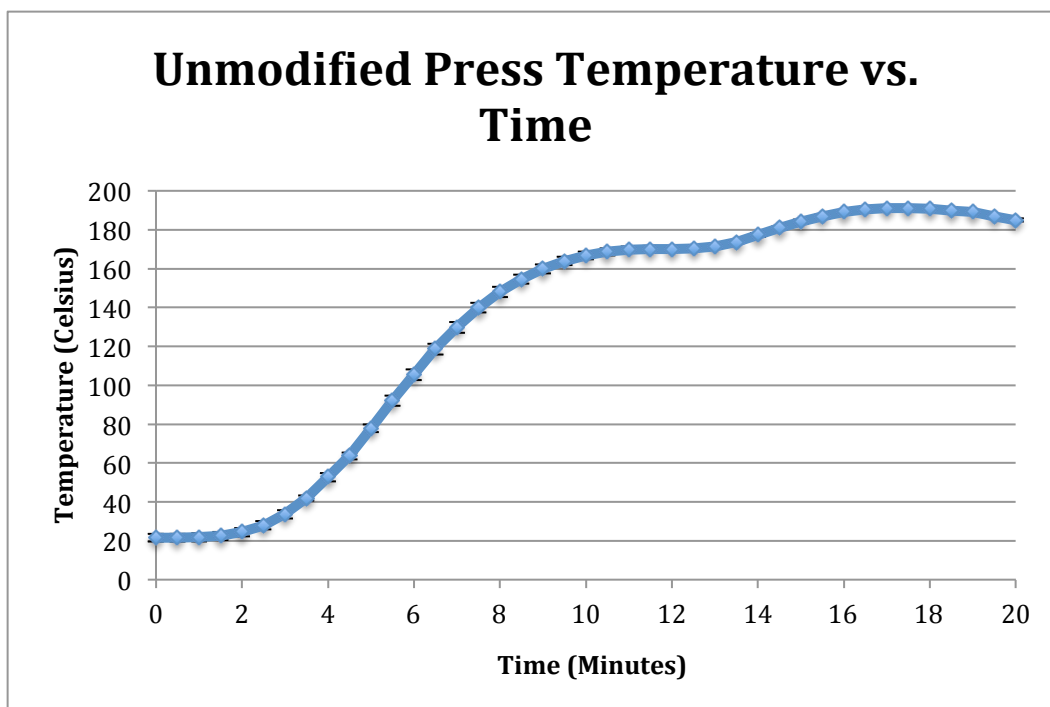


Figure 46: Temperature profile of unmodified sealing press (n=5 trials).

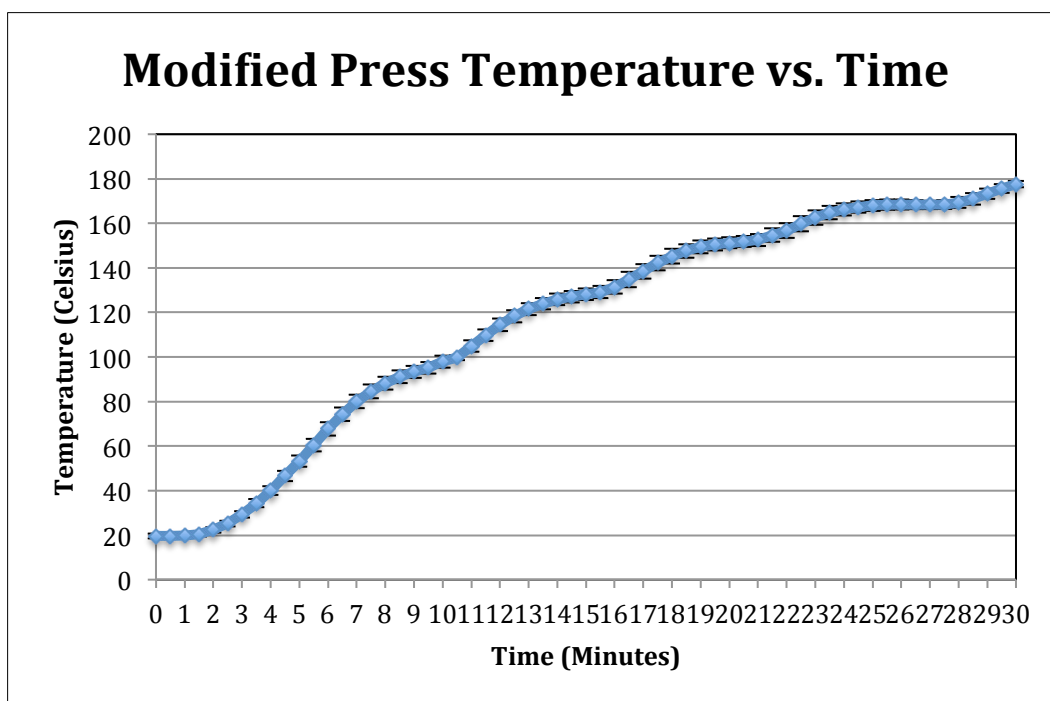


Figure 47: Temperature profile of modified sealing press (n=5 trials).

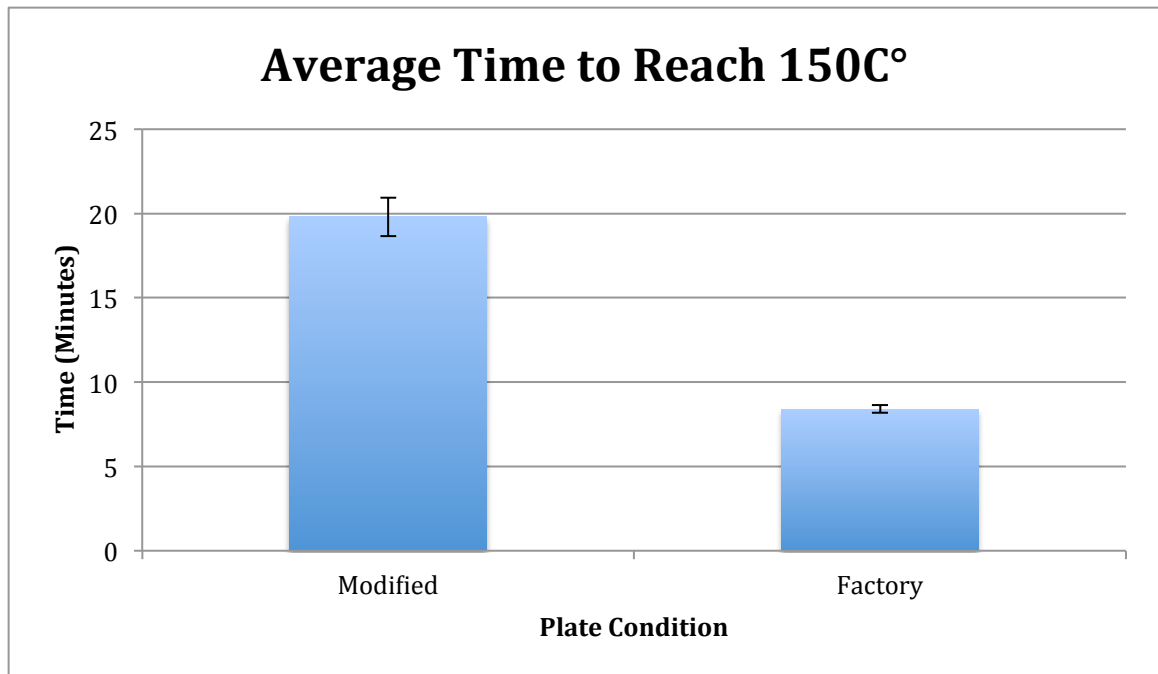


Figure 48: Average time to reach sample preparation temperature (to nearest 30 seconds) ($p < 0.001$; $n = 5$ trials).

IV.2. ASTM Peel Testing

The ASTM F88 protocol was followed for peel testing of the different sample areas at each dwell time and thickness condition. There was a large amount of inconsistency in the profiles of each of the load vs. position graphs recorded for each specimen, but there were some general trends that seemed to develop.

IV.2.1. Data Aggregation

During sample preparation for the ASTM F88 Peel test, it was determined that the 7.5-mil Mylar thickness did not allow for a seal to be created with the respective 10 and 30 second dwell times. There was an ineffective and incomplete seal formed, particularly in areas A and B (internal areas) of the fluid channel design (see Figure 35). As a result

of the small number of samples that were able to be collected from areas C and D (external areas) of the 7.5mil-constructs no thick specimens were used in data analysis.

Due to design constraints, samples in areas A and B could only be cut to 1/8" widths compared to the 1" width of areas C and D. After normalizing to the 1" seal width (by multiplying the strength recorded by a factor of 8), there was no significant difference between the two groups (internal and external seal area) ($t(129) = 0.491$, $p=0.631$) (Table 6). After normalizing data, all specimen areas were aggregated based on material thickness and dwell time. Because the 7.5-mil thickness was eliminated from the analysis a simple 2x2 ANOVA was performed in SPSS.

<u>Sample Areas</u>	<u>Mean Strength (lbs)</u>	<u>t-value</u>	<u>df</u>	<u>p-value</u>
A and B (w/o normalization) Internal Area	0.846 ± 0.582	-12.895	81.295	1.4302E-21
A and B (w/ normalization) Internal Area	6.767 ± 4.655	0.491	129	0.631
C, D External Area	6.402 ± 3.723	--	--	--

Table 6: Data aggregated based on seal area.

IV.2.2. Two-Way-ANOVA

A two-way ANOVA was performed to determine the effects of material thickness and dwell time on overall seal strength for the aggregated data. All samples for each thickness (2 mil, 5mil) and dwell time (10sec, 30sec) regardless of their sample area were

aggregated into one set for analysis (see Appendix C). Significance was set to $p=0.05$ a priori. The average, standard deviation, and number of samples for each group can be found in Table 7.

Thickness	Dwell Time	Mean	Std. Deviation	N
2mil	10seconds	6.0729	2.81311	35
	30seconds	6.5273	3.27530	33
	Total	6.2934	3.03180	68
5mil	10seconds	7.8876	5.09691	33
	30seconds	5.7266	4.78229	32
	Total	6.8237	5.02519	65
Total	10seconds	6.9535	4.15432	68
	30seconds	6.1331	4.07485	65
	Total	6.5526	4.12068	133

Table 7: Aggregated data from ASTM F88 testing.

There were no significant differences found in either the thickness' ($F(129,1) = .512, p=.476$) or dwell time's ($F(129,1) = 1.449, p=.231$) effect on peel strength. These tests had an observed power of .109 and .223 respectively (Figure 50, 51). Furthermore, the analysis of the dual effect of Thickness and Dwell Time on peel strength showed a positive relationship to seal strength, but did not reach significance ($F(129,1) = 3.404, p=0.067; \text{power}=.449$) (Figure 52). Figure 49 shows the standard deviation as a percentage of the mean, and the 5mil group showed a much higher corresponding variance of seal strength

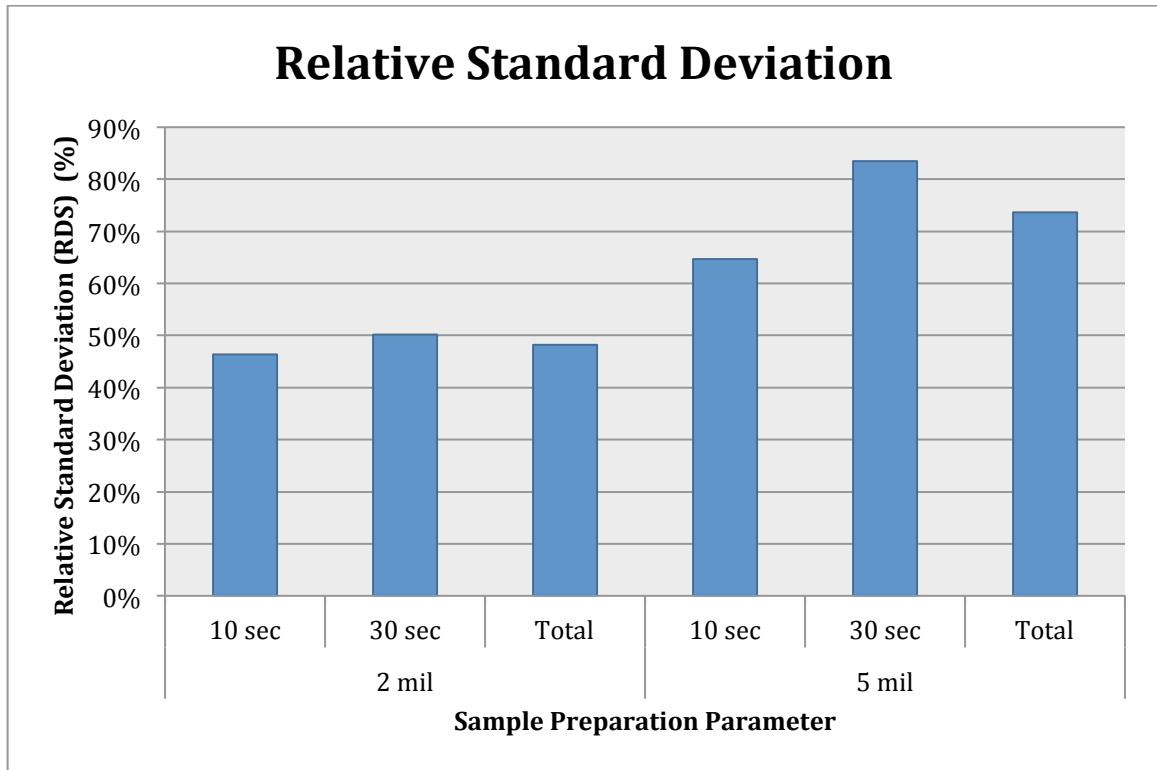


Figure 49: Relative Standard Deviation of ASTM F88. Taken as standard deviation divided by mean, multiplied by 100 (Keeny, Texas A&M).

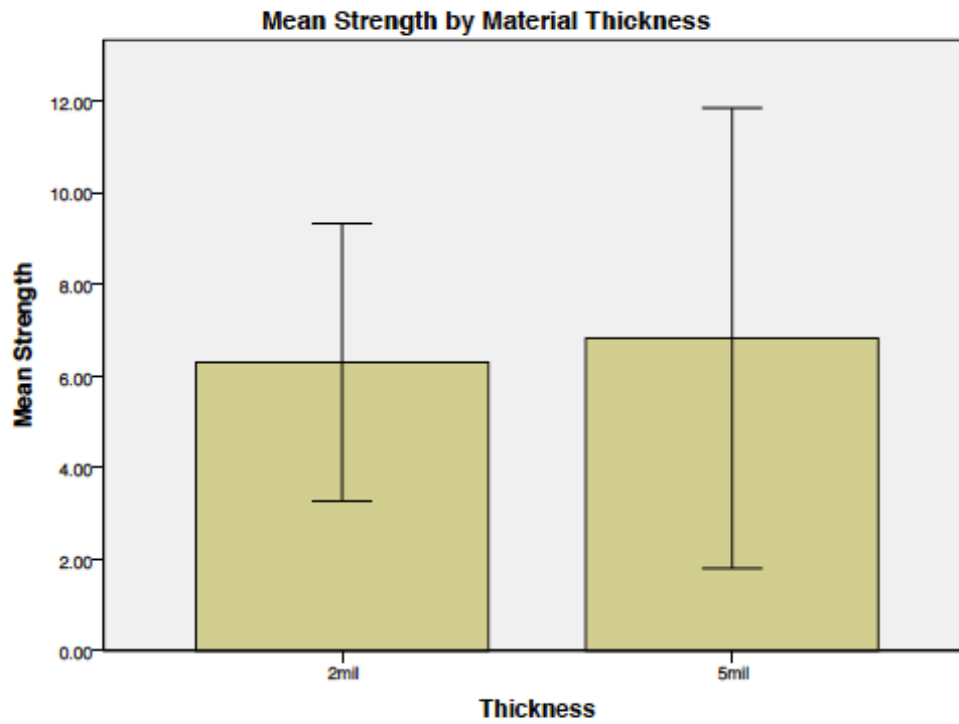


Figure 50: Mean Peel Strength by Material Thickness in Pounds (Error Bars: +/- 1 SD).

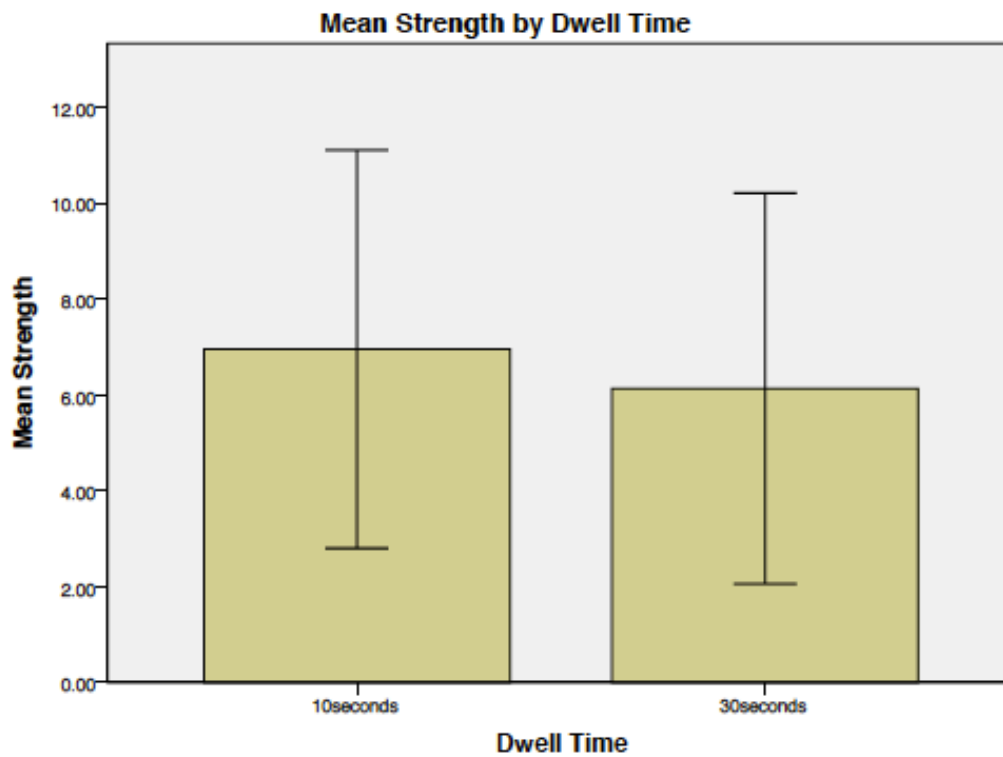


Figure 51: Mean Peel Strength by Dwell Time in Pounds (Error Bars: +/- 1 SD).

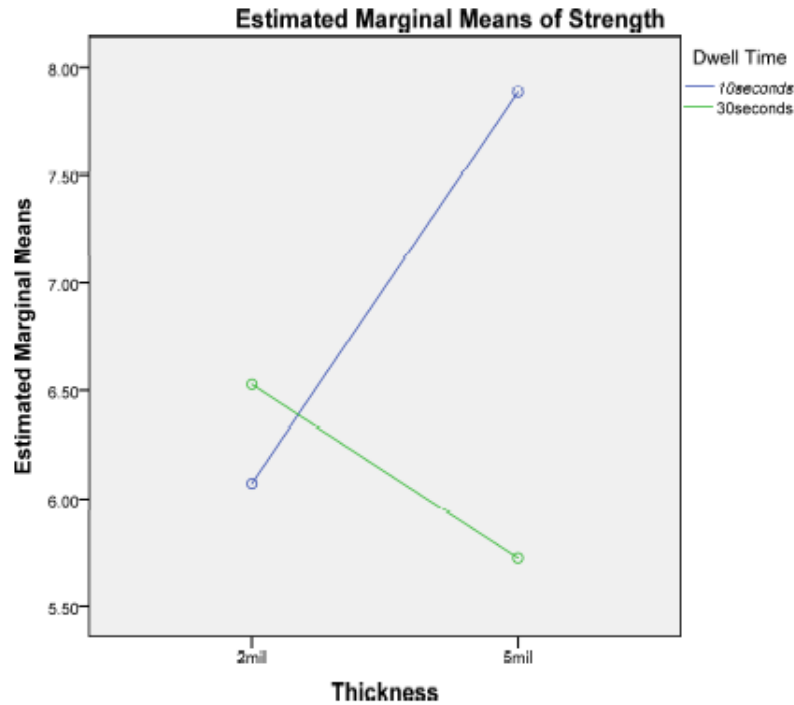


Figure 52: Thickness and Dwell Time Interaction via Means of Strength.

IV.2.3. Method of Sample Break

An additional factor that was recorded during the ASTM peel testing protocol was the method of specimen break. This is an important design consideration to determine if the highest forces seen resulted in material break (which would indicate the material properties are a factor in peel strength), an adhesive peel (which would indicate the seal formed was insufficient), or a combination of both (presence of adhesive peel and material break). When observing the load vs. position graphs of these two conditions, there were stark differences as seen in Figures 53 and 54. A Two-Way ANOVA was performed between sample break (material break, adhesive peel, or both) and the presence of delamination (yes or no) to determine if there were significant effects of these

conditions on peel strength. It was hypothesized that the method of sample break would have a significant effect on peel strength at a $p=0.05$ level set a priori.

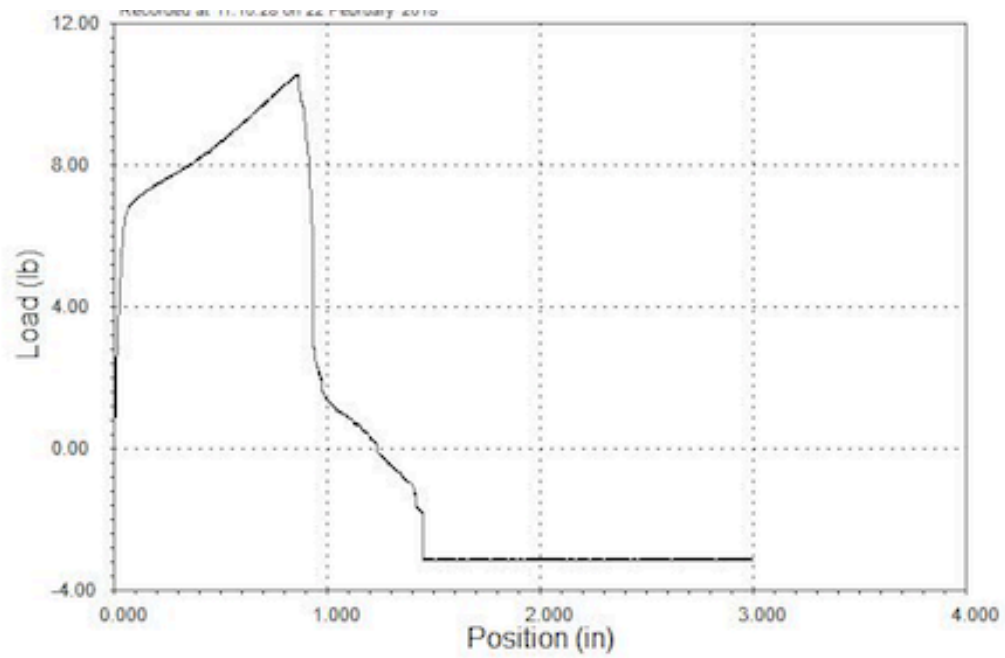


Figure 53: Graph of position vs. load in sample undergoing a material break with delamination.

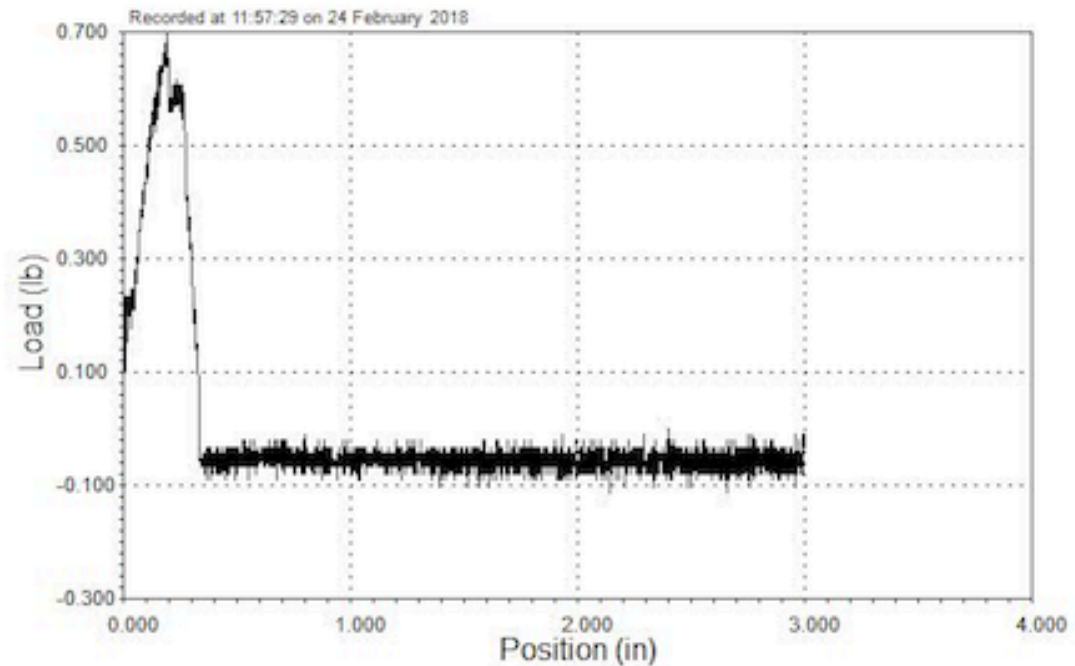


Figure 54: Graph of position vs. load in sample undergoing an adhesive peel without delamination.

The mean, standard deviation, and sample number for each of the method of peel conditions and corresponding sample strength can be seen below in Table 8.

Method of Sample Break	Delamination	Mean	Std. Deviation	N
MaterialBreak	Delamination	8.6762	3.09283	42
	NoDelamination	9.2750	3.14870	8
	Total	8.7720	3.07723	50
Both	Delamination	9.5078	3.73463	18
	NoDelamination	4.7050	.38891	2
	Total	9.0275	3.83047	20
AdhesivePeel	Delamination	7.1363	2.69843	27
	NoDelamination	1.6572	1.39946	36
	Total	4.0054	3.41022	63
Total	Delamination	8.3703	3.21144	87
	NoDelamination	3.1146	3.40987	46
	Total	6.5526	4.12068	133

Table 8: Aggregated data from ASTM F88 testing via method of break and delamination.

Results from the ANOVA showed significant differences between both the method of sample break ($F(127,2) = 26.827, p < 0.001$) and presence of delamination ($F(127,1) = 16.181, p < 0.001$) on corresponding peel strength. There was also an observed significant interaction of both method of sample break and the presence of delamination ($F(127,2) = 11.628, p < 0.001$). These tests had observed powers of 1.000, .979, and .993 respectively. Graphically the results can be seen in Figure 55 for the method of material break, and Figure 56 for the presence of delamination. There was a corresponding decrease in sample strength across all method of break groups when the samples showed no delamination, with the exception of the material break condition which showed a slightly higher average peel strength than the specimens that showed delamination (Figure 57).

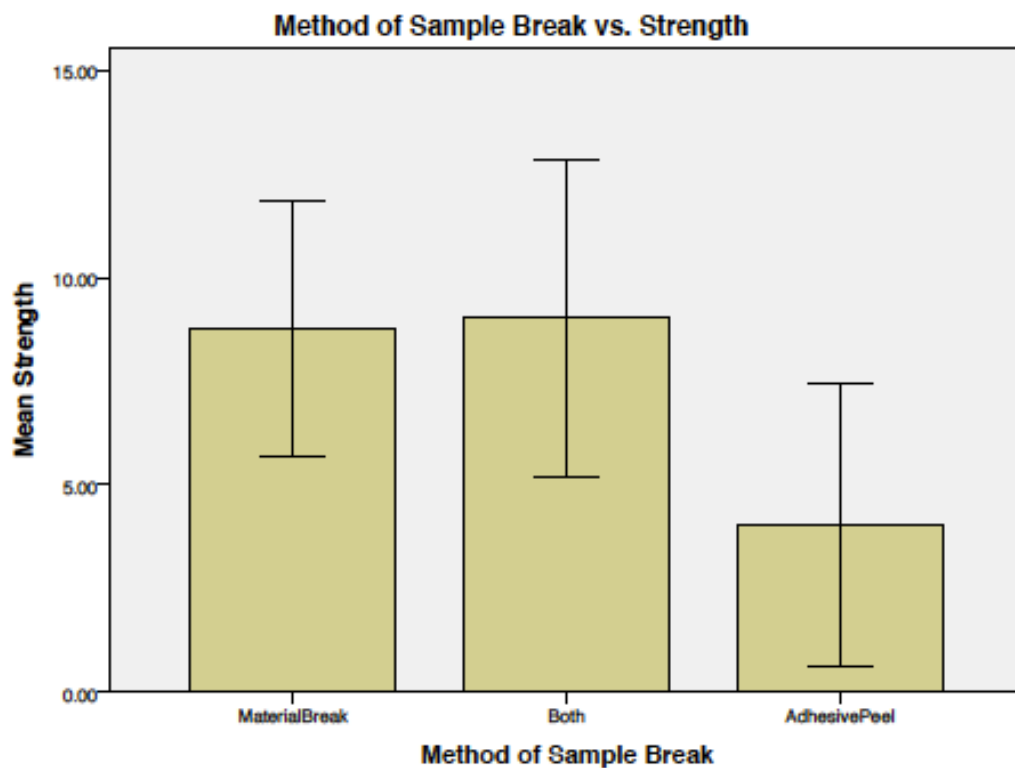


Figure 55: Method of Sample Break vs. Strength (lbs) (Error Bars: +/- 1 SD). Material Break and Both (Material Break and Adhesive Peel) showed significant differences ($p < 0.001$) compared to Adhesive Peel alone.

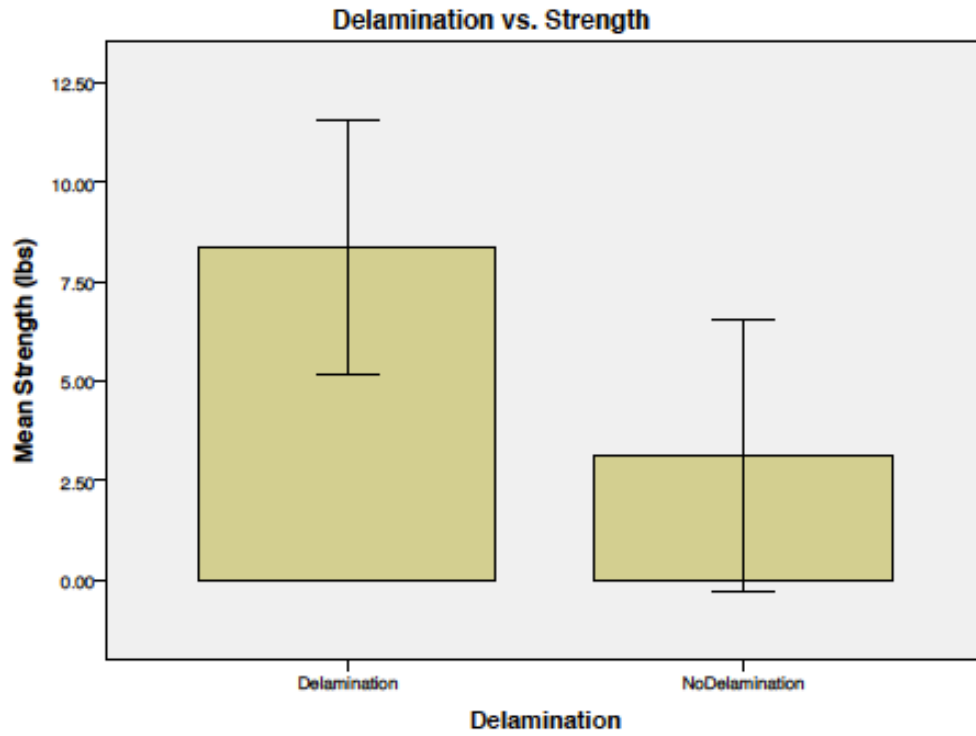


Figure 56: Presence of Delamination vs. Strength (lbs) (Error Bars: +/- 1 SD). Delamination showed significantly higher peel strength than No Delamination ($p < 0.001$).

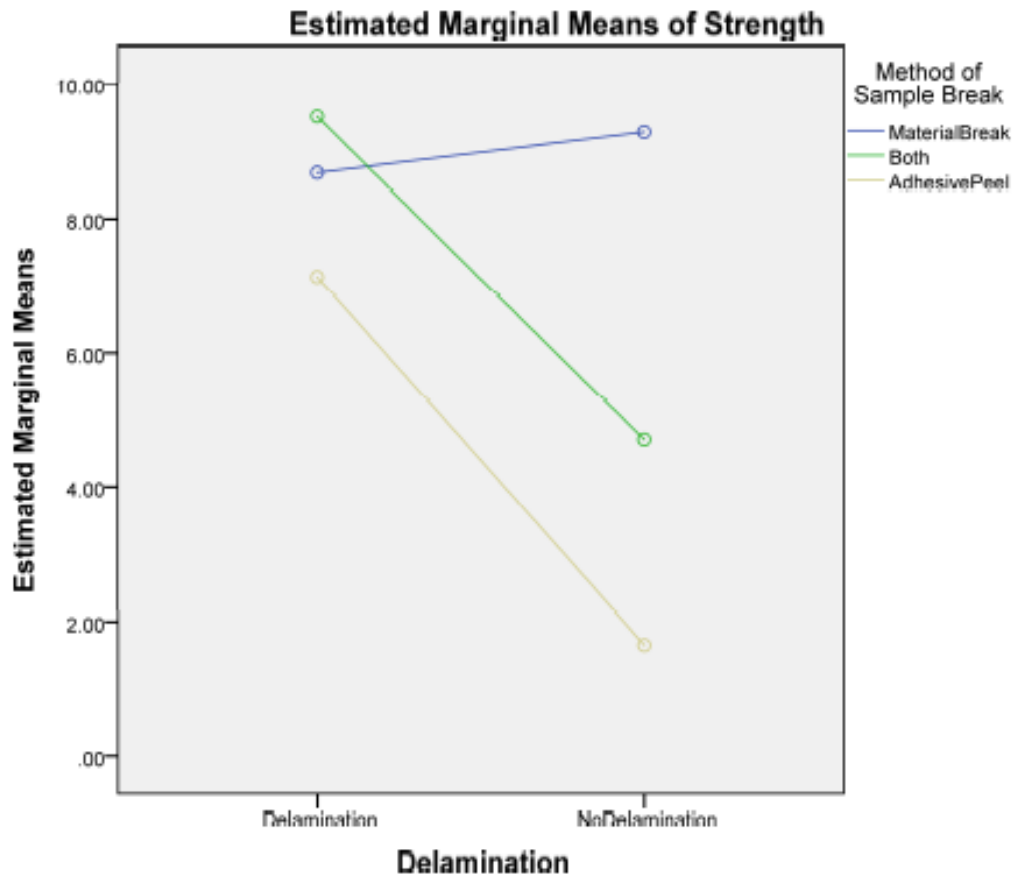


Figure 57: Aggregated Results of Delamination and Method of Sample Break Interaction.

A Tukey's HSD post-hoc analysis of the results showed a significant difference between the material break and adhesive peel groups (Mean difference = 4.766, $p < 0.001$) and between the material break/adhesive peel (both) and adhesive peel groups (Mean difference = 5.0221, $p < 0.001$). There was no significant difference between the material break and material break/adhesive peel (both) groups (Mean difference = .2555, $p = 0.934$).

Results showed that the specimens that underwent a material break were significantly stronger than those that underwent an adhesive peel (Mean difference =

4.766, $p < 0.001$). 57.4% of the 2mil samples underwent a material break alone (with another 16.2% undergoing both a material break and adhesive peel together), compared to just 16.9% of the samples in the 5mil thickness (with 13.8% undergoing both material break and adhesive peel). The aggregated results of method of sample break based on material thickness is presented below in Table 9 and shown graphically in Figure 58.

Thickness	Method of Break	Number of Samples	%
2mil	Material Break	39	57.35
	Both	11	16.17
	Adhesive Peel	18	26.47
	Total	68	100
5mil	Material Break	11	16.92
	Both	9	13.84
	Adhesive Peel	45	69.23
	Total	65	100

Table 9: Thickness vs. method of break in ASTM F88.

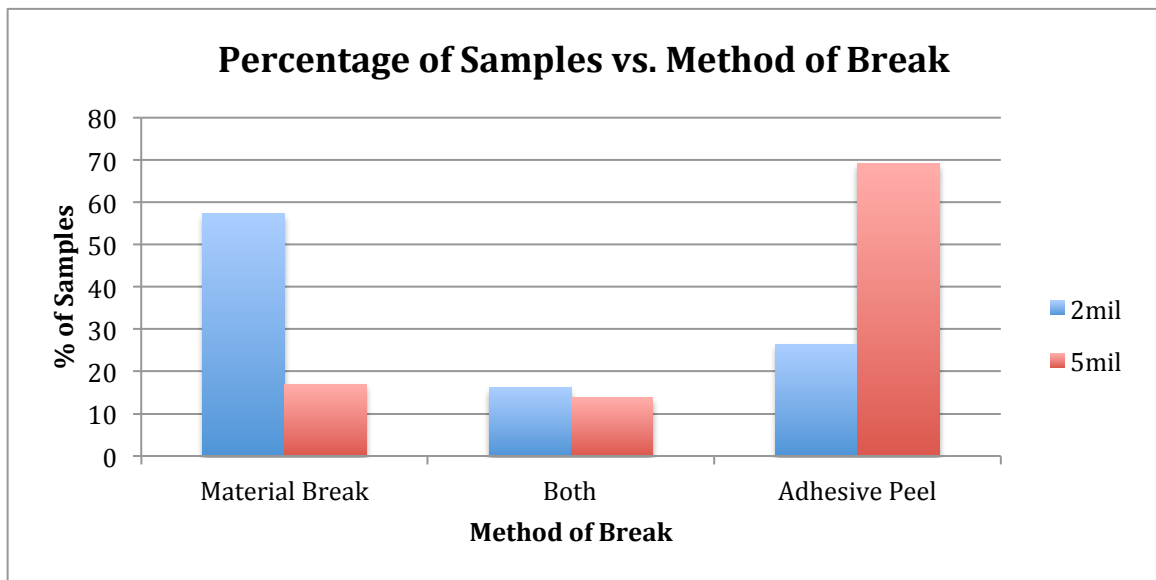


Figure 58: Thickness vs. Method of Break in ASTM F88 (shown as percentage of samples).

Results showed a difference between the 10 and 30-second dwell time in the percentages of samples that failed via material break. There was a slightly higher percentage at 42.7% compared to 32.3% for 10 second and 30-second dwell times respectively. This data can be seen below in Table 10 and graphically in Figure 59. From this data, both the 10 and 30-second dwell times still need to be considered for the 2mil thickness.

Dwell Time	Method of Break	Number of Samples	%
10 sec	Material Break	29	42.64
	Both	11	16.17
	Adhesive Peel	28	41.17
	Total	68	100
30 sec	Material Break	21	32.31
	Both	9	13.85
	Adhesive Peel	35	53.85
	Total	65	100

Table 10: Dwell time vs. method of break in ASTM F88.

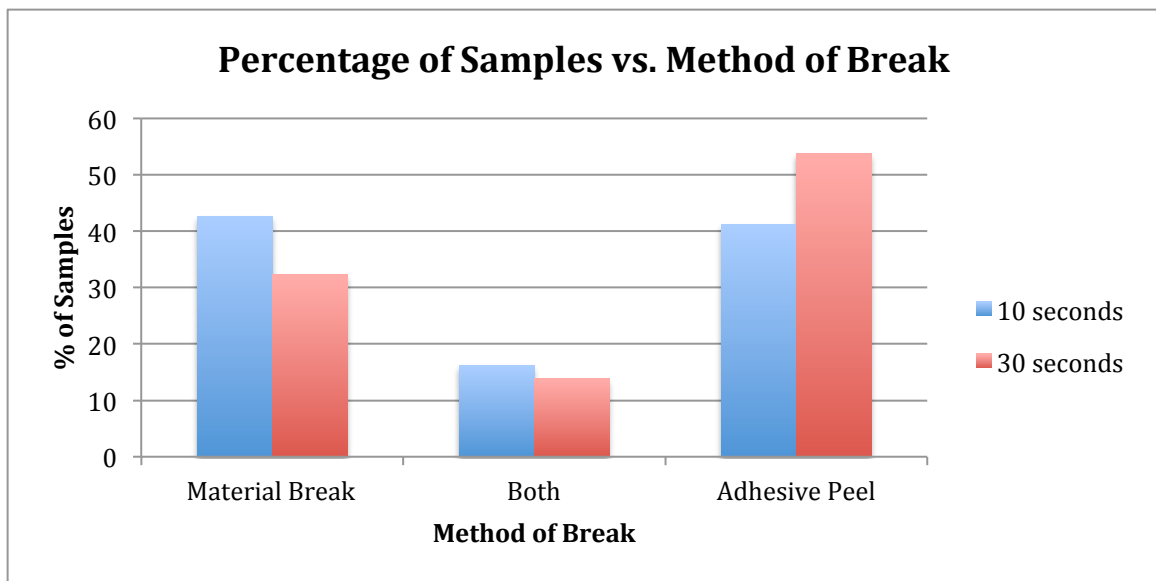


Figure 59: Dwell Time vs. Method of Break in ASTM F88 (shown as percentage of samples).

Looking at the presence of delamination in the thickness and dwell time conditions, there was a higher rate in the 2mil than 5mil (70.6% vs. 60%) and in the 10-second than 30-second (70.6% vs. 60%) dwell time conditions.

IV.3. ASTM Burst Testing

IV.3.1. Sample Preparation

During sample preparation for the ASTM D642 Burst test, several key discoveries were made. As a function of the material properties of the Mylar constructs, the fluid channels flatten closed without fluid flowing through them. This created a particular challenge when filling them with fluid for the burst testing. Furthermore, the long channel design created extremely high-pressure buildup, making it virtually impossible to fill the entire channel length with fluid for burst testing. Although compressed air would fill the entire construct, filling it with an incompressible fluid such as water did not create enough outward pressure to open these channels. As a result of this finding, the constructs were cut in top-and-bottom halves (Figure 40), decreasing the residual pressure buildup and allowing for the lower portion of the FCS to be tested in the Burst Test.

IV.3.2. Data Aggregation and Analysis

A plot of the load vs. deformation graph of one of the samples can be seen below in Figure 60. The local maximum at 0.38in and corresponding drop in the load measurement correlates with the burst of the sample.

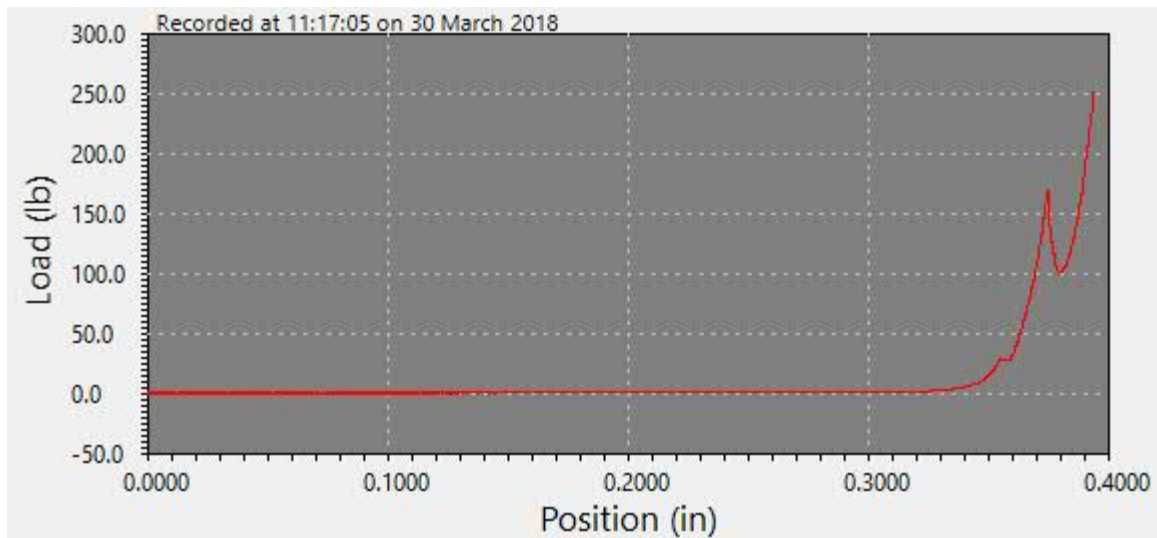


Figure 60: Plot of Load vs. Position in ASTM D642 Burst Test.

N=9 samples were obtained from the 2mil, 10-second dwell time and n=10 were taken from the 2mil, 30-second dwell time. Descriptive statistics was able to detect the presence of two outliers in the 10-second dwell time (Figure 61), which were eliminated in data post-processing for both burst strength and deformation (Appendix E), defined as ≥ 1.5 times the inter-quartile range of the mean burst value. They were eliminated in both groups because their status as outliers indicated the samples were not properly prepared according to the protocol – leading to such high burst strength relative to the other samples. Three samples were corrupted during the testing procedure for the 30-second dwell time, so an equal n=7 for each group was obtained for analysis. The aggregated results of the testing can be seen in Table 11.

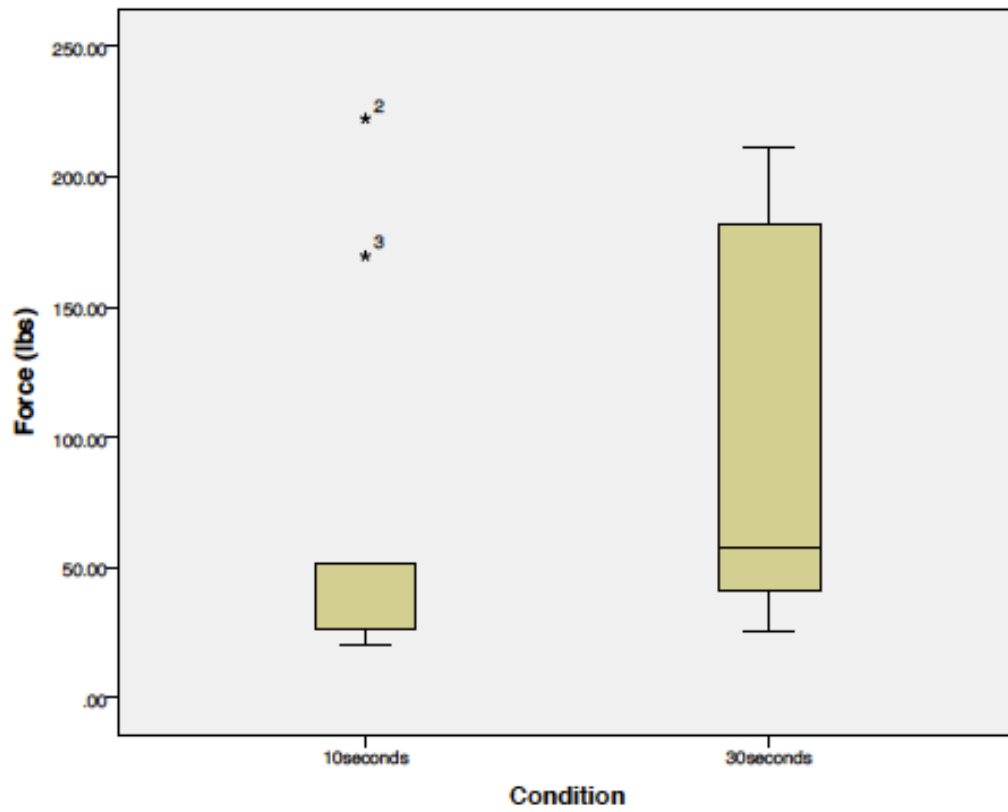


Figure 61: Boxplot to detect presence of outliers in Burst Strength. Two outliers were found in the 10-second dwell time condition. Outlier is defined as ≥ 1.5 -times the inter-quartile range.

	Condition	N	Mean	Std. Deviation	Std. Error Mean
Force (lbs)	2mil,10sec	7	28.67046143	10.45723408	3.952462968
	2mil,30sec	7	105.8139060	81.92572412	30.96501314

Table 11: ASTM D642 burst strength (lbs) with two outliers eliminated.

Levene's test for equality of variances showed a significant difference ($F=64.676$, $p<0.001$), so a two-tailed t-test with unequal variances was chosen to compare the two experimental conditions. The results of this t-test showed that there was significantly higher burst strength in the 2mil, 30-second condition ($t(6.195) = -2.471$, $p=0.047$) than the 2mil, 10-second dwell time condition. This can be seen graphically in Figure 62.

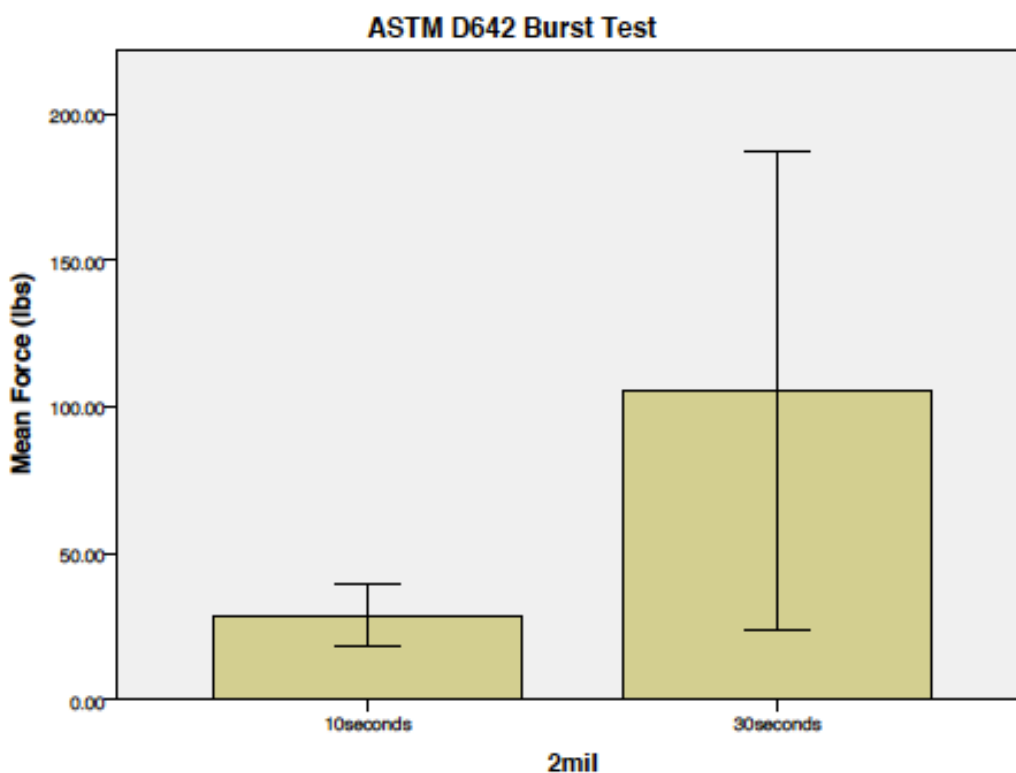


Figure 62: Burst Strength (lbs) results of ASTM D642 Burst Test (Error bars: +/- 1 Standard Deviation) ($p=0.047$).

There was a high standard deviation associated with the 30-second dwell time. The relative standard deviation (RSD) of the 30-second dwell time was 77.42%

compared to 36.47% in the 10-second dwell time. This is indicative of the high between-sample variability seen in the sample preparation for this burst testing protocol.

An additional variable that was considered in this was the deformation of the fixed-platen testing apparatus at which burst occurred. This was standardized for each trial with the use of the ADMET's "home" feature, which set the initial level consistent for each specimen. Descriptive statistics showed no outliers for the values of deformation, so the $n=7$ from the burst strength were used from each group. Results of this comparison can be seen below in Table 12 and Figure 63. Since Levene's test for equality of variances showed no significant difference ($F=.101$, $p=0.756$), a two-tailed t -test with equal variances was used to compare the groups. There was no significant difference between the 10-second and 30-second dwell time in terms of overall deformation at burst ($t(11.923) = -2.008$, $p=0.068$).

	Condition	N	Mean	Std. Deviation	Std. Error Mean
Deformation	10seconds	7	.36180	.008982	.003395
	30seconds	7	.37186	.009735	.003679

Table 12: Aggregated deformation results from ASTM F88.

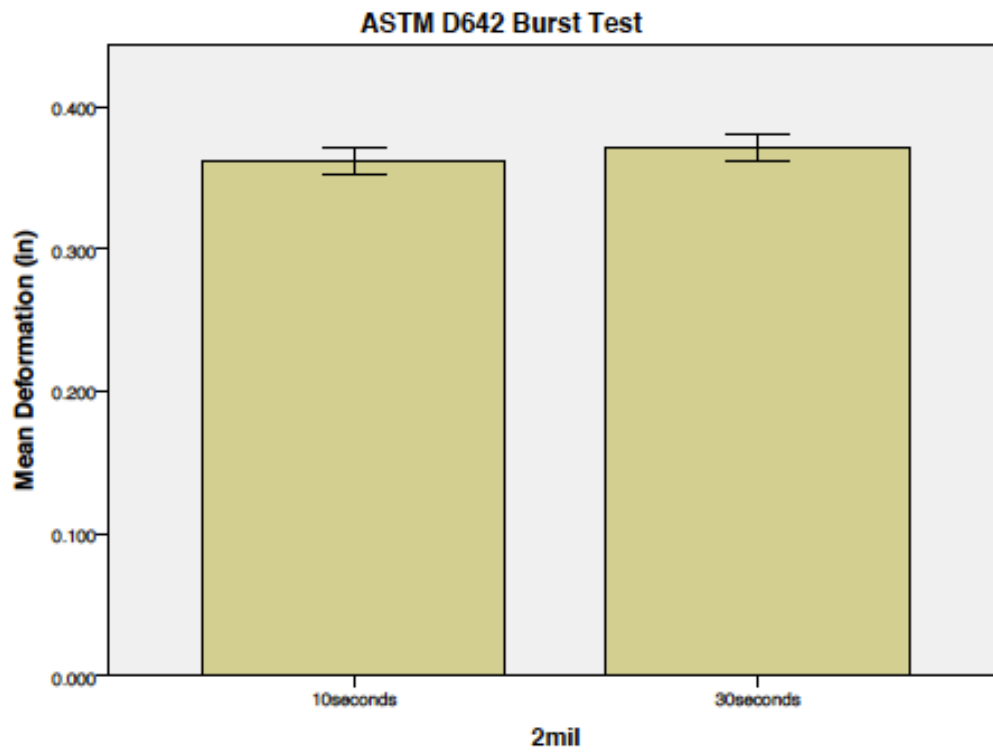


Figure 63: Deformation (in) results of ASTM D642 Burst Test (Error bars: +/- 1 Standard Deviation) ($p=0.068$).

CHAPTER 5: **DISCUSSION**

V.1. Overview

This study created and measured a key component for a physiologically based liquid cooling warming garment that can be used to alleviate the physiological and psychological effects of repetitive/fatiguing tasks. No known published work has used BoPET fluid channel systems that can be integrated into existing technologies easily and effectively. Testing of the prototype BoPET fluid channel system identified key design criteria and limitations, but proved that the concept is valid for creating a heat-sealed FCS. Mechanical peel and burst testing were able to quantify the strength of the sealed systems and determine they were consistent with those that might be seen with commercial fluid chiller systems. Testing showed that different material thickness and heat seal dwell time had no significant impact on the strength of the material, thus other factors such as manufacturability, heat transfer phenomena, and ease of integration into current systems must be considered when determining the materials needed for this application. Furthermore, the sample preparation in burst testing showed the need for a more effective sealing pattern than the current iteration – with larger fluid channels to further open the channels in the constructs and allow for uninterrupted fluid flow throughout the channeled fluid system.

V.2. Temperature Testing

Using thicker plates with the current press system required more time to preheat but proved to be of no consequence in fabricating the fluid channel system. Another issue that needed to be addressed when measuring the temperatures of the modified press device was whether or not there would be residual warping of the aluminum plating that could effect reservoir fabrication. This was particularly necessary for the small width of the internal fluid channels, as any warping could make these impossible to heat seal. No definitive warping temperature could be found in prior literature, but the temperatures reached in the current press design were a factor of 10 below published melting temperatures for 6061 aluminum (Aerospace Specification Metals, Inc.), eliminating this concern. This may be an insignificant issue if channel dimensions are increased. Furthermore, the presence of the “three dimensional dots” that impeded flow in our fluid channel system constructs could also be eliminated with the change of press plate dimensions.

V.3. Fluid Pressure Calculations

Bernoulli’s equation was used to estimate the internal fluid pressures that could be seen in our fabricated fluid flow constructs, but is not without some limitations. The simplifying assumptions necessary to come to the final pressure values are: the fluid is a constant density, the fluid is incompressible, and there is laminar flow. The first two assumptions are without issue, but the laminar flow assumption may not be applicable in the fluid channel system. Due to the small diameter of the sealed channels, it was calculated that there would be turbulent flow as modeled in Figure 64. While this is

effective for thermodynamic transfer, the peak pressures the system would see could be higher due to fluid pockets caused by turbulence. Also, these are not direct comparisons to the peel or burst strength, but serve as an additional method to quantify the internal pressures our system would see based on it's current design.

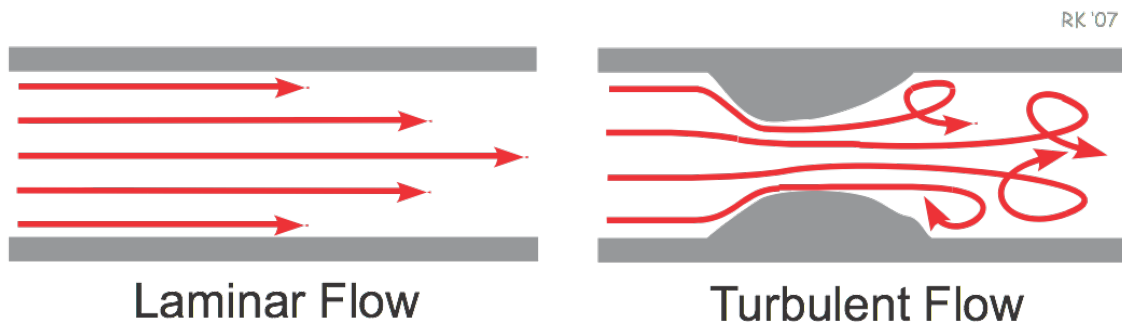


Figure 64: Laminar vs. Turbulent Flow Characteristics (Klabunde).

The turbulent flow allows for better heat transfer due to the fact that there is mixing of the heat within the flow channel, whereas in laminar flow there could be distinct “layers” as seen in Figure 64. This could cause the heat to not transfer as effectively. Further calculations for pressures in turbulent flow are needed for the next stage of this project and are important considerations when designing future iterations of fluid channel constructs.

One way to significantly reduce the fluid pressures seen in the system is to increase the internal diameter of the flow channels (while keeping other parameters consistent). As seen in Figures 65 and 66, by simply doubling the size of the channels from .125in to .25in in diameter, the pressures seen in the system would drop by 10.5%,

and would be only 6.4% higher than the static system pressure alone. For the next iteration of designs, this is an easy way to optimize the system and allow for larger flow channels. This could further increase the heat transfer capabilities and make seals more effective, with larger sealing area between flow channels.

$$Velocity = \frac{.53 \text{ ft}^3/\text{min}}{\pi(.00833 \text{ ft})^2} = 2431 \text{ ft/min} = 12.35 \text{ m/s}$$

$$Pressure (Peak) = 4.4 \text{ psi} + \frac{\rho V^2}{2}$$

$$Pressure (Peak) = 30336.9 \text{ Pa} + \frac{(1000 \text{ kg/m}^3)(12.35 \text{ m/s})^2}{2} = 36511.9 \text{ Pa}$$

$$\mathbf{Pressure (Peak) = 5.23 \text{ Psi}}$$

Figure 65: Calculations of Peak Pressures in FCS with smallest cross-sectional area (See Appendix A).

$$Velocity = \frac{.53 \text{ ft}^3/\text{min}}{\pi(.02083 \text{ ft})^2} = 388.82 \text{ ft/min} = 1.975 \text{ m/s}$$

$$Pressure (Peak) = Pressure (Static) + Pressure (Dynamic) = 4.4 \text{ psi} + \frac{\rho V^2}{2}$$

$$Pressure (Peak) = 30336.9 \text{ Pa} + \frac{(1000 \text{ kg/m}^3)(1.975 \text{ m/s})^2}{2} = 32287.2 \text{ Pa}$$

$$\mathbf{Pressure (Peak) = 4.683 \text{ Psi}}$$

Figure 66: Fluid pressure calculations with internal diameter of 1/4" (.02083ft). (See Appendix A)

V.4. Peel Testing

Based on the results of the ASTM F88 protocol for peel testing, several interesting concepts were uncovered about this type of fluid channel system. Although imperfect, this test was a particularly simple method to quantify the strength of the seal in our system at four distinct regions. After each specimen sample result was normalized by area, there was no significant difference between areas, which allowed the thickness and dwell times effects to be evaluated as a whole.

Using the current protocol the 5mil and 7.5mil thicknesses proved to be ineffective and were not able to be sealed to accommodate fluid flow. Although this was not a manufacturing setting and a high degree of variability existed between each sample, there was a high failure rate associated with the preparation of samples, especially for the 7.5mil material thickness. This was seen many times in the internal specimen areas (A and B in Figure 40) with some groups only allowing for n=1 samples to be pulled. There was extremely high standard deviation in each of the groups, which is a direct result of a low sample number and inconsistency with the sealing method. The relative standard deviation of the 5mil thickness was higher than the 2mil thickness— an indication that its use may not be the most beneficial for the FCS application in terms of manufacturing consistency.

Interesting correlations were found when comparing the method of sample break and presence of delamination. It was shown that there was a statistically significant increase in peel strength when the sample experienced material failure vs. an adhesive peel condition. Material failure was seen in the majority (57.3%) of the 2mil samples, but in very few (16.9%) of the 5mil samples. There was a smaller difference between the 10-

second and 30-second dwell time conditions (42.7% vs. 32.3%). Since the average of the specimens that failed via material break is significantly higher at 8.77 +/- 3.07 pounds vs. the adhesive peel at 4.0 +/- 3.41 pounds the material properties of the thinner material are better in terms of peel strength. Furthermore, there was a significantly higher strength with the presence of delamination (8.37 +/- 3.21 pounds) than with no delamination (3.11 +/- 3.41 pounds). The higher rate of delamination in the 2mil condition shows its use would be beneficial for our application. Since there were no significant effects of any dwell time or material thickness conditions on the peel strength, these choices should be left up to other factors such as method of material break, presence of delamination, thermal transfer to high-density zones, and manufacturability.

V.5. Burst Testing

The ASTM burst test was able to give another quantification for the strength of the developed fluid channel system. Based on the results of the ASTM peel test done previously, only the 2mil thickness at 10-second and 30-second dwell times was tested for burst strength.

The outliers seen in the Burst Strength test are a further indication of the inconsistency of the sealing of the small fluid channels. Although outliers are a part of natural variability, the two outliers seen on the upper end of the data in the 10-second dwell time (222.2 and 169.54 lbs) can be attributed to the method of specimen preparation. Because these two samples were well beyond the ≥ 1.5 -times inter-quartile range these cannot be attributed to natural variability alone. The outer edges of the samples were heat-sealed with the flat iron; they may have affected the corresponding

seal strength in these two samples – causing them to be significantly higher than the other samples. Once these samples were removed from data analysis however, there was a significant difference in burst strength seen between the 10-second and 30-second dwell time conditions ($p=0.047$). This is an indication that the 2mil thickness at 30-second dwell time is the most effective for this fluid channel system application.

There was a high relative standard deviation associated with the 30-second dwell time (77.42%) compared to the 10-second dwell time (36.47%). This can be contributed to the removal of the outliers in the 10-second condition, but also is an indication of the between-sample variability in this method of manufacture. In a manufacturing setting, the quality control of this system can be better maintained, eliminating this high variability.

There was no significant difference in deformation ($p=0.068$) between the 10-second and 30-second groups. There was a positive interaction however that the 30-second group allows for more deformation than the 10-second group. A larger sample size may indicate a more significant interaction between dwell time and overall deformation.

Several of the specimens were also affected by the “pooling” of liquid in the tight corners of the construct. Because the corners in some areas were at a >90 -degree angle, the radius of curvature needed to be large to mitigate the affects of these fluid pockets. This is an important design consideration that must be taken into account for future iterations of the sealing press plates. These pockets could cause backup of the fluid channels and interfere with the thermodynamics of the fluid channel system as a whole. An example of this can be seen in Figure 67.



Figure 67: Presence of fluid pockets at >90 degree corners.

The final factor observed in this protocol is the overall specimen failure rate associated with preparation for the ASTM burst test. A total of $n=9$ and $n=11$ samples (10 second and 30 second groups respectively) were able to be heat-sealed to a point where fluid could be incorporated into the constructs. This is a 77.5% and 72.5% failure rate in the incorporation of fluid into only the lower portion of the constructs after 40 samples were sealed for each condition. This is an extremely high failure rate that should be mitigated in a manufacturing setting. This could be a function of the current preparation methodology, temperatures, or film thickness and further work will have to lower this failure rate by optimizing these conditions. Additionally, the area of specimen break is an interesting factor in order to analyze possible stress concentrations in the FCS, but this was not able to be definitively determined in this experimental procedure.

V.6. Manufacturing Concerns

Although this is not a manufacturing study, there are several key observations made about the manufacturability of this particular fluid channel system. For the mass production of this type of system, being able to optimize manufacturing cost and time is of high importance. Interestingly, there was a higher average maximum peel strength at the 30 second dwell time for the 2mil samples, but at the 10 second dwell time for the 5mil samples as shown in Figure 52. Because there were no statistically significant differences between the thicknesses or dwell times seen, the most ideal material for further use in this system is the one that is most easily manufactured. The thinnest material tested in this scenario (2mil) is easiest to manipulate and would be the least expensive overall. Furthermore, it would allow for the highest degree of heat transfer from fluid to end-user due to the fact that it would be the thinnest barrier between the fluid and the high-density zone. Finally, the thin material would also allow for the most conformity to the user's body as the thicker materials have more rigidity and are less compliant when fluid flow is incorporated.

Several variables that were held constant throughout specimen preparation need to be further studied and optimized for a manufacturing setting. The temperature, dwell times, and sealing pressures used were effective in creating fluid flow constructs for our purposes, but there was a particularly high specimen failure rate, especially in the thicker materials. This is further reasoning to choose a thinner material that would seal more effectively. The possible effects of higher sealing pressures, different temperatures, and other dwell times cannot be ignored. On a larger scale, setting these parameters to their ideal level would decrease the failure rate associated with manufacture. The high failure

rate that was seen within the specimens appeared to be a direct result of the small internal sealing area between the fluid flow areas. Specimens would seal on the outer edges (where there was more sealing area) but would rupture on the internal fluid channels with the addition of fluid. There appeared to be a benefit to a larger sealing area, as the areas of the fluid channel that came into contact with the largest sealing area appeared to seal the most effectively. The presence of material shrinkage as seen below in Figure 68 was the most common method of specimen failure. This tended to occur when samples were not placed in enough tension during preparation or the seal press construct would make contact with the BoPET and shift during heating.

In order to improve and standardize material tension during the current preparation method, a “tension plate” should be fabricated. By using a scrap piece of aluminum with sharp corners to place the BoPET in tension with the current method, there is a finite amount the material can be stretched. Fabrication of a more specific tension plate would eliminate the effects of material shrinkage and lower between-sample variability. Every effort should be made in a manufacturing setting to avoid material shrinkage.

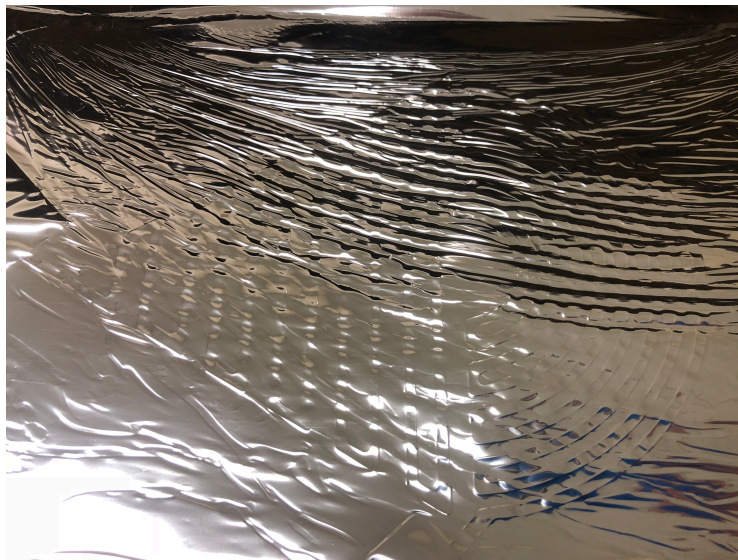


Figure 68: Material shrinkage during specimen preparation.

A final manufacturing consideration is the addition of the fluid channel system into pre-existing protective garments, the final step in full integration of the LCWG. This type of system could be easily incorporated as an additional layer on the internal compartment of protective equipment, which would eliminate its use as an additional layer. The current iteration includes “snaps” as shown in Figure 47 to incorporate it into existing technologies easily, but these snaps would not be necessary if the system were “printed” (heat sealed together) as a part of the existing PPE. This would allow for internal fluid flow to several high-density regions that could be chosen specifically by the wearer. For example, if a physician requests a cooling intervention in their deltoid, antebrachial, and sural regions, those fluid inlets/outlets could be opened with a peel-away closure, while fluid constructs covering other regions of the body (i.e. head, lower back, etc.) are left closed. This would allow one system to work for a number of areas without having to be modified specifically for each individual end-user.

V.7. Further Design Considerations and Future Work

Based on the experimental data and qualitative observations obtained from sample preparation there were several design changes that are necessary to allow for full functionality of the FCS that was developed. First and foremost, the internal flow diameter and channeling pattern needs to be redesigned to allow for greater seal contact area, larger fluid volumes, and corresponding lower internal fluid pressures. It is hypothesized that this would not only decrease the manufacturing failure rate, but would increase the strength of internal flow channels. The minimum flow diameter that should be used in the development of the new plates is .25in, with at least .375in in between each channel for a sealing area. Several new designs have been considered, with some shown below in Figure 69. These designs will be manufactured and used for further development of the FCS, but are by no means the end-all for the most effective design. Further quantification of the fluid properties and peel/burst testing must be accomplished to prove their efficacy.

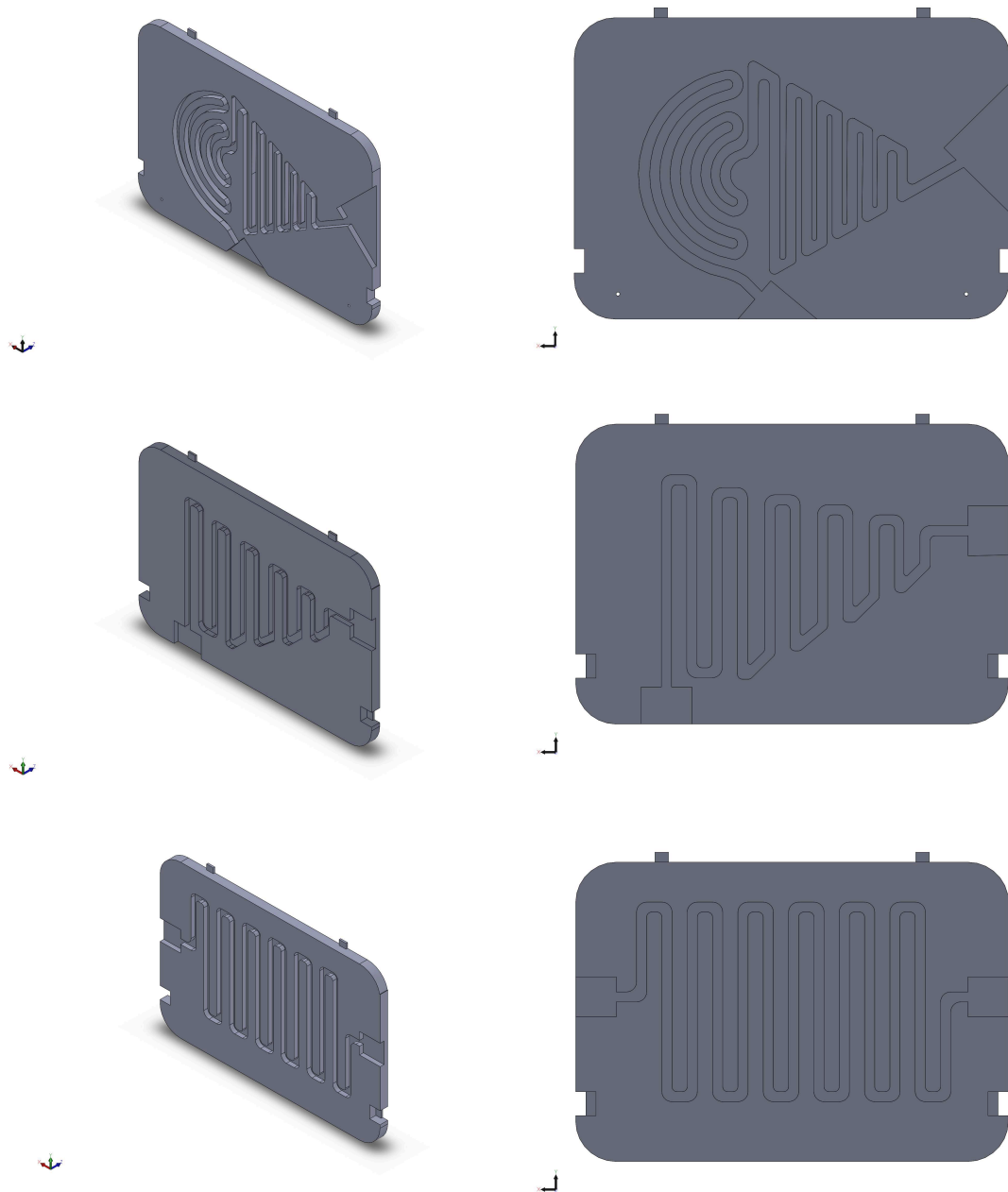


Figure 69: Isometric (Left) and Front (Right) views of additional FCS designs.

Further work is necessary in the redesign of the fluid channels. Particularly seen in the sample preparation for the ASTM D642 Burst Test, the collapse of the material in such a small fluid channel, with small sealing areas, did not facilitate sustainable fluid

flow characteristics. Furthermore, final integration of the valve system into the developed fluid channel construct needs to be accomplished. Although strides have been made in the independent design of both the fluid channel system and the valve connections, full integration has yet to be completed. The material properties of the BoPET and PLA valves may need to be reevaluated for the most cost effective and most manufacturable combination of the two systems.

One particular aspect of this system that is of high importance is the 3-dimensional space that would be occupied when fluid flow is incorporated into the system. The flow would cause the system to “flatten” away from the user’s body and occupy the 3-dimensional space directly outward, away from the high-density zone. This can be corrected with the use of snaps by holding the system flush with the user’s targeted cooling area. Future iterations should aim to eliminate the use of these and incorporate the FCS directly into the personal protective garments.

Finally, the thermodynamic heat transfer properties of the system need to be studied and established. Although it is anticipated that this system should be much easier to control than the current, commercially available systems the system’s thermodynamic properties of will need to be established before full integration into current technologies. The idea has also been discussed to include additional layers of material within the fluid channel system to allow for temperature, haptic, or EMG feedback from the user. These feedback mechanisms would allow for the system to self-regulate the temperature-modulation intervention.

V.8. Conclusions

The fabrication of a fluid channel system made from heat-sealed thin-film BoPET has shown to be a viable option for LCWG systems. Although several steps will need to be taken before a final commercial product design is confirmed, the iterative prototypes of fluid channel design, quantification of the strength of the heat sealed materials, and development of a low-profile valve connection have led to the filing of a provisional patent for the present invention. The methodologies used in this work were able to show the 2mil thickness at 30 second dwell time was the best for this type of fluid channel system application and can be modified to any high-density region throughout a user's anatomy. This method of providing physiologically targeted cooling to wearers in high temperature and high fatigue environments shows extreme promise as a cost-effective and disruptive challenge to existing technologies.

APPENDIX A – Bernoulli and Reynolds Number Equation Variables

$$\text{Pressure (Peak)} = \text{Pressure (Static)} + \text{Pressure (Dynamic)}$$

$$* \text{Pressure (Static)} = 4.4 \text{ psi}, \text{ Pressure (Dynamic)} = \frac{\rho V^2}{2}$$

$$\# \rho = \text{Density of Fluid (water, 5C)} = 1000 \text{ kg/m}^3$$

$$V = \text{Fluid Velocity} = \frac{\text{Flow Rate (ft}^3/\text{min)}}{\text{Cross – Sectional Area (ft}^2\text{)}}$$

$$* \text{Flow Rate} = 3.96 \frac{\text{Gallons}}{\text{Minute}} = .53 \text{ ft}^3/\text{min}$$

$$+ \text{Cross – Sectional Area (ft}^2\text{)} = \pi(\text{Radius of FCS})^2$$

$$+ \text{Radius of FCS} = .0625 \text{ in}, .05 \text{ in}, .125 \text{ in}$$

$$\text{Reynolds Number} = \frac{\rho V D}{\mu}$$

$$\# \rho = \text{Density of Fluid (water, 5C)} = 1000 \text{ kg/m}^3$$

$$V = \text{Fluid Velocity} = \frac{\text{Flow Rate (ft}^3/\text{min)}}{\text{Cross – Sectional Area (ft}^2\text{)}}$$

$$\# \mu = \text{kinematic viscosity} = 8.9 * 10^{-4} \text{ kg/m} * \text{s}, +D = \text{diameter} = .125 \text{ in}$$

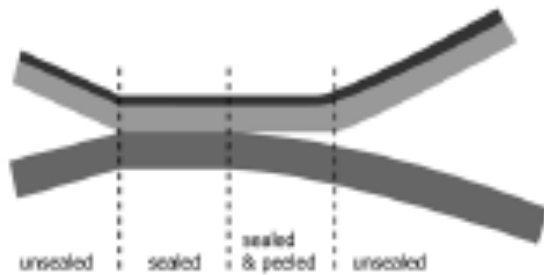
* Taken from Thermofisher Scientific

Taken from Engineer's Toolbox

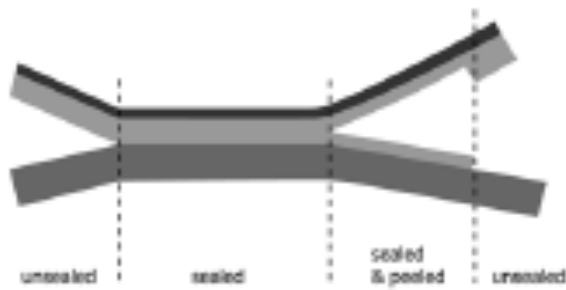
+ Measurement from fluid channel system

APPENDIX B –Method of Sample Break (ASTM International, F88)

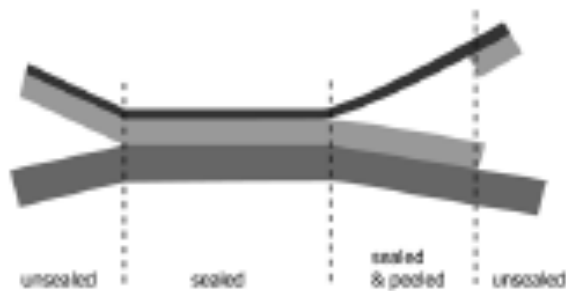
SEAL SEPARATION MODES



ADHESIVE PEEL



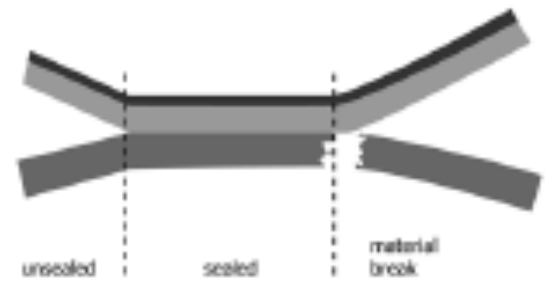
COHESIVE PEEL



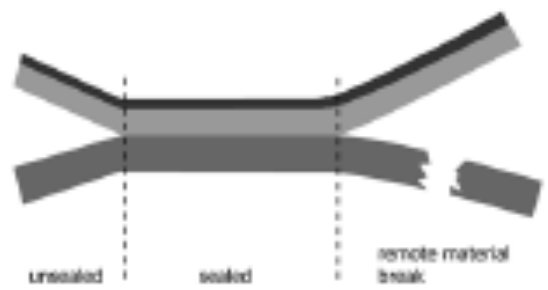
DELAMINATION

INTERFERENCES

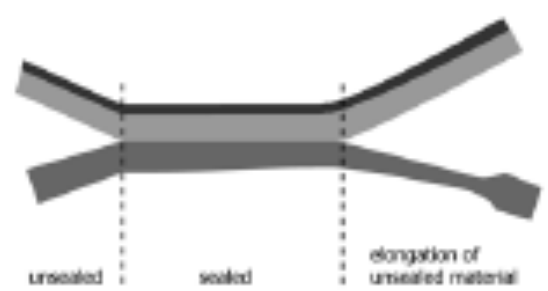
Though the diagrams show only one web being affected, it is possible for either or both webs to partially or fully exhibit interferences. Delamination, when not a designed seal separation mode, is an interference.



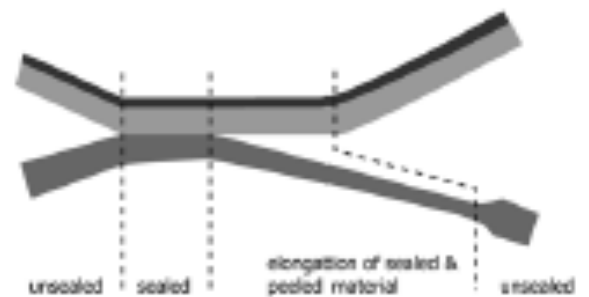
MATERIAL BREAK



MATERIAL BREAK (REMOTE)



MATERIAL ELONGATION



PEEL WITH ELONGATION

APPENDIX C – Temperature Data

Unmodified Plates

Time	Trial 1	Trial 2	Trial 3	Trial 4	Trial 5	Average	Standard Deviation
0	23.1	19.1	22.4	19.1	24.1	21.56	2.08
0.5	23.2	19.1	22.4	19.1	24.1	21.58	2.095137227
1	23.5	19.2	22.7	19.3	24.2	21.78	2.119811312
1.5	24.3	20.1	23.4	19.9	25	22.54	2.135977528
2	26.3	22.1	25.1	21.7	26.9	24.42	2.14140141
2.5	30.3	26	28.5	25	30.2	28	2.162406067
3	36.2	31.9	34	30.5	35.5	33.62	2.146066169
3.5	44.3	41.1	41.7	40.2	42.7	42	1.408545349
4	55.6	50.8	53.4	49.7	54.1	52.72	2.166471786
4.5	66.5	61.9	64.3	62.1	63	63.56	1.696584805
5	80.8	76.4	79.4	75.2	77.3	77.82	2.026228023
5.5	95.7	90.3	94.8	89.6	89.9	92.06	2.629524672
6	110.3	104.6	106.4	103.6	102.3	105.44	2.77459907
6.5	123.2	118.5	119.7	116.6	115	118.6	2.804995544
7	134.7	129.8	130.4	128	126.2	129.82	2.848438169
7.5	143.9	139.6	140.3	139.3	136.3	139.88	2.431789465
8	151.7	147.7	148.7	147.6	143.5	147.84	2.628763968
8.5	157.8	154.6	155.2	154.9	150.4	154.58	2.380252087
9	162.8	159.9	160.5	160.3	155.7	159.84	2.304430515
9.5	166.4	164	164.5	164.5	160.1	163.9	2.069782597
10	168.8	166.6	167.5	167.3	163	166.64	1.95407267
10.5	170.5	168.5	169.4	169.3	165.2	168.58	1.805990033
11	171.4	169.6	170.5	170.3	166.8	169.72	1.568948693
11.5	171.6	169.9	171	170.7	167.2	170.08	1.540649214
12	171.3	169.8	171.1	170.6	167.7	170.1	1.30690474
12.5	171.3	169.8	170.9	170.7	168.5	170.24	0.99919968
13	172.3	170.8	171.4	171.8	170	171.26	0.798999374
13.5	174.9	173.3	173.3	174.3	172.9	173.74	0.74188948
14	178.1	176.7	176.5	178.5	176.4	177.24	0.88
14.5	181.7	180.3	180.1	181.9	179.8	180.76	0.866256313
15	185.1	183.7	183.5	185.3	183	184.12	0.913016977
15.5	188	186.6	186.3	188	185.6	186.9	0.954986911
16	190.4	188.7	188.4	190.1	187.5	189.02	1.083328205
16.5	191.7	190.1	190.1	191.6	188.7	190.44	1.112834219
17	192.4	190.7	190.9	192.2	189.4	191.12	1.094349122
17.5	192.5	190.8	191.1	192.3	189.5	191.24	1.091054536

18	191.9	190.4	190.9	191.6	189	190.76	1.024890238
18.5	190.6	189.4	190.1	190.7	188.1	189.78	0.957914401
19	189.4	188.1	188.9	189.3	189.9	189.12	0.601331855
19.5	187.5	186.5	187.4	187.6	185.3	186.86	0.873155198
20	185.6	184.7	185.5	185.6	183.6	185	0.777174369

Modified Plates

Time	Trial 1	Trial 2	Trial 3	Trial 4	Trial 5	Average	Standard Deviation
0	19.2	18.8	19.9	19	21.6	19.7	1.140175425
0.5	19.2	18.9	19.8	19	21.5	19.68	1.075639345
1	19.4	18.9	19.9	19.1	21.7	19.8	1.126942767
1.5	20.4	19.5	20.5	19.9	22.4	20.54	1.114899099
2	22.6	21	22.1	21.7	24.1	22.3	1.164044673
2.5	25.8	23.6	25	24.7	27.1	25.24	1.304990421
3	30.4	27.2	29.2	28.8	31.2	29.36	1.538830725
3.5	35.9	31.8	34.3	33.6	36.1	34.34	1.770028248
4	42.1	37.1	40.7	39.1	41.5	40.1	2.019900988
4.5	48.9	43.1	47.8	45.3	47.8	46.58	2.350957252
5	55.8	49.7	54.9	51.6	54.3	53.26	2.532390175
5.5	63.3	56.7	62.3	58.4	61.2	60.38	2.754450943
6	70.9	63.7	69.8	65.5	68.8	67.74	3.028696089
6.5	78.2	70.6	75.6	72.2	74.6	74.24	2.961080884
7	84.2	76.7	81	77.7	80.3	79.98	2.954149624
7.5	89.1	81	85.1	82.6	84.9	84.54	3.063168294
8	92.7	84.8	88.5	86.5	88.4	88.18	2.950762613
8.5	95.5	88	91.2	89.6	91.1	91.08	2.794100929
9	97.7	90.5	93.2	91.9	93.3	93.32	2.700370345
9.5	99.4	92.6	95.2	93.4	94.9	95.1	2.630589288
10	101.7		97.5	95.4	97	97.9	2.687005769
10.5		99.6	101.1	98.3	99.9	99.725	1.15
11	108.9	104.1	105.5	102.1	103.9	104.9	2.541653005
11.5	113.6	109.1	110.5	106.6	108.6	109.68	2.599423013
12	118.8	113.8	114.9	111.4	113.1	114.4	2.76857364
12.5	122.9	118	118.4	115.5	116.9	118.34	2.786216072
13	126	121.3	121.2	118.9	120.1	121.5	2.697220792
13.5	128.4	123.8	123.4	121.6	122.7	123.98	2.608064416
14	130.3	125.6	125	123.6	124.5	125.8	2.620114501
14.5	131.5	126.9	126.1	125.1	125.7	127.06	2.566709956

15	132.5	127.8	127.3	126.1	126.6	128.06	2.565735762
15.5	133.9	128.7	128.9	126.9	127.3	129.14	2.797856322
16	136.2	130.8	132	128.7	129.2	131.38	2.995329698
16.5	140.3	133.9	135.6	131.6	132.2	134.72	3.488122704
17	143.5	138	139.7	135.4	135.8	138.48	3.301060436
17.5	147.3	141.9	143.1	139	139.7	142.2	3.293933818
18	150.5	145	145.6	142.2	142.8	145.22	3.280548735
18.5	152.7	147.5	147.5	144.8	145.6	147.62	3.076849038
19	154.1	149.3	148.9	146.8	147.6	149.34	2.84306173
19.5	155	150.6	149.7	148.3	148.9	150.5	2.659887216
20	155.7	151.3	150.3	149.3	149.9	151.3	2.565151068
20.5	156	151.7	151.1	149.7	150.5	151.8	2.461706725
21	156.9	152.2	152.5	150.1	150.7	152.48	2.666833328
21.5	158.6	153.7	155.3	151.3		154.725	3.061998258
22	161.4	156.3	158.5	153.5	154	156.74	3.279176726
22.5	164.7	159.4	161.3	156.5	157	159.78	3.359613073
23	167.5	162.4	163.6	159.5	159.9	162.58	3.238363784
23.5	169.5	164.7	165.1	162.1	162.5	164.78	2.948219802
24	170.8	166.5	166.3	163.8	164.2	166.32	2.781546333
24.5	171.6	167.6	166.9	165.2	165.5	167.36	2.567683781
25	172.1	168.3	167.2	166	166.5	168.02	2.438647166
25.5	172.1	168.6	167.2	166.6	167	168.3	2.253885534
26	172.2	168.7	167.2	166.9	167.2	168.44	2.216528818
26.5	171.9	168.5	167.2	167	167.3	168.38	2.05353354
27	171.4	168.2	168	166.7	167	168.26	1.867618805
27.5	170.8	168.1	170.1	166.6	166.6	168.44	1.950128201
28	170.5	168.9	172.8	167.4	166.9	169.3	2.409356761
28.5	170.9	170.9	175.3	169.3	168.4	170.96	2.652922916
29	172.6	173.8	177.1	172	170.8	173.26	2.403747075
29.5	175.2	176.3	178.5	174.5	173.5	175.6	1.915724406
30	178.1	178.4	179.3	176.4	175.9	177.62	1.423727502

APPENDIX D – Peel Test Data

Thickness (mil)	Dwell Time (s)	Strength (lbs)
2	10	5.12
2	10	6.64
2	10	0.96
2	10	4
2	10	9.92
2	10	0.72
2	10	7.2
2	10	7.36
2	10	4.16
2	10	1.12
2	10	6.08
2	10	9.12
2	10	6.24
2	10	6.08
2	10	8.8
2	10	3.86
2	10	8.81
2	10	0.57
2	10	7.84
2	10	7.86
2	10	6.93
2	10	7.45
2	10	5.54
2	10	6.54
2	10	5.64
2	10	10.53
2	10	7.71
2	10	2.55
2	10	3.01
2	10	6.63
2	10	8.28
2	10	2.93
2	10	7.32
2	10	11.65
2	10	7.38
2	30	0.56

2	30	5.12
2	30	0.8
2	30	12.24
2	30	6.24
2	30	0.72
2	30	8.72
2	30	9.84
2	30	9.2
2	30	7.2
2	30	14.32
2	30	7.44
2	30	8.8
2	30	3.68
2	30	4.67
2	30	6.42
2	30	5.17
2	30	1.5
2	30	4.55
2	30	2.43
2	30	7.74
2	30	6.68
2	30	7.95
2	30	7.1
2	30	8.46
2	30	5.46
2	30	12.45
2	30	4.43
2	30	4.98
2	30	7.38
2	30	6.92
2	30	7.64
2	30	8.59
5	10	0.8
5	10	1.12
5	10	1.12
5	10	14.4
5	10	12.8
5	10	14.08
5	10	4.48
5	10	13.76
5	10	14.72

5	10	11.36
5	10	10.72
5	10	5.52
5	10	10.88
5	10	1.96
5	10	12.75
5	10	4.58
5	10	0.76
5	10	1.88
5	10	4.21
5	10	9.31
5	10	1.39
5	10	6.82
5	10	0.35
5	10	9.73
5	10	10.93
5	10	12.08
5	10	9.88
5	10	7.24
5	10	5.29
5	10	16.41
5	10	14.38
5	10	3.55
5	10	11.03
5	30	1.12
5	30	0.48
5	30	0.64
5	30	5.2
5	30	0.96
5	30	5.6
5	30	11.6
5	30	3.52
5	30	1.2
5	30	15.52
5	30	6.16
5	30	10.88
5	30	15.12
5	30	0.38
5	30	0.21
5	30	5.75
5	30	7.06

5	30	1.95
5	30	2.13
5	30	9.93
5	30	6.13
5	30	2.23
5	30	6.92
5	30	1.05
5	30	12.31
5	30	7.97
5	30	1.23
5	30	5.25
5	30	10.36
5	30	13.76
5	30	0.62
5	30	10.01

APPENDIX E – Burst Test Data

2mil, 10 sec	Force (lbs)	Deformation (in)
1	21.153145	0.34806573
* 2	222.19524	0.38873985
* 3	169.54	0.38
4	51.411797	0.36822477
5	27.746786	0.3636522
6	26.618774	0.37382162
7	26.735064	0.3630668
8	20.315859	0.35180682
9	26.711805	0.3639733
2mil, 30sec		
1	25.932665	0.363825
2	191.69238	0.38536516
3	56.307606	0.37274763
4	26.293161	0.36366707
5	211.38028	0.38375458
** 6	No Data	No Data
7	57.78449	0.3612765
8	171.30676	0.37236026
** 9	No Data	No Data
** 10	No Data	No Data

* Eliminated from data analysis in post-processing (≥ 1.5 times the inter-quartile range).

** Samples corrupted

VII. LIST OF REFERENCES

- Advantage Engineering, Inc. "Turbulent and Laminar Flow." *FYI #156*, Advantage Engineering, Inc.,
www.advantageengineering.com/fyi/156/advantageFYI156.php.
- Aerospace Specification Metals Inc. "Aluminum 6061-T6; 6061-T651." *ASM Material Data Sheet*, asm.matweb.com/search/SpecificMaterial.asp?bassnum=MA6061t6.
- Anderson, Thomas L., et al. Interface for Use Between Medical Instrumentation and a Patient. US Patent US 2005/0215901 A1, 29 Sept. 2005.
- Anderson, Thomas P., et al. Multifunction Warming Device with an Upper Body Connective Apparatus. US Patent US 2007/0093885 A1, 26 Apr. 2007.
- Andritz Group. "ANDRITZ Biax Line for BOPET Film Production." *BOPET - Andritz Group*, Andritz Group, www.andritz.com/oi-bopet-andritz-biax. Accessed Jan. 2016.
- Arcade Museum. "Curling Mylar." *Pinball Magic*, Arcade Museum, 18 Mar. 2010, forums.arcade-museum.com/archive/index.php/t-126448.html.
- ASTM International. *Standard Practice for Conditioning and Testing Flexible Barrier Packaging*. Test Protocol no. E171M - 11, West Conshohocken, PA, ASTM International, 2015.
- ASTM International. *Standard Terminology Relating to Primary Barrier Packaging*. Test Protocol no. F17 - 17, West Conshohocken, PA, ASTM International, 2017.
- ASTM International. *Standard Test Method for Determining Compressive Resistance of Shipping Containers, Components, and Unit Loads*. Test Standard no. D642 - 15, West Conshohocken, PA, ASTM International, 2015.
- ASTM International. *Standard Test Method for Seal Strength of Flexible Barrier Materials*. Test Standard no. F88-15M, West Conshohocken, PA, ASTM International, 2015.

- ASTM International. *Standard Test Method for Tensile Properties of Thin Plastic Sheeting*. Test Protocol no. D882 - 12, West Conshohocken, PA, ASTM International, 2012.
- Beij, K. Hilding. *Pressure Losses for Fluid Flow in 90 Degree Pipe Bends*. Research report no. RP1110, US Department of Commerce, July 1938.
- Benson, Tom, editor. "Reynolds Number." *Reynolds Number*, National Aeronautics and Space Administration, 12 June 2014, www.grc.nasa.gov/www/BGH/reynolds.html.
- Berg, Regan J., et al. "The Impact of Heat Stress on Operative Performance and Cognitive Function During Simulated Laparoscopic Operative Tasks." *Minimally Invasive Surgery*, vol. 157, no. 1, Jan. 2015, pp. 87-95.
- Berg, Regan James, et al. "The Impact of Heat Stress on Performance and Cognitive Function During Simulated Laparoscopic Surgical Tasks." *Journal of the American College of Surgeons*, vol. 215, no. 3, Sept. 2012.
- Berguer, R., et al. "Ergonomic Problems Associated with Laparoscopic Surgery." *Surgical Endoscopy*, vol. 13, no. 5, May 1999, pp. 466-68.
- Bernal, William. *Relating Burst Pressure to Seal Peel Strength in Pouches*. 2012. Clemson, MS thesis. *Tiger Prints*, Clemson University, tigerprints.clemson.edu/cgi/viewcontent.cgi?article=2490&context=all_theses.
- Bletsos, Ioannis V., et al. Coated Sheet Materials and Packages Made Therewith. US Patent US 2004/0028931A1, 12 Feb. 2004.
- Bond, Curtis J., and John G. Ulm. Quick-Disconnect Service-Line Connector and Valve Assembly. US Patent 4,421,146, 20 Dec. 1983.
- Bongers, Coen C.W.G., et al. "Precooling and percooling (cooling during exercise) both improve performance in the heat: a meta-analytical review." *British Journal of Sports Medicine*, vol. 49, no. 6, Mar. 2016, pp. 377-84.
- Borg, Gunnar. *Borg's Perceived Exertion and Pain Scales*. Human Kinetics, 1998.
- Brister, Mark C., et al. Intra-gastric Device. US Patent US 2012/0191123 A1, 26 July 2012.

- Budd, Grahame E. "Wet-bulb globe temperature (WBGT)—its history and its limitations." *Journal of Science and Medicine in Sport*, vol. 11, no. 1, Jan. 2008, pp. 20-32.
- Carpenter, James E., et al. "The Effects of Muscle Fatigue on Shoulder Joint Position Sense." *American Journal of Sports Medicine*, vol. 26, no. 2, Mar. 1998, pp. 262-65.
- Cleary, Michelle A., et al. "Thermoregulatory, Cardiovascular, and Perceptual Responses to Intermittent Cooling During Exercise in a Hot, Humid Outdoor Environment." *Journal of Strength and Conditioning Research*, vol. 28, Mar. 2014, pp. 792-806.
CoolOR Zipper Vest with Cool58 Packs - Polar Products Inc. Polar Products Inc., www.polarproducts.com/polarshop/pc/CoolOR-Zipper-Vest-with-Cool58-Packs-p160.htm.
- Corbeil, Philippe, et al. "Perturbation of the postural control system induced by muscular fatigue." *Gait & Posture*, vol. 18, no. 2, Oct. 2003, pp. 92-100.
- Cultua. "Where does the Cephalic Vein Originate?" *Cultua.info*, 2018, cultua.info/where-does-the-cephalic-vein-originated/.
- Cuschieri, Alfred. "Whither Minimal Access Surgery: Tribulations and Expectations." *The American Journal of Surgery*, vol. 169, no. 1, Jan. 1995, pp. 9-19.
- Dean, W. Clark. Medical Cooling Vest and System Employing the Same. US Patent US 6,349,412 B1, 26 Feb. 2002.
- DeMeuse, Mark T., editor. *Biaxial Stretching of Film: Principles and Applications*. Cornwall, Woodhead Publishing, 2011.
- De Muinck, Ebo Jacques, and Jaap Jeroen Sondaar. Butterfly Valve. US Patent US 9,377,111 B2, 28 June 2016.
- Dimitrova, Nonna, and George Dimitrov. "Interpretation of EMG changes with fatigue: facts, pitfalls, and fallacies." *Journal of Electromyography and Kinesiology*, vol. 13, no. 1, Feb. 2003, pp. 13-36.
- Duke, Derek A. Medical garment ventilation system. US Patent 7,490,606B2, 17 Feb. 2009.
- Dunning, James E., et al. System and Method for Providing Even Heat Distribution and Cooling Return Pads. US Patent US 2008/0249520 A1, 9 Oct. 2008.

- Eijsvogels, Thijs M.H., et al. "Cooling during Exercise in Temperate Conditions: Impact on Performance and Thermoregulation." *International Journal of Sports Medicine*, vol. 35, no. 10, 2014, pp. 840-46.
- Ellis, Kent D., et al. Personal Warming Systems and Apparatuses for Use in Hospitals and Other Settings, and Associated Methods of Manufacture and Use. US Patent US 6,933,469 B2, 23 Aug. 2005.
- Encyclopedia Astronautica, and Mark Wade. "Echo." *Echo*, Encyclopedia Astronautica, www.astronautix.com/craft/echo.htm. Accessed Jan. 2016.
- Erickson, Brandon J., et al. "The Impact of Fatigue on Baseball Pitching Mechanics in Adolescent Male Pitchers." *Journal of Arthroscopic and Related Surgery*, vol. 32, no. 5, May 2016, pp. 762-71.
- Farah, Shady, et al. "Physical and mechanical properties of PLA, and their functions in widespread applications — A comprehensive review." *Advanced Drug Delivery Reviews*, vol. 107, 15 Dec. 2016, pp. 367-92.
- Farley, James M., et al. Heat Sealable Films and Articles Made Therefrom. US Patent 5,530,065, 25 June 1996.
- Ferber, John A. Bulk Consumables Pouch. US Patent D694649S, 3 Dec. 2013.
- Filingeri, Davide, et al. "Mild evaporative cooling applied to the torso provides thermoregulatory benefits during running in the heat." *Scandinavian Journal of Medicine and Science in Sports*, vol. 25, no. S1, June 2015, pp. 200-10.
- Fisher Scientific. "Fisherbrand™ Isotemp™ Refrigerated/Heated Bath Circulators: 5.4-6.5L, 115V/60Hz." *Fisherbrand Isotemp Refrigerated/Heated Bath Circulators: 5.4-6.5L, 115V/60Hz*, Thermofisher Scientific, www.fishersci.com/shop/products/fisher-scientific-isotemp-refrigerated-heated-bath-circulators-5-4-6-5l-115v-60hz-4/p-4105182.
- Friedman, Mitchell A. Dispensing Valve for Fluids. US Patent US 6,742,680 B2, 1 June 2004.
- Fuller, Jason R., et al. "Posture-movement changes following repetitive motion-induced shoulder muscle fatigue." *Journal of Electromyography and Kinesiology*, vol. 19, no. 6, Dec. 2009, pp. 1043-52.

- Galleano, Raffaele, et al. "Can Armrests Improve Comfort and Task Performance in Laparoscopic Surgery?" *Annals of Surgery*, vol. 243, no. 2, Mar. 2006, pp. 329-33.
- Hagihara, Tadashi. Self-Standing Bag Container Equipped with Vacuum and Flow Rate Control Functions. US Patent US 6,578,740 B1, 17 June 2003.
- Halim, Isa, et al. "Assessment of Muscle Fatigue Associated with Prolonged Standing in the Workplace." *Safety and Health at Work*, vol. 3, no. 1, Mar. 2012, pp. 31-42.
- Hartviksen, Karl. "Ice Therapy in Spasticity." *Acta Neurologica Scandinavica*, vol. 38, no. S3, 1962, pp. 79-84.
- Herrera, Esperanza, et al. "Motor and Sensory Nerve Conduction Are Affected Differently by Ice Pack, Ice Massage, and Cold Water Immersion." *Physical Therapy*, vol. 90, no. 4, Apr. 2010, pp. 581-91.
- Hsu, Patricia A., and Brian C. Cooley. "Effect of Exercise on Microsurgical Hand Tremor." *Microsurgery*, vol. 23, no. 4, Aug. 2003, pp. 323-27.
- Jankovic, Joseph, and Fahn Stanley. "Physiologic and Pathologic Tremors: Diagnosis, Mechanism, and Management." *Annals of Internal Medicine*, vol. 93, no. 3, 1 Sept. 1980.
- Jenkins, Donny Ray. Body Heating/Cooling Apparatus. US Patent US 6,942,015 B1, 13 Sept. 2005.
- Jensen, Lauren, et al. "Muscle-Cooling Intervention to Reduce Fatigue and Fatigue-Induced Tremor in Novice and Experienced Surgeons: A Preliminary Investigation." *The Surgery Journal*, vol. 2, no. 4, Nov. 2016, pp. 1-5.
- Keeney, Wendy Lisabeth, compiler. *Average, Standard Deviation and Relative Standard Deviation*. Texas A&M University.
- Kilbom, Asa, and Jan Persson. "Work technique and its consequences for musculoskeletal disorders." *Ergonomics*, vol. 30, no. 2, 1987, pp. 273-79.
- Klabunde, Richard E. "Turbulent Flow." *CV Physiology | Turbulent Flow*, 3 1 2018, www.cvphysiology.com/Hemodynamics/H007.
- Koewler, Danial E. Patient Temperature Control System with Variable Gradient Warming/Cooling. US Patent US 8,647,374 B2, 11 Feb. 2014.

- Koscheyev, Victor S., et al. Multi-Zone Cooling/Warming Garment. US Patent 7,089,995 B2, 15 Aug. 2006. Regents of the University of Minnesota
- Lakie, M., et al. "Limb Temperature and Human Tremors." *Journal of Neurology, Neurosurgery, and Psychiatry*, vol. 57, no. 1, Jan. 1994, pp. 35-42.
- Locker, Anatol. "PETG Filament Guide 2018 – Explained, Compared & Reviewed." *PETG Filament Guide 2018*, edited by All3DP, 8 Mar. 2018, all3dp.com/1/petg-filament-3d-printing/.
- Lumen Learning. "Fluid Dynamics and Its Biological and Medical Applications." *Flow Rate and Its Relation to Fluid Velocity*, Lumen Learning, courses.lumenlearning.com/physics/chapter/12-1-flow-rate-and-its-relation-to-velocity/.
- Maffiuletti, NA, and R. Lepers. "Muscular and Mental Fatigue in Surgeons." Received by Annals of the Royal College of Surgeons of London, Jan. 2012. Memo.
- Merrick, Mark A., et al. "Cold Modalities With Different Thermodynamic Properties Produce Different Surface and Intramuscular Temperatures." *Journal of Athletic Training*, vol. 38, no. 1, January-March 2003, pp. 28-33.
- . "The Effects Of Ice And Compression Wraps On Intramuscular Temperatures At Various Depths." *Journal of Athletic Training*, vol. 28, no. 3, Fall 1993, pp. 241-45.
- Molloy, Michael C. Configured Pad for Therapeutic Cooling Effect. US Patent 5,086,771, 11 Feb. 1992.
- Montgomery, Paul G., et al. "The effect of recovery strategies on physical performance and cumulative fatigue in competitive basketball." *Journal of Sports Sciences*, vol. 26, no. 11, 2008, pp. 1135-45.
- Morrison, S., et al. "The Effects of Unilateral Muscle Fatigue on Bilateral Physiological Tremor." *Experimental Brain Research*, vol. 167, no. 4, 3 Aug. 2005, pp. 609-21.
- Murphy, John. "Temperature and Humidity Control in Surgery Rooms." *ASHRAE Journal*, vol. 48, 2006, pp. H18-H25.
- Myrer, J. William, et al. "Cold- and Hot-Pack Contrast Therapy: Subcutaneous and Intramuscular Temperature Change." *Journal of Athletic Training*, vol. 32, no. 3, Sept. 1997, pp. 238-41.

- Niedospial, John J., Jr, and Charles Quirico. Twist Valve. US Patent 6,156,025, 5 Dec. 2000.
- Nielsen, Lau, and Erik Dige. Tap for a Bag-In-Box. US Patent US 2009/0159594 A1, 25 June 2009.
- Nur, Nurhayati Mohd, et al. "Muscle activity, time to fatigue, and maximum task duration at different levels of production standard time." *Journal of Physical Therapy Science*, vol. 27, no. 7, July 2015, pp. 2323-26.
- Omega Engineering. *Revised Thermocouple Reference Tables*. Omega Engineering.
- P., Kellene. "Mylar the Magnificent." *Mylar the Magnificent | Preparedness Pro*, Preparedness Pro, 24 Nov. 2009, www.preparednesspro.com/mylar-the-magnificent.
- Paradis, Joseph R. Control of Fluid Flow. US Patent 5,699,821, 23 Dec. 1997.
- Pavalarajan, Ganesh B., et al. Surgical Helmet. US Patent EP2853169 A1, 1 Apr. 2015. Zimmer Surgical, Inc.
- Pfister, William R., et al. Heat-Sealable Membrane for Transdermal Drug Release. US Patent 4,951,657, 28 Aug. 1990.
- Pilcher, June J., et al. "Effects of hot and cold temperature exposure on performance: a meta-analytic review." *Ergonomics*, vol. 45, no. 10, 2002, pp. 682-98.
- Pressure Drop Along Pipe Length of Uniform Diameter*. Engineer's Edge, Inc., www.engineersedge.com/fluid_flow/pressure_drop/pressure_drop.htm.
- Rampinini, Ermanno, et al. "Technical performance during soccer matches of the Italian Serie A league: Effect of fatigue and competitive level." *Journal of Science and Medicine in Sport*, vol. 12, no. 1, Jan. 2009, pp. 227-33.
- Reader, S. R., and H. M. Whyte. "Tissue Temperature Gradients." *Journal of Applied Physiology*, vol. 4, 1951, pp. 396-402.
- Roman-Liu, Danuta, et al. "Quantitative assessment of upper limb muscle fatigue depending on the conditions of repetitive task load." *Journal of Electromyography and Kinesiology*, vol. 14, no. 6, Dec. 2004, pp. 671-82.
- Rose, Joseph Lorney, and Kirk Alan Dobbs. Tubed Lamination Heat Transfer Articles and Method of Manufacture. US Patent 5,755,275, 26 May 1998.

- Schaar, Charles H. Differential Heat-Sealability in Differentially Crystalline Sheet Materials, Products Made Therefrom, and Process and Apparatus for Making. US Patent 3,012,918, 12 Dec. 1961.
- Slack, Paul, et al. "The Effect of Operating Time on Surgeon's Muscular Fatigue." *Royal College of Surgeons of England*, 2008, pp. 651-57.
- Slack, Paul S., et al. "The Effect of Operating Time on Surgeon's Hand Tremor." *European Archives of Oto-Rhino-Laryngology*, 2009, pp. 137-41.
- Smolko, Daniel D., and Gregory J. Kevorkian. Vented Closures for Containers. US Patent US 2004/0173556 A1, 9 Sept. 2004.
- Solid State Cooling Systems. "ThermoCube 200/300/400." *Solid State Cooling Systems: ThermoCube 200/300/400*, Solid State Cooling Systems, www.sscooling.com/products/benchtopy-chillers/item/thermocube-air-cooled-200-300-400-w-liquid-recirculating-chiller-for-lab-laser-semiconductor?category_id=249.
- Sommerich, Carolyn M., et al. "Occupational risk factors associated with soft tissue disorders of the shoulder: a review of recent investigations in literature." *Ergonomics*, vol. 36, no. 6, July 1993, pp. 697-717.
- Stackhouse, Wyman H., et al. Surgical Gown. US Patent 5,253,642, 19 Oct. 1993. Stackhouse, Inc.
- Staugaitis, C., and L. Kobren. *Mechanical And Physical Properties of the Echo II Metal-Polymer Laminate*. Technical report no. D-3409, NASA Goddard Space Flight Center, 1966.
- Stevens, Christopher, et al. "Cooling during exercise: an overlooked strategy for enhancing endurance performance in the heat." *Sports Medicine*, vol. 47, no. 5, 2017, pp. 829-41.
- Teijin DuPont Films Japan Limited. "Mylar." *Mylar Tetoron Film*, Teijin DuPont Films Japan Limited, teijindupontfilms.jp/english/product/pet_ma.html. Accessed Feb. 2016.
- Thermocouples*. Spectris, Inc., www.omega.com/prodinfo/thermocouples.html.
- 30 Watt Lightweight Soldering Iron*. Harbor Freight Tools, www.harborfreight.com/30-watt-lightweight-soldering-iron-69060.html.

- Tripp, Brady L., et al. "Functional Fatigue and Upper Extremity Sensorimotor System Acuity in Baseball Athletes." *Journal of Athletic Training*, vol. 42, no. 1, January-March 2007, pp. 90-98.
- USA Lab Equipment. "SEALER SALES KF-150 CST 6' PORTABLE DIRECT HEAT SEALER." *SEALER SALES KF-150 CST 6" PORTABLE DIRECT HEAT SEALER - USA Lab Equipment*, USA Lab Equipment, 2018, www.usalabequipment.com/sealer-sales-kf-150-cst-6-portable-direct-heat-sealer/.
- VanDerWoude, Brian J., et al. Personal Protection System. US Patent US0213523 A1, 28 Sept. 2006. Stryker Corporation
- VanDerWoude, Brian James, and Douglas Lee Campbell. Personal Protection System With Head Unit Having Easy Access Controls and Protective Covering Having Glare Avoiding Face Shield. US Patent US20090151054 A1, 18 June 2009.
- Walton, Mark, et al. "Effects of Ice Packs on Tissue Temperatures at Various Depths Before and After Quadriceps Hematoma: Studies Using Sheep." *Journal of Orthopaedic and Sports Physical Therapy*, vol. 8, no. 6, 1986, pp. 294-300.
- Wyatt, Charles C., et al. Personal Warming Systems and Apparatuses for Use in Hospitals and Other Settings, and Associated Methods of Manufacture and Use. US Patent US 6,967,309 B2, 22 Nov. 2005.
- Zacoi, Thomas N. Apparatus for Controlling the Temperature of an Area of the Body. US Patent 5,190,032, 2 Mar. 1993.

VII. Biography

Justin Baris was born on April 17th, 1995 in St. Louis, Missouri to Mitchell and Lynda Baris. He has one brother, Alec who is 2.5 years his junior. He was raised in St. Louis all of his life with a particular interest in the medical field since the age of 10 years old. He attended Marquette High School in Chesterfield, Missouri where he was a 4-year letterman on both the Tennis and Cross Country teams and had a particular love for science and mathematics courses. He came to Tulane University and joined the Biomedical Engineering program in the fall of 2013. He decided to pursue the 4+1 BSE/MS in Biomedical Engineering degree program and after graduation he plans to pursue a career in the medical device industry, helping physicians provide the best care possible for their patients.